

## **Optimal Impulsive Control for Cancer Therapy**

**João Pedro Lourenço dos Santos Belfo**

Thesis to obtain the Master of Science Degree in

## **Electrical and Computer Engineering**

Supervisor: Professor João Manuel Lage de Miranda Lemos

### **Examination Committee**

Chairperson: Professor João Fernando Cardoso Silva Sequeira

Supervisor: Professor João Manuel Lage de Miranda Lemos

Member of the Committee: Professor João Manuel de Freitas Xavier

**October, 2018**



***Mathematics reveals its secrets only to those who approach it with pure love, for its own beauty***

-Archimedes



**Declaration:** I declare that this document is an original work of my own authorship and that it fulfills all the requirements of the Code of Conduct and Good Practices of the Universidade de Lisboa.



## Acknowledgments

The last 5 years were the best and most difficult years of my life. I have met many different persons, some are my best friends. Many things happen in this period: I have studied a lot, went to parties, I did Erasmus in Finland etc... It was a roller coaster of emotions. Now that everything is ending, is time to thank all the people and institutions that contributed to this adventure and to this dissertation. This is a very complex task, since many people contributed in a direct or indirect way. For those persons, I want to express my huge gratitude.

I would like to express a special thank to my supervisor Professor João Miranda Lemos for all the guidance, assistance, availability and all the laughs since the day I showed my interest in this topic. Professor João is, without a doubt, the person behind all ideas of this dissertation. I felt always motivated to work in this dissertation and to meet with Professor João to discuss issues and concepts.

I also would like to thank to INESC-ID for the access to its facilities, to the PERSEIDS project, where this dissertation is inserted and to my friend Margarida Nabais for her revision of this dissertation.

Finally, I would like to express the most special thank to my family for making this last 5 years possible, specially my father. Also a special thank to my friends Rafael, Francisco and Pedro for all the help and laughs.



The work of this dissertation was performed within the framework of the project PERSEIDS, Personalizing cancer therapy through integrated modeling and decision, financed by FCT under contract PTDC/EMS-SIS/0642/2014.



## Abstract

Currently, mortality due to cancer is still one of the most important problems, even when considering the scientific advances that allowed the implementation of more effective solutions to treat or even cure some diseases. This work focuses on the chemotherapy optimization, where the number of therapy sessions  $N$ , drug dosage in each session  $A_n$ , and time intervals between sessions  $T_n$  correspond to variables that are to be optimized. This is achieved through the design of a controller to minimize tumor size in cancer and also the treatment side effects, depending on those variables.

In order to achieve such goal, Pharmacokinetic, Pharmacodynamic and Tumor Growth models and mathematical models for subsystems that affect the tumor growth, like the Immune System and Angiogenesis, are studied to develop a single mathematical model that translates the relationship between the Tumor volume and the three treatment variables. This relationship is then studied using optimal impulsive control techniques in order to create a function to be minimized, whose minimum value translates the intended objective of treatment optimization. The problem is divided into three problem and various concepts like optimal control, convexity, robustness, receding horizon, minimum attention control, pseudo-spectral analysis, sensitivity analysis and parameter quantization are considered in each problem. In the first problem, only the drug dosages are considered to be variable and the results suggest that the objective function used is convex. In the second and third problems, besides the dosages, time intervals are now variable which leads to a non convex objective function. Optimization algorithms are used using different initial conditions and the solution that corresponds to a lower objective function value is chosen. A pseudo-spectral approach is used in order to reduce problem dimension and the results suggest a convex approximation problem.

**Keywords:** Optimal Impulsive Control, Nonlinear Optimization, Receding Horizon Control, Minimum Attention Control, Pseudo-spectral Analysis.



## Resumo

Actualmente, a mortalidade devido a o cancro continua a ser um dos problemas mais importantes, mesmo considerando os avanços científicos que permitiram a implementação de soluções mais eficazes de tratamento ou até mesmo cura de certas doenças. Este trabalho foca-se na optimização da quimioterapia, onde é necessário optimizar o numero de sessões  $N$ , as dosagens de fármaco em cada sessão  $A_n$  e os intervalos de tempo entre cada sessão. Este objetivo é atingido através do projecto de um controlador que minimiza o volume do tumor e também os efeitos secundários do tratamento.

Os modelos Farmacocinéticos, Farmacodinâmicos, de crescimento do tumor e modelos de subsistemas que possam influenciar o crescimento do tumor são estudados de modo a criar um único modelo que traduza a relação entre o volume do tumor e os três parâmetros do tratamento. Esta relação é então estudada usando técnicas de controlo ótimo por forma a criar-se uma função, cujo minímo traduza o que se pretende minimizar. O problema de optimização é dividido em três problemas nos quais são considerados diferentes conceitos tais como controlo ótimo, convexidade, robustez, controlo de horizonte recidido, controlo de atenção mínima, análise pseudo-espectral, análise de sensibilidades e quantização das variáveis de controlo. No primeiro problema, apenas variam as dosagens de fármaco e os resultados sugerem uma função objetivo convexa. No segundo e terceiro problema, ambas as dosagens e intervalos de tempo variam, levando à não convexidade. São usados algoritmos de optimização que consideram pontos iniciais diferentes e é escolhida a solução que apresenta menor valor da função objetivo. Uma abordagem pseudo-espectral é usada com o objetivo de reduzir a dimensão do problema e os resultados sugerem a convexidade do problema aproximado.

**Palavras-chave:** Controlo Óptimo Impulsivo, Optimização Não Linear, Controlo de Horizonte Recidido, Controlo de Atenção Mínima, Análise Pseudo-espectral.



# Contents

Acknowledgments . . . . .	vii
Abstract . . . . .	ix
Resumo . . . . .	xi
List of Figures . . . . .	xv
List of Tables . . . . .	xix
<b>1 Introduction</b>	<b>1</b>
1.1 Motivation . . . . .	1
1.2 Problem Formulation . . . . .	2
1.3 State of the art . . . . .	5
1.4 Contributions . . . . .	7
1.5 Report Outline . . . . .	7
<b>2 Pharmacodynamical Model</b>	<b>9</b>
2.1 Pharmacokinetics . . . . .	9
2.1.1 Types of models . . . . .	10
2.1.2 Compartmental models . . . . .	10
2.1.3 Positive Systems . . . . .	12
2.1.4 Controllability and Observability . . . . .	13
2.1.5 Example: A 2 compartment model . . . . .	14
2.1.6 Dirac Impulse Sequence . . . . .	14
2.1.6.1 Second Order System Response . . . . .	17
2.1.6.2 Pharmacokinetic Model Response . . . . .	20
2.2 Pharmacodynamics . . . . .	23
2.3 Important Remarks . . . . .	24
<b>3 Tumor Growth Models</b>	<b>27</b>
3.1 Logistic Growth Model . . . . .	27
3.1.1 Solution of the Logistic equation . . . . .	28
3.1.2 Tumor Volume Evolution . . . . .	29
3.2 Gompertz Growth Model . . . . .	32
3.3 Interacting Subsystems . . . . .	33

3.3.1 Immune System . . . . .	33
3.3.2 Angiogenesis . . . . .	34
3.4 Important Remarks . . . . .	35
<b>4 Global Cancer Therapy Model</b>	<b>37</b>
<b>5 Optimal Impulsive Control</b>	<b>41</b>
5.1 Optimal Control . . . . .	41
5.2 Optimal Impulsive Control and PK model . . . . .	42
5.3 Maximum Principle for Impulse Optimal Control . . . . .	45
5.4 Variable amplitudes and fixed time intervals . . . . .	48
5.4.1 Influence of parameter $\rho$ . . . . .	55
5.4.2 Influence of parameter $T$ . . . . .	57
5.4.3 Receding Horizon Control . . . . .	59
5.5 Variable amplitudes and periodic time intervals . . . . .	64
5.5.1 Influence of the Immune System . . . . .	67
5.5.2 Influence of the Angiogenesis Process . . . . .	69
5.6 Variable amplitudes and time intervals . . . . .	72
5.6.1 Minimum Attention Control . . . . .	72
5.6.2 Fixing N . . . . .	76
5.6.3 Pseudo-spectral Analysis . . . . .	80
5.7 Important Remarks . . . . .	83
<b>6 Results and Discussion</b>	<b>85</b>
6.1 Sensitivity Analysis . . . . .	85
6.1.1 Parameter Variation . . . . .	85
6.1.2 Modelling Errors . . . . .	91
6.1.3 Quantization . . . . .	92
6.2 Using the Gompertz Growth Model . . . . .	94
<b>7 Conclusions</b>	<b>97</b>
7.1 Future Work . . . . .	99
<b>Bibliography</b>	<b>101</b>
<b>A Solution of the Logistic Equation</b>	<b>A1</b>
<b>B Important remarks of chapter 5</b>	<b>B1</b>

# List of Figures

1.1	Mortality in Portugal, in 2014. Source: Eurostat Database (data refer to 2014) . . . . .	1
1.2	Block diagram of the overall system, including the Pharmacokinetic models, Pharmacodynamic models and tumor growth models . . . . .	3
1.3	Block diagram for the overall system with the controller that minimizes the tumor dynamics . . . . .	4
1.4	Block diagram for the overall system with a different control architecture . . . . .	4
2.1	Classification of modeling approaches . . . . .	10
2.2	General compartment model architectures . . . . .	11
2.3	Catenary model with 2 compartments . . . . .	14
2.4	Dirac impulse approximation represented by a rectangle $\epsilon = 1$ . . . . .	16
2.5	Unit step with $\epsilon = 2$ . . . . .	17
2.6	Second Order System response to a Dirac impulse with zero initial conditions . . . . .	18
2.7	Second order system response to a rectangle impulse for different values of height $A = 1/\epsilon$ , $\omega_n = 3$ Hz . . . . .	19
2.8	Second order system response to a sequence of Dirac Impulses with period $T = 10$ hours, $\xi = 0.5$ and $\omega_n = 3$ Hz . . . . .	20
2.9	Variation of the concentrations . . . . .	22
2.10	Average Concentration Variation depending on the Administration Period T . . . . .	22
2.11	Drug effect as a function of drug concentration, with $u_{max} = 1$ . . . . .	24
3.1	Logistic and Generalized Logistic Models, with $K = 10$ , $a = 0.09$ and $V_0 = 1mm^3$ . . . . .	29
3.2	Gompertz Model, with $\beta = 0.02$ , $a = 0.09$ and $V_0 = 1mm^3$ . . . . .	30
3.3	Gompertz Model, with $b = 0.02$ , $a = 0.09$ and $V_0 = 1mm^3$ . . . . .	33
4.1	Block diagram considered in the first problem: Administration model, Pharmacokinetics, Pharmacodynamics and Logistic model . . . . .	37
4.2	Time evolution of the logistic equation solution denominator $D(t) = V_0 + (K - V_0)e^{-a(t-t_0)}$ for $K = [-1, -0.5, 0.5, 2]$ , with $a = 0.01$ and $V_i = 10$ . . . . .	39
4.3	Tumor volume time evolution for different values of $K$ , with $a = 0.1$ , $V_i = 10$ and $t \geq 0$ . . . . .	39
5.1	Objective functions values described in (5.3) and (5.4) for variable amplitudes, with $N = 2$ , $\rho = 1$ and a constant reference $r(t) = 0.6$ . . . . .	43

5.2	Concentration variation with optimal amplitudes . . . . .	44
5.3	Concentration variation with 10 optimal amplitudes, with $T_i = 5, i = 1, \dots, N$ . . . . .	44
5.4	Objective function as a function of $(v(t_1), t_1)$ , for $T = 2$ . . . . .	48
5.5	Output signals of Administration model, $I(t)$ , Pharmacokinetics, $c(t)$ , and Pharmacodynamics, $u(t)$ . . . . .	49
5.6	Tumor evolution over time when applied the Dirac impulse sequence described in fig.5.5. . . . .	49
5.7	Squared Volume time evolution when applied the Dirac impulse sequence described in fig.5.5 . . . . .	51
5.8	Tumor volume and squared volume for $V(0) = 0.5 \text{ mm}^3$ , when applied the Dirac impulse sequence described in figure 5.5 . . . . .	51
5.9	Tumor volume and squared volume for $V(0) = 2 \text{ mm}^3$ , when applied the Dirac impulse sequence described in figure 5.5 . . . . .	52
5.10	Surface and contour of $V^2$ considering $N = 2, T_1 = 3 \text{ days}, \rho = 0.5$ and $T = 30 \text{ days}$ . . . . .	52
5.11	Surface and contour of $ V $ considering $N = 2, T_1 = 3 \text{ days}, \rho = 0.5$ and $T = 30 \text{ days}$ . . . . .	53
5.12	Surface and contour of different objective functions considering $N = 2, T_1 = 3 \text{ days}, \rho = 0.5$ and $T = 30 \text{ days}$ . . . . .	54
5.13	Optimal solutions depending on $\rho$ , for different values of $C_{max}$ , with $\alpha = 0.9$ . . . . .	56
5.14	Optimal output signals of Administration model, $I(t)$ , Pharmacokinetics, $c(t)$ , and Pharmacodynamics, $u(t)$ , using a percentage decay with $\alpha = 0.9, N = 10, T_n = 3$ for $n = 1, \dots, N - 1$ and $C_{max} = 10 \text{ mg/kg}$ . . . . .	57
5.15	Optimal solutions depending on $T$ , for different values of $C_{max}$ , with $\alpha = 0.9, N = 10$ and $\rho = 0.3$ . . . . .	58
5.16	Optimal solutions for $T = 136$ and $T = 138$ , with $\alpha = 0.9, N = 10$ and $\rho = 0.3$ . . . . .	59
5.17	Receding Horizon illustration of three iterations, with $N = 4$ . . . . .	60
5.18	Receding Horizon Control simulation considering the two variations . . . . .	61
5.19	Optimal solution for $T = 150, N = 30, T_n = 5$ for $n = 1, \dots, N - 1$ and $\rho = 0.3$ . . . . .	62
5.20	Receding Horizon Control simulation considering the variation two, with changes in the parameter $u_{max}$ as perturbation. . . . .	63
5.21	Optimal Impulsive Control Simulation with changes in the parameter $u_{max}$ as perturbation. . . . .	63
5.22	Objective function as a function of the second amplitude and the time interval, considering $T = 15 \text{ days}, N = 2$ and $A_1 = 1 \text{ mg/kg}$ . . . . .	64
5.23	Tumor volume time evolution considering solutions from different initial conditions in the optimization method . . . . .	65
5.24	Optimal solutions and tumor volume evolutions for each solution, for $\omega = 2, \omega = 5$ and $\omega = 10$ . . . . .	66
5.25	Optimal solution considering periodic time interval, with $N = 10, T_1^C = 5$ and $\omega_N = 2$ . The optimal time interval is $T_1^* = 4.8049 \text{ days}$ . . . . .	67
5.26	Optimal solutions considering the influence of the Immune System. . . . .	68
5.27	Relationship between the tumor volume and the immune system. . . . .	69

5.28 Relationship between the tumor volume and the angiogenesis process. . . . .	70
5.29 Optimal solutions considering the influence of the angiogenesis process. . . . .	70
5.30 Relationship between the tumor volume, the immune system and the angiogenesis process. . . . .	71
5.31 Optimal solutions considering the influence of the angiogenesis process and the immune system. . . . .	71
5.32 Optimal solutions considering exponential, pair of exponential, negative linear and negative quadratic penalization functions with constant weights. It is also considered the integral of $ V $ and the sum of squared amplitudes in the objective function. . . . .	74
5.33 Optimal solutions considering both exponential and par of exponential functions with linear weights. . . . .	76
5.34 Optimal solution considering restriction 5.30. . . . .	77
5.35 Optimal solution considering the objective function presented in equation (5.32). . . . .	78
5.36 Objective function values of the optimal solutions considering different $\Omega$ values. . . . .	79
5.37 Behavior of the tumor volume during treatment and its final value considering the optimal solutions for different $\Omega$ values. . . . .	80
5.38 Optimal solution considering the objective function presented in equation (5.34). . . . .	80
5.39 Normalization of time $t$ in $\tau \in [-1, 1]$ for each of the time intervals $t_0 \geq t \geq t_1$ , $t_1 \geq t \geq t_2$ , $t_2 \geq t \geq t_f$ , where $x$ correspond to the state variable and $u_q$ correspond to the Dirac impulse sequence considered [36]. . . . .	81
5.40 Optimal solution using a pseudo-spectral method, considering the objective function presented in equation (5.32). . . . .	83
6.1 Optimal solution considering the objective function 6.1. . . . .	86
6.2 Optimal solution considering the objective function 6.1, for $V(0) = 5 \text{ mm}^3$ . . . . .	87
6.3 Optimal solution considering the objective function 6.1, for $V(0) = 3 \text{ mm}^3$ . . . . .	87
6.4 Optimal solution considering the objective function 6.1, for $V(0) = 3 \text{ mm}^3$ , considering non proportional amplitudes weights to the initial volume. . . . .	88
6.5 Optimal solution considering the objective function 6.1, for $u_{max} = 0.5$ . . . . .	89
6.6 Optimal solution considering the objective function 6.1, for $u_{max} = 1.5$ . . . . .	90
6.7 Optimal solution considering the objective function 6.1, for $K = 10$ . . . . .	90
6.8 Tumor volume time evolution and tumor final value as functions of the error $V(0) - 1$ , where $V(0) \in [0.4, 15] \text{ mm}^3$ and the value 1 correspond to the initial volume used for the optimal solution considered. . . . .	91
6.9 Tumor volume time evolution and tumor final value as functions of the error $u_{max} - 1$ , where $u_{max} \in [0.5, 1.5] \text{ mm}^3$ and the value 1 correspond to the initial $u_{max}$ value used for the optimal solution considered. . . . .	92
6.10 Tumor volume time evolution and tumor final value as functions of the error $K - 5$ , where $K \in [1, 10] \text{ mm}^3$ and the value 5 correspond to the initial $K$ value used for the optimal solution considered. . . . .	93

6.11 Objective function considered in figure 5.34 evaluated for different quantization values . . .	93
6.12 Original solution and solution considering quantization of 1. . . . .	94
6.13 Tumor volume time evolution considering both Logistic and Gompertz growth models. . .	95
6.14 Optimal solutions considering constant time intervals $T_n = 3$ , $N = 10$ and $T = 30$ days. . .	95

# List of Tables

2.1	Pharmacokinetic parameters for Bevacizumab and Atezolizumab . . . . .	21
2.2	Pharmacodynamic parameters for Bevacizumab and Atezolizumab . . . . .	23
4.1	Parameters of each block used in simulations . . . . .	38
5.1	Advantages and Disadvantages of $V^2$ and $ V $ . . . . .	53
5.2	Amplitudes found to be optimal for each objective function presented in figure 5.12 and the corresponding tumor volume final value. . . . .	55
B.1	Important remarks of chapter 5. . . . .	B2



# Chapter 1

## Introduction

### 1.1 Motivation

Cancer is presently one of the main causes of death in human populations. For instance in Portugal, cardiovascular diseases and cancer are the largest contributors to mortality. Figure 1.1 represents the mortality in Portugal in 2014, where it was possible to conclude that women frequently die from cardiovascular diseases and men from cancer [25]. Cancer is a general name for a group of diseases that are characterized by a genetic disorder caused by DNA mutations, that spontaneously happen or are induced by environmental aggressions. These genetic modifications are inherited and pass to other cells in the cell division. The modified cells will be subject to Darwinian selection (survival of the fittest cell). Because of this selection, advantages are given to a unique cell (that will give origin to the tumor) so that every tumor is clonal, meaning that they are derived from the same cell [21].

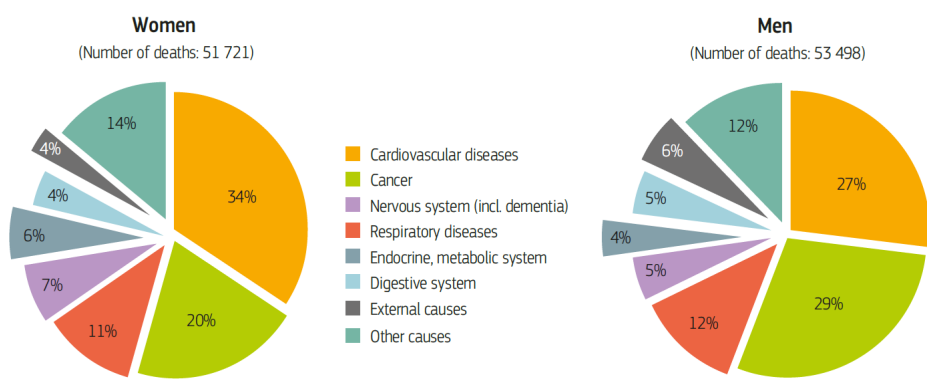


Figure 1.1: Mortality in Portugal, in 2014. Source: Eurostat Database (data refer to 2014).

The health care industry has experienced dramatic changes during the last 25 years. The scientific advances have allowed the implementation of more effective solutions to treat or even cure some diseases. However, mortality due to cancer is still one of the most important problems for this industry. This leads to an increasing investigation to find a solution in terms of prevention through regular exams, creation of more effective and less toxic drugs and more efficient treatments. The comprehension of the

cellular and molecular abnormalities in cancer cells is leading to a revolution in cancer treatment [10]. Some cancers are curable, while others are virtually fatal. The only hope to control cancer is to learn more about its pathology including its behavior on a dynamical system.

There are many types of cancer treatment such as surgery, radiation therapy, chemotherapy, immunotherapy, etc. The type of treatment that a patient receives depends on the type of cancer and on how advanced it is. Chemotherapy involves the administration of a drug into the human body. Those drugs are designed to kill cancer cells and, because of that, they cause side effects, being therefore very important not to administrate too much drug but also not too few concentration. There is an equilibrium point for the drug concentration that allows the drug to kill the cancer cells and, at the same time, reduce the side effects to the minimum possible. After a chemotherapy session, there will be fewer cancer cells in the human body. The next session has to be planned in order to kill a different number of cancer cells. So, each time a patient is subject to a chemotherapy session, the dynamical state of the tumor changes and it is necessary to exam again the tumor in order to administrate the exact amount of drug to optimize the process of killing cancer cells.

The above treatment plan is not easy to establish. Because of the limited resources and side effects of any kind of treatment, it is natural that the problem of how to plan cancer therapies to achieve the best case scenario arises [38]. Nowadays, methods to precisely plan a cancer treatment are being studied. Those methods involve modeling and control engineering methods in order to create a system that models the human organism and also the tumor dynamics. According to these methods, optimal control methods are widely used to minimize the tumor dynamics [38]. The complexity of the problem increases in the presence of constraints on the toxicity and on the human organism drug resistance. Although much of the published research on applying control methods to therapy design consider continuous control variables, in many cases the administration of the therapy is made in the form of a swallow action, for instance swallowing a pill, that is best modeled in mathematical terms as a Dirac impulse function. This type of actuation leads to the consideration of impulsive control methods. In this work, optimal impulsive methods are considered to approach the problem of planning cancer therapies.

## 1.2 Problem Formulation

The main goal of this dissertation is to design a controller to plan a therapy to minimize tumor size in cancer while reaching a compromise with also minimizing the therapy toxic effects. This therapy corresponds to the administration of drugs into the human body in a way that is modeled by a train of impulses. Drug administration depends on 3 different parameters:

- drug dosage of each administration,  $A_n$ ;
- time interval between administrations,  $T_n$ ;
- total number of drug administrations,  $N$ .

To plan a therapy, it is necessary to optimize the tumor dynamic response with respect to these 3 parameters. In this work, it is assumed that the drug is administrated in the form of pills. From a

mathematical point of view, this corresponds to a manipulated input represented by a sequence of Dirac - delta functions that cause a sudden change of drug concentration at times in which pills are taken by the patient.

Before designing the controller, it is necessary to understand:

- (P1) how the drug administrations is modeled;
- (P2) the relationship between the tumor dynamics and the drug administration. In other words, it is necessary to define the tumor dynamic response with respect to drug dosage  $A_i$ , the time interval between administrations  $T_i$ , and the total number of administrations  $N$ .

It is possible to subdivide the problem (P2) in three different problems, that can be studied separately:

(P2.1) how the drug is distributed in the human organism – the models that approach this problem are named Pharmacokinetic models – (P2.2) how the human organism reacts to a certain amount of drug in a certain organ or tissue, and the influence of other subsystems and phenomena (for instance, immune system, angiogenesis, etc...) – the models that approach this problem are called Pharmacodynamic models – and (P2.3) how the tumor develops in the presence of the drug.

These problems are connected. For instance, the study results of (P2.1) are the inputs of (P2.2), and the study results of (P2.2) are the inputs of (P2.3). In other words, it is only possible to study the drug effect on the human organism if the amount of drug that is inside of a certain organ is known. The input for the PK models is a signal that models the drug administration, with respect to the three parameters  $A_i$ ,  $T_i$  and  $N$ . Figure 1.2 represents the block diagram of the overall system, including the block that creates input signal for the PK mode, PD model and Tumor growth model.

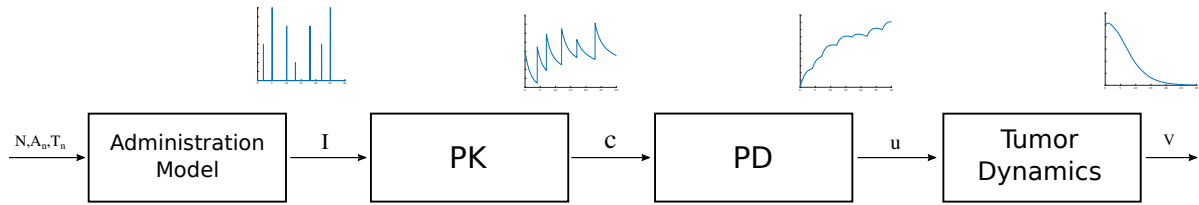


Figure 1.2: Block diagram of the overall system, including the Pharmacokinetic models, Pharmacodynamic models and tumor growth models

That being said, the third problem of this work concerns (P3) the design of the controller that minimizes tumor size with respect to the parameters of the signal that modulates the drug administration. This problem also includes the compromise between minimizing the tumor size and the therapy toxic effects. This compromise appears in the form of restrictions to the system. The toxicity sets a limit to the maximum drug concentration in the organism, while the organism drug resistance sets a limit to the minimum drug concentration in the system. Besides that, the impulse amplitudes generated by the controller cannot be negative, meaning that it does not make sense to administrate a negative amount of drug. So, the controller has as input the tumor size, and as output the optimal parameters that minimize tumor volume.

It is also possible to subdivide (P3) in three problems, assuming fixed and variable parameters. These problems are optimization problems where it is assumed that:

- (P3.1) the time interval between each administration,  $T_n$ , and the number of administrations,  $N$ , are fixed to a certain known value, and variable drug dosage  $A_n$ .
- (P3.2) the number of administrations  $N$  is fixed to a known value, the time interval between each administration  $T_n$  is fixed to an unknown value ( $T_n$  constant/periodic but unknown), and variable drug dosage  $A_n$ .
- (P3.3) each of the three parameters have unknowns and unfixed values. In other words, unknown values for drug dosage  $A_n$  and time interval  $T_n$  for each administration, and unknown number of administrations  $N$ .

Figure 1.3 represents the block diagram of the overall system with the controller.

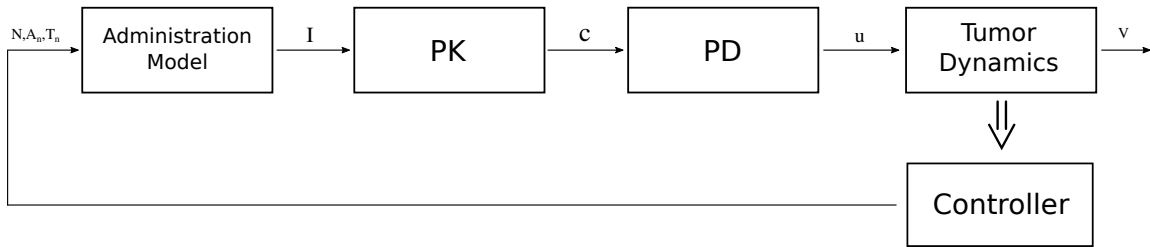


Figure 1.3: Block diagram for the overall system with the controller that minimizes the tumor dynamics

The above constraints change the controller computations. The three control variables may not be the same in their presence. For example, in a situation where there is a small amount of drug in the organism, the controller computes an administration with a large drug dosage. But, in order to not violate the maximum drug concentration constraint, this dose is not possible. So, maybe the time interval between this administration and the previous one needs to be smaller. This change might cause the addition of more administrations as well. This is why the constraints can change all the control variables.

Although the controller model described in figure 1.3 is the model considered in this work, it is possible to define another model, where the controller block can be divided into two blocks: a master and a slave controller. Figure 1.4 represents this new control architecture.

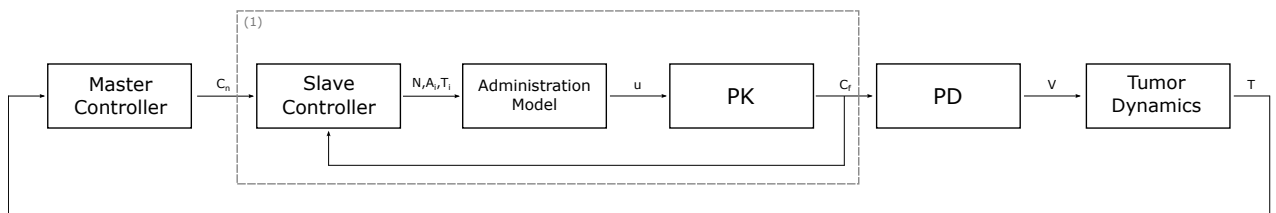


Figure 1.4: Block diagram for the overall system with a different control architecture

The master controller has as input the tumor size and computes the necessary drug concentration in

plasma,  $c_n$  for the tumor volume to be minimized. The slave controller uses the necessary concentration in plasma to compute the three parameters, with respect to the restrictions, such that the error between the final concentration  $c_f$  and the necessary concentration  $c_n$  is minimized. The controllers are designed such that the system inside the box (1) in figure 1.4 is faster than the rest of the system. In this way, while the master controller computes the necessary concentration, the slave controller is continuously adjusting the parameters to minimize the error  $c_f - c_n$ . From another perspective, this new controller model can be seen as a system that can be split in two parts: one that solves an optimal control problem with only one variable - tumor dynamics with respect to the concentration in plasma - and another part that solves the optimal impulsive control problem with the three administration parameters – corresponding to the blocks inside the box (1) in figure.

These three problems define the work to be done, having in mind that the controllers are to be designed in an optimal control framework, and such as to deal with impulsive manipulates variable signals. It is possible to add a fourth problem: assuming two or more drug to administrate, instead of having just one. This last problem yields a closer approach of the therapies that are done nowadays.

### 1.3 State of the art

The importance of cancer prevention, detection, treatment and management led to an increasing interest in learning and studying more about cancer development. Mathematical modeling had a significant importance in this domain since they suggest that cancer treatment can be a formal optimization problem. Tumor size in cancer, toxicity and drug resistance are the most important factors in planning a chemotherapy treatment and this is why most of the studies about chemotherapy treatment optimization explore various possible ways of modeling the interactions between these factors [37].

Depending on the type of tumor, different treatments can be used. If it is located on one single area, surgery and radiation therapy are the most common therapies used. If the tumor is transmitted to other parts of the body, the chemotherapy is more suited. The disadvantage of chemotherapy is that it destroys normal cells, besides the cancer cells, leading to toxicity issues. Because there is a tradeoff between killing the tumor and minimizing toxicity, there is an increasing interest in optimizing chemotherapy. So far, clinical trials have been used to plan chemotherapy efficiently. Due to the high costs and duration of trials, mathematical modeling is now one of the most used tools to optimize chemotherapy.

The idea of applying optimal control to various diseases began in mid-1970 [37]. Since then, many publications were made. For instance in 1975 [42], in 1984 [43] and in 1990 [44]. In [37], a review of optimization methods is made with many different references.

In order to minimize tumor size in cancer, the relationship between tumor size and the drug administered needs to be modeled. Here is where Pharmacokinetic (PK) and Pharmacodynamical (PD) models enter. PK describes the drug concentration-time courses in body. In other words, it tells us what the body does to the drug in terms of absorption, distribution, reaction and excretion of the drug. PD describes the observed effect resulting from a certain drug concentration [23]. Since 1937, PK/PD relationships have been studied and they allowed the prediction of temporal patterns of drug administration [27][23]. With

these relationships, science is able to test drug treatments before applying the treatment to the patient. There are many different models used in PK and PD. The most commonly used models to represent the PK behavior are Physiologically Based Pharmacokinetic Models (PBPM). Actually, the first PK model described in literature is a PBPM model [27]. In PBPM, the model equations follow the principles of mass transport, fluid dynamics, and biochemistry in order to predict the drug fate in the body [19]. Compartmental models are the most PBPM models used, where each compartment corresponds to groups of organs or/and tissues where drug flow and effect is similar. Depending on how the compartments are connected, there are different types of compartmental models: mammillary model, catenary model, cyclic model, and many others. About the PD models, there are also different models that represent the effect that a certain amount of drug has on the body: fixed effect model, linear model, log-linear model,  $E_{max}$ -model, sigmoid  $E_{max}$ -model and the Hill equation [19]. The most common model used is the Hill equation, which introduces a saturation effect in the concentration behavior [35].

Besides drug distribution and effect in the body, cancer was also a target of mathematical modeling and it has been an object of study for more than 60 years [3]. The interest of studying cancer and the development of cancer treatments is increasing, since treatments have significant potential to enhance quality of life and increase life-expectancies, which may, in turn, leading to considerable economic and social benefits [1]. There are several different tumor growth models. Most of them came from fitting experimental data. The most used models are: exponential-linear model, Logistic model, Gompertz model, Dynamic carrying capacity model, Mendelsohn model and von Bertalanffy model [3] [28]. Besides the study of tumor growth models and laws, subsystems that affect its growth have been also object of study, like the Immune System and Angiogenesis. The Immune system is the defense system of the human organism and its study became very important since it can fight cancer. In some types of cancer, is possible to use the immune system in a form of cancer treatment called Immunotherapy. Immunotherapy is not as widely used as, for instance, surgery or chemotherapy. However it causes fewer side effects than other treatments and it can help other cancer treatments work better, has shown in [28]. The Angiogenesis process corresponds to the growth of new capillaries from existing blood vessels. This process is very important not only during fetal development but also in tissue repair after surgery. However, the existence of new blood vessels can contribute to the proliferation of cancer and other diseases [47]. New studies reported that tumors can grow along existing vessels without evoking new vessel growth. The new vessels created by the angiogenesis process supply tumors with oxygen and nutrients, allowing them to grow [33]. This led to the investigation of drugs that can mediate angiogenesis, leading to anti-angiogenesis processes. Adding the knowledge about pathological processes, it is possible to diagnose and treat some of those diseases. For instance, in [45] is shown that immunotherapy, when applied alone, cannot eradicate the tumor while its combination with anti-angiogenesis process can eradicate.

The concepts previously stated in this section can be combined in order to create a mathematical model that translates the relationship between a drug administration and the tumor evolution in time. These types of models have been widely used in order to study different drugs and treatments like immunotherapy, chemotherapy and many others [45]. Thanks to models like these, it is possible to deal with complex physical and physiological relationships with an engineering point of view, where already

studied and investigated theory can be used.

In an Engineering Control point of view, the goal of killing the tumor corresponds to taking a variable to zero through the design of a specific controller. The choice of what type of controller should be designed depends on the problem formulation. Many different techniques can be used, for instance, adaptive control, predictive control, optimal control, etc. It is also important to have in mind that the controller design must adapt to a real scenario. For instance, it does not make sense to administer a huge amount of drug to kill the tumor, since it will also kill other healthy cells.

As previously stated, the goal in this work is to optimize a therapy in order to minimize tumor in size, keeping in mind toxicity and drug resistance issues. Because the goal of this work is to optimize the drug administration, optimal control techniques are more suitable for the design of the controller.

Optimal Control (OC) techniques are a set of mathematical methods developed to find optimal ways of controlling a certain dynamical system [40]. First, the problem needs to be formulated into an optimization problem which will be then minimized/maximized. The problem formulation must be such that its minimum/maximum corresponds to what is actually wanted. Optimal Control theory is an extension of the calculus of variations that was created after the invention of calculus by Newton and Leibniz. The first problem considered by the calculus of variation was the Brachistrone problem, where the goal was to connect two points such that a bead sliding along the curve (that connects the two points) would move from one point to another in the shortest time, under the influence of gravity [40]. Afterwards, the addition of control variables to the state equations led to the creation of optimal control theory. OC theory has many different applications: food technology, environmental engineering, noise reduction, economic systems and many others [4] [8]. In most of them the control variables are assumed to vary continuously in time. However in many situations, instantaneous changes can occur leading to a different problem and, consequently, to a different type of control theory named Optimal Impulse Control (OIC) (or Optimal Impulsive Control). OIC is being investigated for many years and it can be applied to different areas: finance, economics, medicine and many others.

## 1.4 Contributions

This dissertation contribution can be divided in two parts. First, a global model that translates the relationship between tumor evolution in time and a sequence of drug administrations as treatment is studied, including the study of properties and particularities of the models used. Secondly, Optimal Impulse Control (OIC) techniques are used to design a controller to plan the therapy. In addition, different control concepts are also applied and discussed, for instance, Receding Horizon Control, Minimum Attention Control and Pseudo-spectral approach.

## 1.5 Report Outline

This dissertation can be divided in two main parts: the first part correspond to the study and definition of the global mathematical model used in this work (corresponding to chapters 2, 3 and 4); the second part

correspond to the controller design, where different methods and concepts are studied (corresponding to chapters 5 and 6). In the first chapter (chapter 1) an introduction to the work of this report has been done including an explanation of the motivation and the main goals for this work. Thereafter, this work is divided in the following way:

- In Chapter 2, a review of the Pharmacokinetics and Pharmacodynamics is made, including a discussion about the mathematical definition of the PK and PD models.
- In Chapter 3, a review of Tumor growth models, Immune Systems and Angiogenesis is made, including a mathematical discussion about attainability.
- In Chapter 4, the mathematical model that relates the tumor volume with the input parameters, used in this work is described.
- In Chapter 5, a review of Optimal Control and Impulsive Control is made, including the explanation of the approaches used to address the problem of this work.
- In Chapter 6, a discussion is made and results are demonstrated.
- In Chapter 7, the report review and the conclusions are described.

# **Chapter 2**

## **Pharmacodynamical Model**

### **2.1 Pharmacokinetics**

Pharmacokinetics (PK) studies the fate of a drug in the body. In a qualitative way, it can be defined as what the body does to the drug. In other words, it represents the steps that the drug takes since the administration until the excretion, called ADME process. These steps are [7]:

- Absorption: this is the phase that goes from the way that the administration is made until the drug reaches the blood flow.
- Distribution: in this phase, the drug will be distributed by the blood flow to every part of the organism, possibly reaching the part where it will act.
- Reaction (metabolism): this phase represents how the organism reacts to the drug. Only part of the drug concentration will reach the blood flow. This fraction of administrated dosage of unchanged drug that reaches the blood circulation is called Bioavailability. Depending on this parameter, the organism will react differently to the drug.
- Excretion: in this phase, the drug is transformed in a better compound for excretion. The liver and kidneys are the most important organs for eliminating the drug.

The drug concentration variation depends on a variety of factors that are related to the way the organism reacts to the drug and to the substance properties, as well as the drug administration method which can be one of the following: Intravenous (IV), Constant Infusion Therapy (CIT) or Oral Administration (PO) [45]. In this work it is considered an PO therapy for exploring the PK behavior.

Although the availability of the drug is a function of the amount of drug being administered, it also depends on the extent and rate of its absorption, distribution, metabolism and excretion (ADME). However, there are some restrictions on the amount of drug. For instance, there is a risk of toxicity in the case of big amounts of drug. The fundamental hypothesis of pharmacokinetics is that a relationship between the pharmacological or toxic response to a drug and the concentration of the drug in the blood exists. However, for some drugs this relationships are neither clear nor simple [29]. Nonetheless, pharmacoki-

netics plays an important role in a dose-efficacy scheme, providing a quantitative relationship between dose and plasma concentration.

Mathematics is used for the description of drug absorption, distribution, reaction (metabolism) and excretion. Some pharmacokinetic parameters (e.g., bioavailability, volume of distribution and others) are defined by mathematic equations. They can be obtained by direct measurement or through calculation using experimental data, based on developed mathematical equations. But more complex mathematical manipulations have been used to describe pharmacokinetics.

### 2.1.1 Types of models

Figure 2.1 demonstrates two general approaches for pharmacokinetic modeling: empirical and mechanistic modeling.

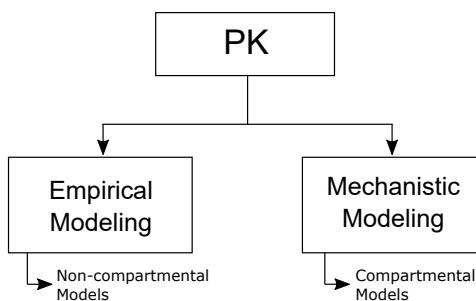


Figure 2.1: Classification of modeling approaches

Empirical modeling aims at evaluating experimental data by means of mathematical modeling. In pharmacokinetics, the experimental data refers to time series measurements of drug concentration in plasma or blood. Based on the estimated parameters, typical PK characteristics are determined to characterize the drug (e.g., area under the concentration time curve (AUC), elimination half-life ( $t_{1/2}$ ), total plasma clearance). In the other hand, mechanistic modeling uses the knowledge of biochemical, physiological and/or physical processes involved in drug disposition and drug response into pharmacokinetic model development to derive the model structure and the model parameters [32]. Currently, the most frequently mechanistic models used are physiology-based pharmacokinetic (PBPK) models. Those models aim at incorporating the most relevant ADME process involved in drug disposition and can be used to predict the time course of drug concentration in plasma or blood. PBPK models are usually multi-compartmental models, where each compartment corresponds to predefined organs or tissues, and each interconnection (between compartments) corresponds to blood or lymph flows. Because empirical modeling creates models by observations and experiments, it includes non-compartmental models, that are the opposite of compartmental models.

### 2.1.2 Compartmental models

Compartmental models are based on dividing the organism into spaces with identical dynamic (typically divided into one, two or three spaces/compartments). Figure 2.2 represents the most general used compartment models. In the catenary model (fig. 2.2a), the compartments are arranged in a chain, with

each cell connecting only to its neighbors, while in the mammillary model, there is a central compartment with peripheral compartments connecting only to it. There are other compartmental models. For instance, cyclic model (like the catenary model but the first and last cell are connected), closed model, open model, etc.

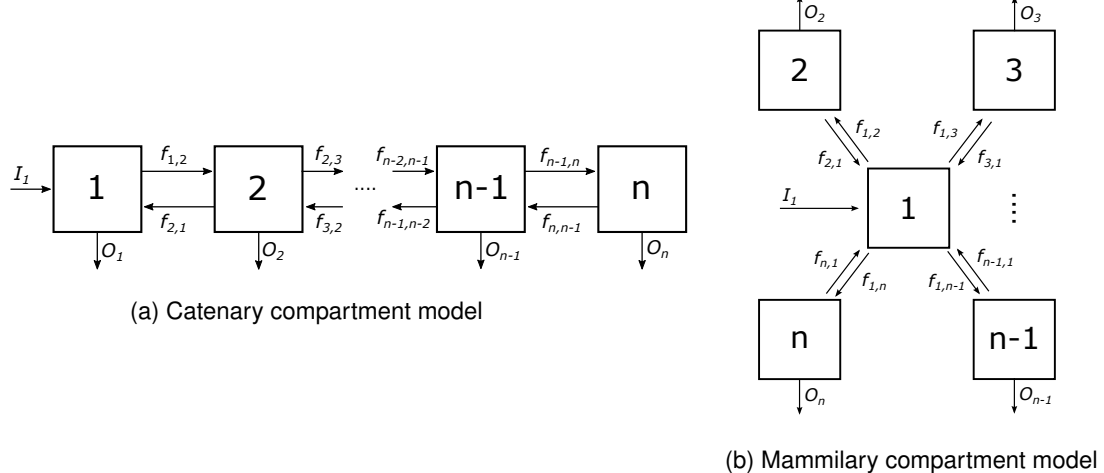


Figure 2.2: General compartment model architectures

Compartmental models have two important characteristics: mass conservation and positivity. In other words, the compartmental models are governed by a law of mass conservation (that states that for any system closed to all transfers of matter and energy, the mass of the system must remain constant over time, as system mass cannot change, add or remove quantity) and its state variables are constrained to remain non-negative along time. Using the mass conservation law, a system of differential equations for concentration or quantity of substance on each compartment can be written. Each compartment contains a variable quantity (or drug quantity)  $c_i(t)$  of some drug. Grouping all the quantities in one vector, it is possible to write  $c(t) = (c_1(t), c_2(t), \dots, c_n(t))^T$  called the state vector. The connections between compartment  $i$  and  $j$  are represented by a function  $f_{i,j}(c(t))$ , and the input (injected from the outside to some compartments) and output (expelled from some compartments to the outside) are expressed by  $I_i(t)$  and  $O_i(c(t))$  [2]. So, the quantity variation in a compartment  $i$  can be expressed by the sum of all the inputs from others compartments or from the outside, minus the sum of all the outputs to other compartments or to the outside, assuming that, initially, the concentration inside the compartments is zero. In other words, in a general case where is assumed that all the compartments have non-zero connections between them and that all compartments have input and output functions, the variation of the state vector  $\dot{c}(t)$  can be written by

$$\dot{c}_i = \sum_{j \neq i} f_{ji}(c) - \sum_{j \neq i} f_{ij}(c) - O_i(c) + I_i, \quad i = 1, \dots, n. \quad (2.1)$$

The model defined in equation (2.1) makes sense only if the quantities in all the compartments remain non-negative along time. Actually the flow ( $f_{i,j}(c(t))$ ), inflow ( $I_i(t)$ ) and outflow ( $O_i(c)$ ) functions are defined to be non-negative for all time [2]. Making an analogy to a real case, it does not make

sense to administrate a negative amount of drug to a patient, as well as expelling to the outside and transferring to other organs a negative amount of drug. Furthermore, it is not possible to have positive flows from an empty compartment. These last statement implies that if  $c_i = 0$ , then  $f_{i,j}(c) = 0$  and  $O_i(c) = 0$ . Under this condition, it is possible to say that

$$f_{i,j}(c) = r_{i,j}(c)c_i, \quad O_i(c) = q_i(c)c_i, \quad (2.2)$$

where  $r_{i,j}(c)$  and  $q_i(c)$  are defined to be continuous and non-negative for all values of  $c$  [2]. Rewriting equation(2.1) the following is obtained

$$\dot{c}_i = \sum_{j \neq i} r_{j,i}(c)c_j - \sum_{j \neq i} r_{i,j}(c)c_i - q_i(c)c_i + I_i, \quad i = 1, \dots, n. \quad (2.3)$$

Models of this form are used to represent industrial processes (chemical reactors [18], griding circuits [16]), queuing systems [13], and many others, for instance lipoprotein metabolism and potassium ion transfer models [46].

### 2.1.3 Positive Systems

Compartmental models have many interesting properties which are widely documented in the literature. As previously stated, compartmental models are positive systems. It can be proved that if  $c$  is positive and the initial conditions are non-negative for all compartments, then equation (2.3) remains positive (higher or equal to zero) for all time. The other property, previously stated, is that the compartment system is mass conservative. In the special case of a system without inflows ( $I_i = 0, i = 1, \dots, n$ ) and outflows ( $O_i(c) = 0, i = 1, \dots, n$ ), it is easy to verify that the variation of the total mass contained in the system  $dM(c)/dt = 0$  (where  $M(c) = \sum_{i=1}^N c_i$ ), which shows that the total mass is conserved. Another interesting characteristic is that, writing equation (2.3) in matrix form as  $\dot{c} = A(c)c + b$ , matrix  $A(c)$  (called compartmental matrix) follows three properties:

1.  $A(c)$  is a Metzler matrix, meaning that it is a matrix with non-negative off-diagonal entries:  $a_{ij}(c) = r_{ji}(c) \geq 0$ ;
2. The diagonal entries of  $A(c)$  are non-positive:  $a_{ii} = -q_i(c) - \sum_{j \neq i} r_{ij}(c) \leq 0$ ;
3. The matrix  $A(c)$  is diagonally dominant:  $|a_{ii}|(c) \geq \sum_{j \neq i} r_{ij}(c)$ .

An important aspect that Metzler matrices give to a state space model is stability, in addition to the fact that the state variables remain positive for all time. This characteristic can be verified by the dynamic matrix eigen values analysis. Assuming the state space model previously stated  $\dot{c} = A(c)c + b$ , where  $A(c)$  is a Metzler matrix, the eigen values  $p_i, i = 1, \dots, O$  (where  $O$  is the system order) are computed using the following, where is assumed a second order system ( $O = 2$ )

$$\det(pI - A) = 0 \Rightarrow p_{1,2} = \frac{(a_{11} + a_{22}) \pm \sqrt{(a_{11} + a_{22})^2 - 4(a_{11}a_{22} - a_{12}a_{21})}}{2}. \quad (2.4)$$

The eigenvalues real part is negative, since the diagonal entries of matrix  $A(c)$  are negative. This means that the system is asymptotically stable for all matrix values that follow the three properties above stated [9]. Using the conditions in (2.2), the continuous time system state  $c(t)$  remains non-negative, for non-negative initial conditions.

For a discrete time system  $x(k+1) = Ax(k) + b$  where  $k$  is the discrete time variable, the positivity conditions are different. For the system state to remain non-negative in discrete time systems, the matrix  $A$  must have all entries non-negative. In [22] a discussion about positive discrete systems is made, including stability analysis. It is showed that a positive matrix has a dominant positive eigenvalue and if all the eigenvalues are strictly inside the unit circle, then the system is asymptotically stable and there is a non-negative equilibrium point [22]. The dominant eigenvalue comes from the result of the Frobenius-Perron theorem that says: if  $A$  is a Metzler matrix, then there exists an eigenvalue  $\lambda_0 > 0$  and a non-negative eigenvector  $x_0 > 0$  such that  $Ax_0 = \lambda_0 x_0$  and, if there is other  $\lambda \neq \lambda_0$  of  $A$ , then  $|\lambda| < \lambda_0$  [22]. The eigenvalue  $\lambda_0$  is the dominant eigenvalue and it is called the Frobenius eigenvalue.

## 2.1.4 Controllability and Observability

There are two other important tools to be mentioned: controllability and observability. Controllability is related to the existence (or not) of an input signal that can change the system state to a different state, in finite time [34]. In a more precise way, a system  $\dot{x} = Ax + bu$  is controllable if, given an initial condition  $x(0) = x_0$  and a state  $x_f$ , exists a time instant  $t_f$  and an input signal  $u(t)$  such that  $x(t_f) = x_f$ . For continuous time systems, this definition is equivalent to imposing that from any state the origin is reached in a finite instant  $t_f$ , through a convenient choice of the input signal  $u(t)$  [34]. In the other hand, observability is related to the possibility of knowing the system state  $x(t)$  only by observing the input  $u(t)$  and output  $y(t)$  of the system [34]. This definition can be put in other words: a system  $\dot{x} = Ax + bu$ ,  $y(t) = Cx$  is observable if exists a time instant  $0 < t_0 < +\infty$  such that  $y(t)$ , for  $0 < t < t_0$ , is enough to determine the initial condition of the system  $x(0) = x_0$ .

The conditions for a system to be controllable is related to the matrix  $A$  and the vector  $b$ : using the notation in [34], if the rank of the controllability matrix  $\Gamma_c = [b|Ab|A^2b|\dots|A^{n-1}b]$  is equal to the dimension of the system state  $n = \dim(x(t))$ , then the system is controllable [34]. In the other hand, the conditions for a system to be observable are: if the rank of the observability matrix  $\Gamma_o = [C|CA|CA^2|\dots|CA^{n-1}]^T$  is equal to the dimension of the system state  $n = \dim(x(t))$ , then the system is observable [34]. These tools are important, in the control systems point of view. For instance, there are controllers that need the system state for computations but in real scenarios, the state may not be reached. So, if the system is observable then, by looking to the input and output, it is possible to estimate the state, using observers. Furthermore, if a system needs to be controlled, then it needs to be controllable.

### 2.1.5 Example: A 2 compartment model

Let us now apply equation (2.3) to, for example, a catenary model with 2 compartments, as figure 2.3 suggests.

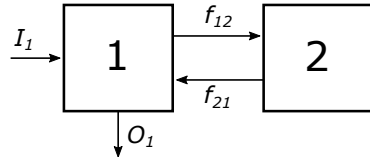


Figure 2.3: Catenary model with 2 compartments

Using the conditions stated in (2.2), the variation of quantity  $\dot{c}$  is given by

$$\begin{bmatrix} \dot{c}_1 \\ \dot{c}_2 \end{bmatrix} = \begin{bmatrix} -r_{12}(c) - q_1(c) & r_{21}(c) \\ r_{12}(c) & -r_{21}(c) \end{bmatrix} \begin{bmatrix} c_1 \\ c_2 \end{bmatrix} + \begin{bmatrix} I_1 \\ 0 \end{bmatrix}. \quad (2.5)$$

For simplicity, this is the compartmental model considered in this work, used for simulation purpose.

Mechanistic modeling can be used to predict drug concentration and drug effect prior to *in vivo* experiments. As soon as the experimental data measurements become available, the comparison of the data to the model predictions can be used to assess the reliability of the model assumptions [32]. The mechanistic modeling independency to experimental data can make it preferable. On the other hand, the main drawback of empirical pharmacokinetic modeling is its need for experimental data that might not be accessible in certain scenarios. However, none of the approaches takes advantage of the other approach in a general situation. In drug discovery and preclinical development, mechanistic modeling is frequently used to optimize the selection of drug candidates based on experimental data that are likely to have the desired *in vivo* pharmacokinetic properties, and to determine the first dose in man based on preclinical data. After entry into clinical development, there is a shift from mechanistic to empirical modeling [32]. Despite of underrepresentation of mechanistic PBPK modeling in the analysis of clinical data, an approach that establishes the link between the mechanistic PBPK models and the empirical models is highly desirable to bridge the gap between preclinical and clinical model development.

In this work, a Catenary model with 2 compartments is used as target model to study the PK behavior. As previously stated, the compartment model input signal  $I_1$  (fig. 2.3) is the Dirac impulse sequence. In the next sections, a discussion about Dirac impulse, Dirac impulse sequence and its mathematical representation is going to be performed.

### 2.1.6 Dirac Impulse Sequence

A Dirac impulse ( $\delta$ -function) is a function that was introduced by the theoretical physicist Paul Dirac (1902-1984) for modelling the density of an idealized point mass. In 1930, Paul Dirac investigated the following function

$$\delta(x) = \begin{cases} +\infty, & \text{for } x = 0 \\ 0, & \text{for } x \neq 0 \end{cases}, \quad (2.6)$$

imposing that

$$\int_{-\infty}^{\infty} \delta(x) dx = 1. \quad (2.7)$$

But this property is not compatible with the definition in eq.(2.6), because, in fact, from eq.(2.6) it follows that the integral must be equal to zero [14]. To circumvent this problem, the creation of a generic function  $\delta_\epsilon(x)$  defined by

$$\delta(x) = \lim_{\epsilon \rightarrow 0^+} \delta_\epsilon(x) = \begin{cases} +\infty, & \text{for } x = 0 \\ 0, & \text{for } x \neq 0 \end{cases}, \quad (2.8)$$

was suggested, for which

$$\int_{-\infty}^{\infty} \delta_\epsilon(x) dx = 1, \quad (2.9)$$

$$\int_{-\infty}^{\infty} \delta(x) dx = \lim_{\epsilon \rightarrow 0^+} \int_{-\infty}^{\infty} \delta_\epsilon(x) dx. \quad (2.10)$$

Thus, the Dirac delta function  $\delta(x)$  is a “generalized function” that satisfies eq.(2.6) and (2.7) and the integral in eq.(2.7) must be interpreted according to eq.(2.10), where  $\delta_\epsilon(x)$  satisfies eq.(2.8) and (2.9). The first formulation of generalized functions was developed by Laurent Schwartz in [39]. Yet another alternative theory of Schwartz was developed by the mathematician Sebastião e Silva, using an axiomatic approach [14].

There are many functions that satisfy eq.(2.8) and (2.9). For instance, there is the following Gaussian

$$\delta_\epsilon(x) = \frac{1}{\epsilon\sqrt{\pi}} e^{-x^2/\epsilon^2}. \quad (2.11)$$

Another example is the function

$$\delta_\epsilon(x) = \begin{cases} \frac{1}{\epsilon}, & \text{for } |x| \leq \frac{\epsilon}{2} \\ 0, & \text{for } x > \frac{\epsilon}{2} \end{cases}. \quad (2.12)$$

This means that the Dirac impulse can be represented by a rectangle with width  $\epsilon$  and height  $A = 1/\epsilon$ .

Figure 2.4 represents the rectangle, with  $\epsilon = 1$ .

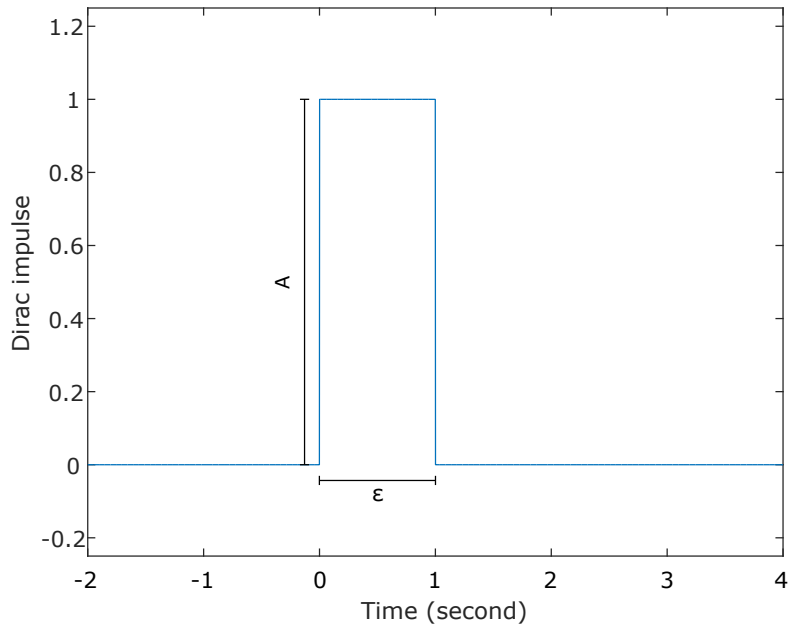


Figure 2.4: Dirac impulse approximation represented by a rectangle  $\epsilon = 1$

There is another way of mathematically representing the Dirac impulse by a rectangle. Assume that it is possible to define the following function

$$u(x) = \begin{cases} 1, & \text{for } x > 0 \\ 0, & \text{for } x < 0 \end{cases}. \quad (2.13)$$

This signal is called unit step. Note that it is discontinuous at  $x = 0$ . So, the Dirac impulse can be defined as

$$\delta(x) = \frac{du(x)}{dx}. \quad (2.14)$$

Because of the step discontinuity, it is possible to define a function  $u_\epsilon(x)$  that does not switch so suddenly [26]. This function is represented in figure 2.5 .

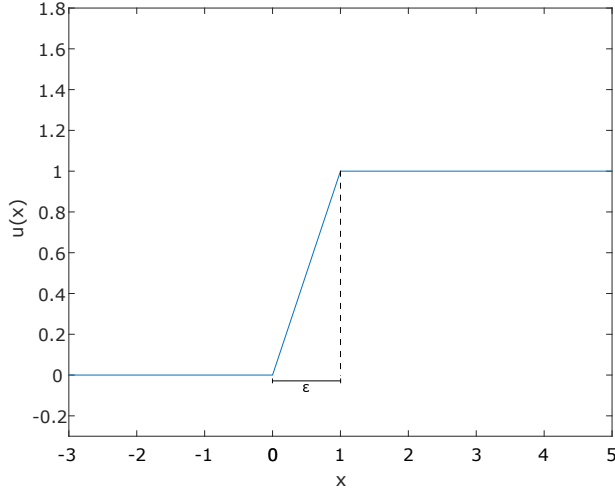


Figure 2.5: Unit step with  $\epsilon = 2$

Using equation (2.14), the Dirac impulse can be also defined by the rectangle (see fig. 2.4) with width  $\epsilon$  and height  $1/\epsilon$ .

Having now an approximated way of describing a Dirac impulse, the Dirac impulse sequence can be written as the sum of time shifted Dirac function represented by

$$u(t) = \sum_{n=0}^{N-1} \alpha_n \delta(t - nT_n), \quad (2.15)$$

where  $N$  is the total number of Dirac impulses,  $\alpha_n$  are the amplitudes for each impulse and  $T_n$  the time interval between each impulse.

The rectangle representation is an easy and intuitive way of describing a Dirac impulse. However, in order to represent properly an impulse, it is necessary to take the width  $\epsilon$  to zero, forcing an infinite height, which can be difficult for computations. In section 2.1.6.1 this representation is tested with a second order system and a different approach for making computations with Dirac impulses is presented.

### 2.1.6.1 Second Order System Response

A second-order linear system is a common description of many dynamic processes, and can be generally described by

$$\frac{d^2y}{dt^2} + 2\xi\omega_n \frac{dy}{dt} + \omega_n^2 y(t) = \omega_n^2 u(t), \quad (2.16)$$

where  $\xi$  and  $\omega_n$  are constant parameters.

Equations like (2.16) arise in many physical systems, including RLC circuits and mechanical systems (for instance, system with a spring and dash-pot attached to a movable mass and a fixed support). Computing the Laplace Transform of equation (2.16), the frequency response for the second order system is

$$H(s) = \frac{Y(s)}{U(s)} = \frac{\omega_n^2}{s^2 + 2\xi\omega_n s + \omega_n^2}. \quad (2.17)$$

The denominator of  $H(s)$  can be factored

$$H(s) = \frac{\omega_n^2}{(s - p_1)(s - p_2)}, \quad (2.18)$$

where

$$p_1 = -\xi\omega_n + \omega_n\sqrt{\xi^2 - 1}, \quad p_2 = -\xi\omega_n - \omega_n\sqrt{\xi^2 - 1}. \quad (2.19)$$

The parameter  $\xi$  is referred to as the damping ratio and  $\omega_n$  as the undamped natural frequency. For  $0 < \xi < 1$ ,  $p_1$  and  $p_2$  are complex and the second order system has an impulse response that has damped oscillatory behavior and, because of that, is referred to as being underdamped. For  $\xi > 1$ ,  $p_1$  and  $p_2$  are real negative and the impulse response is a decaying exponential and, in this case, the system is referred to be overdamped. For  $\xi = 1$ ,  $p_1 = p_2$  and the systems are referred to be critically damped [26]. Figure 2.6 represents the second order system response to an ideal Dirac impulse.

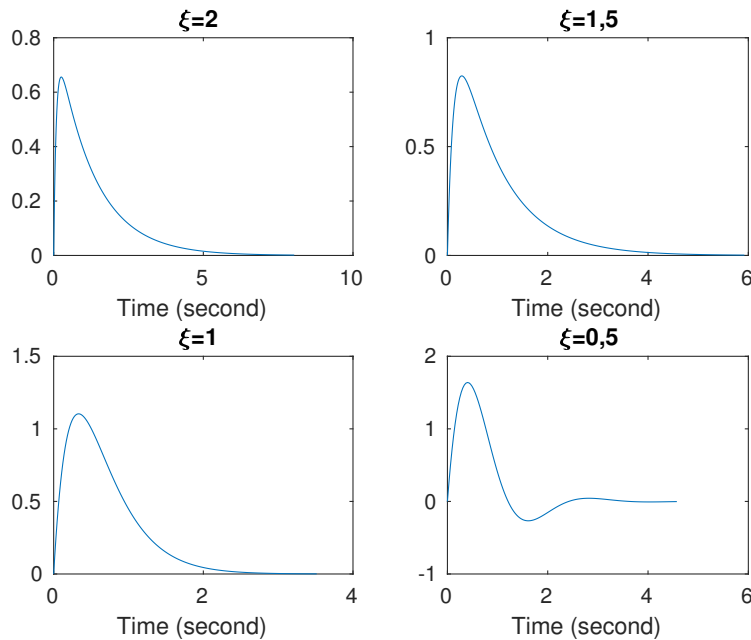


Figure 2.6: Second Order System response to a Dirac impulse with zero initial conditions

As it is possible to verify, when  $\xi$  decreases, the response takes less time to reach its final value. For  $\xi < 1$  the response becomes oscillatory, with oscillation frequency  $\omega_n$ .

Using the rectangle representation of the Dirac impulse, the second order system response is different depending on  $A = 1/\epsilon$ , as it is possible to see in figure 2.7.

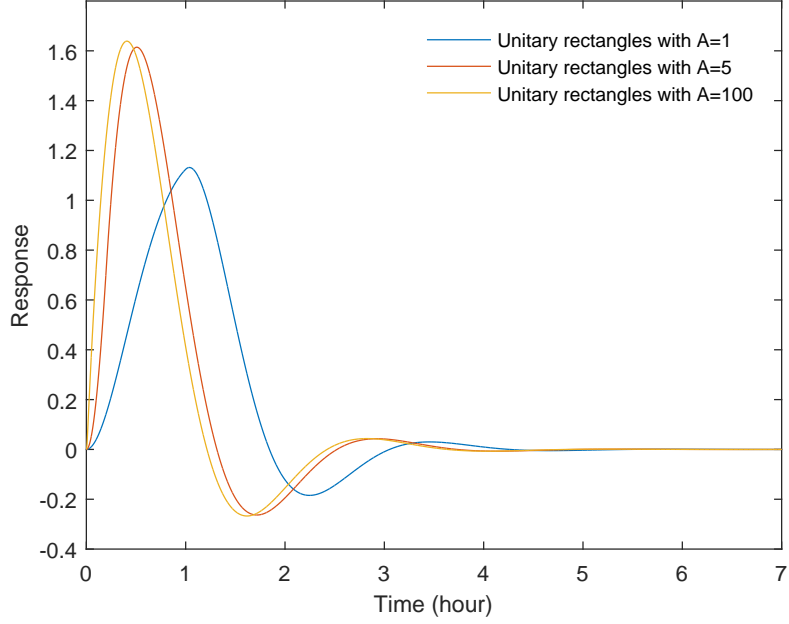


Figure 2.7: Second order system response to a rectangle impulse for different values of height  $A = 1/\epsilon$ ,  $\omega_n = 3 \text{ Hz}$

Because of the uncertainty of knowing what is the value that is sufficiently small for  $\epsilon$ , let us use math for finding another way of doing computations with Dirac impulses. Doing the inverse Laplace Transform of equation (2.17), the following is obtained

$$\ddot{y} + 2\xi\omega_n\dot{y} + \omega_n^2 y = \omega_n^2 u \Rightarrow \ddot{y} = -2\xi\omega_n\dot{y} - \omega_n^2 y + \omega_n^2 u. \quad (2.20)$$

Defining the state variables as

$$\begin{cases} x_1 = y \\ x_2 = \dot{y} \end{cases} \Rightarrow \begin{cases} \dot{x}_1 = x_2 \\ \dot{x}_2 = \ddot{y} = -2\xi\omega_n x_2 - \omega_n^2 x_1 + \omega_n^2 u \end{cases}, \quad (2.21)$$

equation (2.20) can be written in terms of  $\dot{x}_1$  and  $\dot{x}_2$

$$\begin{cases} \dot{x}_1 = x_2 \\ \dot{x}_2 = -2\xi\omega_n x_2 - \omega_n^2 x_1 + \omega_n^2 u \end{cases}. \quad (2.22)$$

Using (2.21) and (2.22), it is possible to represent the second order system in matricial form as

$$\dot{x} = Ax + bu, \quad y = Cx, \quad (2.23)$$

where

$$A = \begin{bmatrix} 0 & 1 \\ -\omega_n^2 & -2\xi\omega_n \end{bmatrix}, \quad b = \begin{bmatrix} 0 \\ \omega_n^2 \end{bmatrix}, \quad C = \begin{bmatrix} 1 & 0 \end{bmatrix}. \quad (2.24)$$

Equation (2.23) represents a model called state model. In a more general way, a state space system can be represented by  $\dot{x} = f(x) + g(x)u$ , with some initial condition  $x(0) = x_0$ . Solving the differential

equation, the following is obtained

$$x(t) = x_0 + \int_0^t f(x(\tau))d\tau + \int_0^t g(x(\tau))u(\tau)d\tau. \quad (2.25)$$

Considering a Dirac impulse as input signal  $u(t) = \alpha\delta(t)$ , and using the Dirac impulse definition in equation (2.7),  $x(t)$  can be written in the following form

$$x(t) = x_0 + \alpha g(x(0)) + \int_0^t f(x(\tau))d\tau \iff \begin{cases} \dot{x} = f(x) \\ x(0) = x_0 + \alpha g(x(0)) \end{cases}. \quad (2.26)$$

This means that, if the input signal of a state-space model is the Dirac impulse, having a model with an input signal and some initial condition is the same that having a model with no input signal and an initial condition that takes that into account.

Using the Dirac impulse sequence defined in (2.15) as input signal for the second order system, the simulation represented in figure 2.8 is obtained.

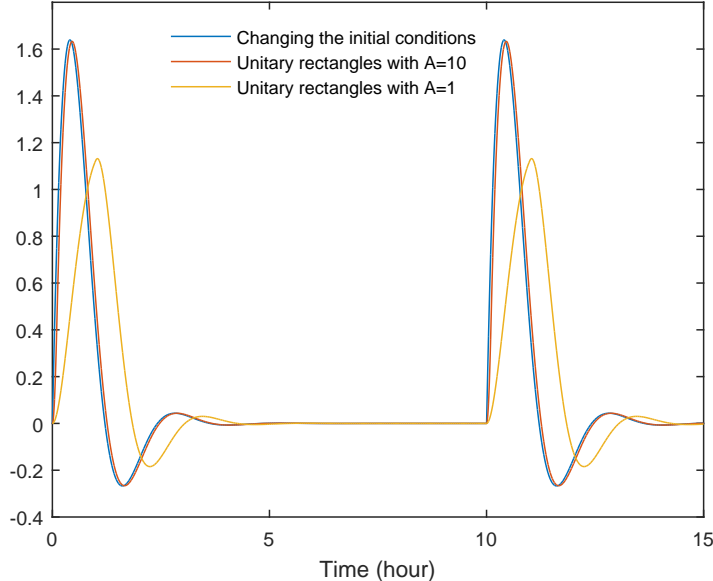


Figure 2.8: Second order system response to a sequence of Dirac Impulses with period  $T = 10$  hours,  $\xi = 0.5$  and  $\omega_n = 3$  Hz

Figure 2.8 shows that changing the initial conditions corresponds to the case where  $\epsilon$  goes to infinity but without the computation problems. This means that the initial conditions change method is preferable to the rectangle representation.

### 2.1.6.2 Pharmacokinetic Model Response

To represent the pharmacokinetics model, a Catenary model with 2 compartments represented in figure 2.3 is considered. Let the functions  $r_{ij}(c)$  and  $q_i(c)$  be some positive constants

$$r_{ij}(c) = K_{ij} \geq 0, \quad q_i(c) = K_{i0} \geq 0. \quad (2.27)$$

So, equation (2.5) can be expressed by

$$\begin{bmatrix} \dot{c}_1 \\ \dot{c}_2 \end{bmatrix} = \begin{bmatrix} -K_{12} - K_{10} & K_{21} \\ K_{12} & -K_{21} \end{bmatrix} \begin{bmatrix} c_1 \\ c_2 \end{bmatrix} + \begin{bmatrix} 1 \\ 0 \end{bmatrix} u, \quad (2.28)$$

where  $u = I_1$  is the input signal. In order to analyze the concentration variation instead of quantity variation, the equation (2.28) must be divided by the volume fo each compartment  $V_i$ . So, equation (2.28) can be written as

$$\begin{bmatrix} \dot{c}_1 \\ \dot{c}_2 \end{bmatrix} = \begin{bmatrix} \frac{1}{V_1}(-K_{12} - K_{10}) & \frac{1}{V_1}K_{21} \\ \frac{1}{V_2}K_{12} & -\frac{1}{V_2}K_{21} \end{bmatrix} \begin{bmatrix} c_1 \\ c_2 \end{bmatrix} + \begin{bmatrix} \frac{1}{V_1} \\ 0 \end{bmatrix} u, \quad (2.29)$$

where vector  $c = [c_1, c_2]^T$  is now the drug concentration.

The constants value depend on the administrated drug. Table 2.1 summarizes some estimated values presented in [45] for two drugs currently used in cancer chemotherapy, where the volume of both compartments are assumed to be equal. Usually drug doses are described in  $mg/kg$ . However, from equation (2.28) results a drug concentration in  $mg/kg/ml$ . In order to make a more straightforward analysis, the concentration outputs are multiplied by the respective volume, being  $c$  given also in  $mg/kg$ .

Table 2.1: Pharmacokinetic parameters for Bevacizumab and Atezolizumab

Parameter	Bevacizumab	Atezolizumab	Units
$K_{12}$	0.223	0.3	$day^{-1}$
$K_{21}$	0.215	0.2455	$day^{-1}$
$K_{10}$	0.0779	0.0643	$day^{-1}$
$V_1$	2660	3110	$ml$
$V_2$	2660	3110	$ml$

Considering the initial condition change method, it is possible to simulate the catenary compartment model. Figure 2.9 represents the variation of concentrations when the Dirac impulse sequence is applied as input signal. In this simulation, it is considered a periodic administration with period T=50 days.

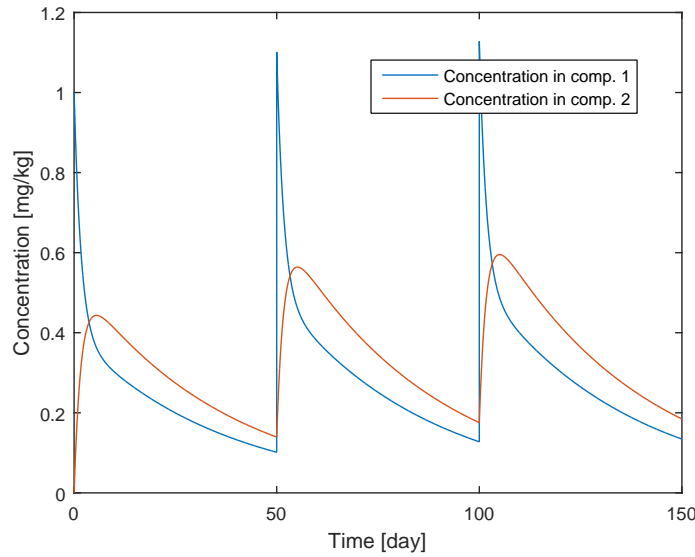


Figure 2.9: Variation of the concentrations

Because there is only an inflow into compartment 1, its concentration increases immediately due to the Dirac impulse (corresponds to the absorption phase). Through the flows between compartments, the concentration in compartment 2 also increases (corresponds to the distribution phase). Meanwhile, the concentration in compartment 1 decreases and a balance between concentrations in both compartments is reached (corresponding to the metabolism phase). Finally, because of the outflow in compartment 1, the concentration in both compartments decreases to zero, until the next drug administration (corresponding to the excretion phase).

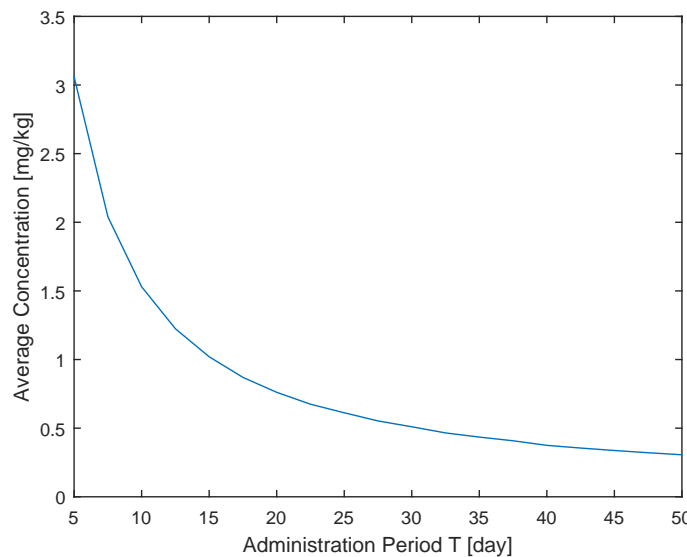


Figure 2.10: Average Concentration Variation depending on the Administration Period T

Depending on the period of the administration, the final value of the concentration in each compartment, before the administration, will be higher or lower. If there is no further administration, the

concentration will go to zero. Figure 2.10 represents the average concentration variation with respect to the administration period. As it is possible to see, when the administration period increases, the average concentration of drug in the organism will decrease. This is due to the constant excretion rate of the organism.

## 2.2 Pharmacodynamics

Pharmacodynamics (PD) aims at defining a relation between drug concentration and effect in the human organism. As for PK modeling, there are also two general approaches for PD modeling: classical modeling (*i.e.* empirical modeling) and mechanistic modeling [32]. In the first, the type of the model and the values of the model parameters are derived from experimental measurements. In mechanistic modeling, the structure of the model is defined by the understanding of biochemical and physical processes involved in drug response. In a general way, the qualitative description of PD models are important to establish appropriate band dosage for patients as well as for compare efficacy and safety of a drug with another. [15]

The simplest PK models describe the relationship between drug effect and drug concentration. These relationships have been widely represented by the Hill Equation introduced by Wagner in 1968 [35]

$$u(t) = u_{max} \frac{c^\alpha(t)}{c_{50}^\alpha + c^\alpha(t)}, \quad (2.30)$$

where  $c_{50}$  is the drug concentration value for which the half-maximal effect is reached and  $\alpha$  the Hill coefficient that describes the steepness of the resulting sigmoid curve (fig. 2.11b). The PD behavior depends on the current drug concentration, on the drug concentration variation but mainly on the  $c_{50}$  value. Table 2.2 shows some values for this parameter [45] for the two drugs previously considered.

Table 2.2: Pharmacodynamic parameters for Bevacizumab and Atezolizumab

Parameter	Bevacizumab	Atezolizumab	Units
$C_{50}$	72	40	$pM$
$C_{50}$	0.1074	0.0578	$\mu g/mL$
$C_{50}$	11.4274	7.1903	$mg/kg$

In figure 2.11 is represented the drug effect as a function of drug concentration.

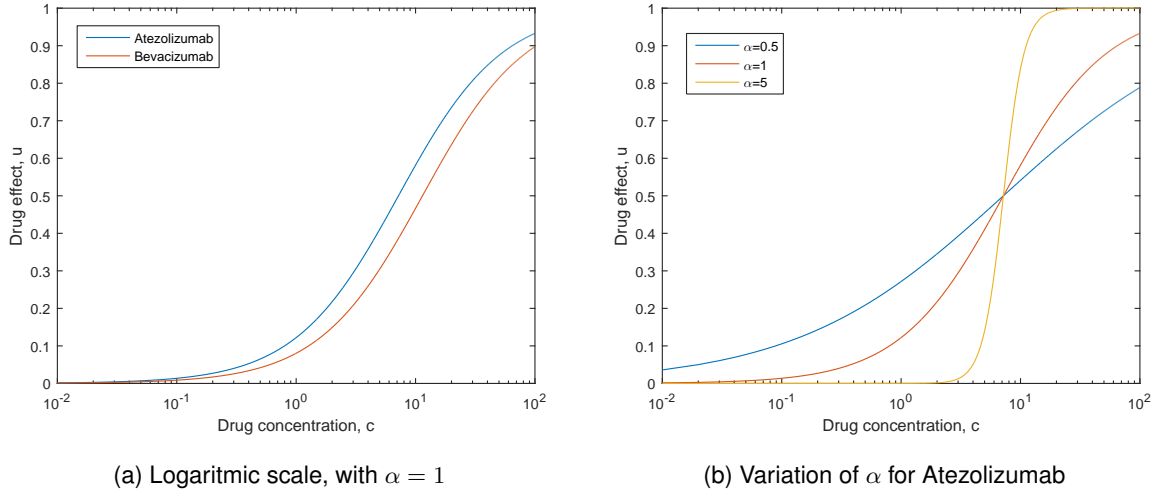


Figure 2.11: Drug effect as a function of drug concentration, with  $u_{max} = 1$

As it is possible to see, the Hill Equation introduces a saturation on the drug concentration variation. It means that for small concentrations, its effect is very small. And for high concentrations, its effect saturates, meaning that higher dosages administrations will not create a higher effect in the tumor. The saturation value is given by the parameter  $u_{max}$ . In other words, for drug concentration in the saturation area, when  $u_{max}$  increase, the effect that amount of drug has on the tumor also increases.

Once knowing the drug concentration approximate effect in the human organism, it is possible to introduce this information (signal  $u(t)$ ) in Tumor Growth Models. There are various mathematical models that try to describe the dynamics of cancer cells population. In fact, finding the right treatment to cure cancer is complex. It depends on many different aspects related to differences between patients, to several cancer growth phases and related to mutations types of cancer cells. Besides that, there are other subsystems that influence tumor dynamics: Immune System (IS), Vascularization, Angiogenesis, etc... In the following chapter a more detailed discussion regarding Tumor Growth Models and some subsystems is performed.

## 2.3 Important Remarks

In this section, the most important conclusions of this chapter are going to be made. About Compartmental Models  $\dot{c} = Ac + bI$ :

- Positive system;
- Mass conservative;
- Matrix  $A$  is a Metzler matrix  $\Rightarrow$  Stability.

About the Dirac impulse sequence:

- Sequence of shifted versions of the Dirac delta function;

- Best ways of input the sequence in a state space model is by reseting and changing initial conditions of the system.

About Pharmacodynamics (PD):

- the Hill equation is the most used PD model;
- Non-linear model;
- Introduces a saturation on the concentration.



# Chapter 3

## Tumor Growth Models

Despite internal complexity, tumor growth dynamics follow relatively simple laws that can be expressed as mathematical equations. Tumor growth dynamics have been the subject of biological study for more than 60 years [3]. The models used for the modelling of tumor growth have 2 general approaches: descriptive models (empirical models) and mechanistic models (explicative models) [28]. Empirical models try to describe experimental data. On the other hand, mechanistic models incorporate the understanding of biological and physical processes and factors as immune systems, therapy resistance, and others [28]. However, in general, tumor growth models are used to test growth hypotheses of theories by assessing their descriptive power against experimental data and to predict the course of tumor dynamics in order to determine the efficacy of a therapy in preclinical drug development [3]. Depending on the scale, approach or integration of spatial structure, there are different mathematical models. For focusing on scalar data of tumor volume, models based on differential equations are more suitable. The Gompertz and Logistic models are the most widely used models in numerous studies involving animal or human data [3]. They are inserted in the group of sigmoid shaped models. Also in this group there is the Bertalanffy models (also sigmoid shaped) and exponential models [28]. Independently of the model used, the descriptive variable is always the total tumor volume  $V$  as a function of time and it is assumed to be proportional to the total number of cancer cells.

### 3.1 Logistic Growth Model

The simplest model of population dynamics is the one with exponential growth

$$\frac{dV}{dt} = aV, \quad (3.1)$$

where  $a$  is the intrinsic growth rate related to proliferation kinetics. In other words,  $a$  represents growth rate per capita. This model suggests an unrestricted tumor growth. Meanwhile, in 1838 Verhulst considered that a stable population would have a saturation level. To achieve this, Verhulst augmented the exponential model suggested in (3.1) by a multiplicative factor  $1 - \frac{V}{K}$ , where  $K$  denotes the maximal

volume (carrying capacity) [38]. So, the Logistic model can be represented by the following

$$\begin{cases} \frac{dV}{dt} = aV(1 - \frac{V}{K}) \\ V(t = 0) = 1\text{mm}^3 \end{cases} . \quad (3.2)$$

In some cases, a generalization of the logistic equation is considered

$$\begin{cases} \frac{dV}{dt} = aV(1 - (\frac{V}{K})^\beta) \\ V(t = 0) = 1\text{mm}^3 \end{cases} , \quad (3.3)$$

called the generalized logistic model [3].

### 3.1.1 Solution of the Logistic equation

There are two different ways of solving the equation (3.2). Understanding that the logistic equation is a Bernoulli equation and use the separable differential equation method to solve the equation is one possible method. The other one is understanding that it is possible to write the Logistic equation in the form of a non-linear differential equation  $\frac{dy}{dx} + P(x)y = y^nQ(x)$  and then perform a change of variable. In appendix A the application of these two methods to the Logistic equation is made. Solving the equation, the following is obtained

$$V(t) = \frac{V_0 K}{V_0 + (K - V_0)e^{-a(t-t_0)}}. \quad (3.4)$$

For  $\beta \neq 1$

$$V(t) = \frac{V_0 K}{(V_0^\beta + (K^\beta - V_0^\beta)e^{-a\beta(t-t_0)})^{\frac{1}{\beta}}}, \quad (3.5)$$

where  $V_0$  denotes the volume at time  $t = 0$ . It is important to notice that  $\frac{dV}{dt}$  in equation (A.10) is convex, meaning that its second derivative is positive for  $\beta < 1$ , and concave, meaning that its second derivative is negative for  $\beta > 1$  [38]. In figure 3.1 the logistic model and the generalized logistic model for different values of  $\beta$  are represented. As it is possible to see, the logistic model has three key features:

- $\lim_{t \rightarrow \infty} V(t) = K$ , means that the cancer cells will ultimately reach its carrying capacity;
- The relative growth rate  $\frac{1}{V} \frac{dV}{dt}$  decreases linearly with increasing tumor volume;
- The volume at the inflection point (where the growth rate is maximum) is exactly half the carrying capacity  $\frac{K}{2}$ .

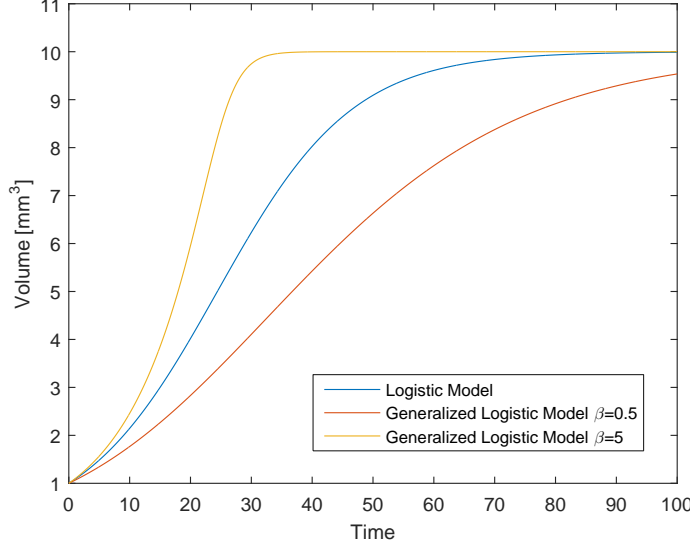


Figure 3.1: Logistic and Generalized Logistic Models, with  $K = 10$ ,  $a = 0.09$  and  $V_0 = 1\text{mm}^3$

In this work is considered that the output  $u(t)$  of the PD model is introduced by an additional term in the differential Logistic model equation

$$\frac{dV}{dt} = aV(t)\left(1 - \frac{V(t)}{K}\right) - \beta u(t)V(t) = (a - \beta u(t))V(t) - \frac{a}{K}V^2(t). \quad (3.6)$$

This term is multiplied by the tumor volume  $V(t)$  to force  $\frac{dV}{dt} = 0$  when  $V(t) = 0$ . This equation continues to be a Bernoulli equation but not a separable differential equation. To solve this equation, the non-linear differential equation method can be used. The steps are the almost the same as before (see appendix A) but the multiplicative function will be now  $e^{\int P(\tau)d\tau} = e^{\int(a-u(\tau))d\tau} = e^{at}e^{-\int u(\tau)d\tau}$ . After multiplying the equation by this function, it is necessary to integrate both sides. If the function  $u(t)$  is known, then it is possible to compute the multiplicative function.

For the specific case of this work, the expression of  $u(t)$  is actually the Hill equation from section 2.2 and the input of the Hill equation is the drug concentration  $c(t)$  from section 2.1. So, the total expression of  $u(t)$  is possible but not easy to compute analytically and, consecutively, neither the expression of  $V(t)$ . However, it is possible to reach some conclusions about equation 3.6 (see next section).

### 3.1.2 Tumor Volume Evolution

Let  $u(t) \leq u_{max}$  and  $V(0) > 0$ . Looking at the Logistic equation (3.6), when  $u$  increases, the time derivative of the volume  $\frac{dV}{dt}$  decreases. So that means that exists a minimum value for  $\frac{dV}{dt}$  when  $u = u_{max}$ . In other words

$$\frac{dV}{dt} \geq \left[ a \left( 1 - \frac{V}{K} \right) - \beta u_{max} \right] V. \quad (3.7)$$

Using this inequality it is possible to calculate the regions where the tumor volume evolves, for  $u = u_{max}$ . For instance, for  $\frac{dV}{dt} > 0$  the following is obtained

$$a \left( 1 - \frac{V}{K} \right) - \beta u_{max} > 0, \Rightarrow V < K - \frac{K\beta u_{max}}{a} \quad (3.8)$$

and for  $\frac{dV}{dt} < 0$

$$a \left( 1 - \frac{V}{K} \right) - \beta u_{max} < 0, \Rightarrow V > K - \frac{K\beta u_{max}}{a}. \quad (3.9)$$

So for  $V(0) > 0$ , between  $0 < V < K - \frac{K\beta u_{max}}{a}$  the volume increases because the derivative is positive, and between  $K - \frac{K\beta u_{max}}{a} < V < K$  the volume decreases because the derivative is negative, depending on the value of  $u_{max}$ . For  $V = K - \frac{K\beta u_{max}}{a}$  the derivative is zero, which means that the volume will be constant. For instance, if  $V(0) = K - \frac{K\beta u_{max}}{a}$ , the volume will not change for all  $t \geq 0$ . Figure 3.2 illustrates what is said here.

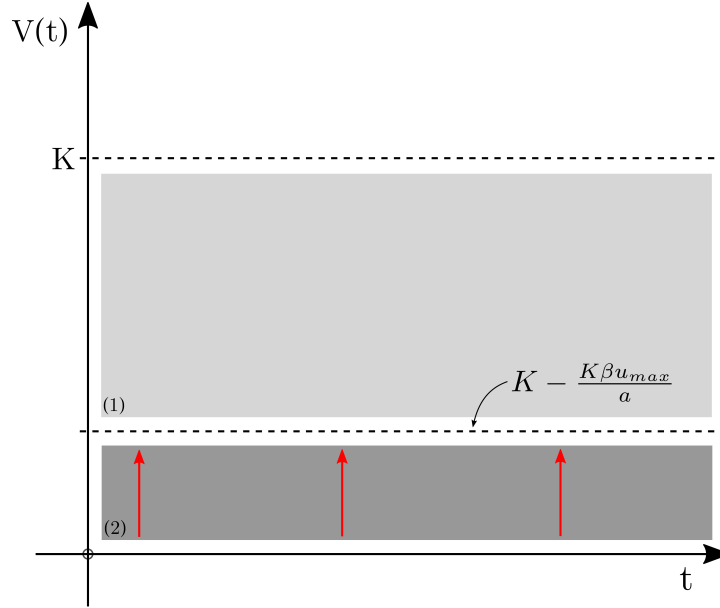


Figure 3.2: Gompertz Model, with  $\beta = 0.02$ ,  $a = 0.09$  and  $V_0 = 1mm^3$

The dark gray zone (2) correspond to the region  $0 < V < K - \frac{K\beta u_{max}}{a}$  and the gray zone (1) correspond to the region  $K - \frac{K\beta u_{max}}{a} < V < K$ . So, in the zone (2) the derivative of the volume is positive which means that, for a initial condition in that region, the volume will always increase, as previously stated. So, with this study, it is possible to conclude that for initial conditions  $V(0) \neq 0$ , the volume will never go to zero and will always converge to the equilibrium point  $V = K - \frac{K\beta u_{max}}{a}$ , where the derivative is zero.

Imagine now that  $V(0)$  is in the region (1) (light gray zone in figure 3.2) and  $K - \frac{K\beta u_{max}}{a} = 0$  by appropriate choice of  $u_{max}$ . Because in this region the volume derivative is negative, the tumor should go to zero, just like when  $K - \frac{K\beta u_{max}}{a} \neq 0$ . Actually this not happens and that can be explained by the Existence and Uniqueness Theorem. This theorem gives the answer to two important questions when a initial value problem (IVP) is considered defined by  $\dot{x} = f(t, x)$ ,  $x(\tau) = A$ , where its solution maybe impossible to calculate explicitly [6]. This theorem give answers for the following questions: (1) is there an existing solution  $x(t)$  for the IVP? (2) if the solution exists, is it unique?

In a first approximation, the Existence and Uniqueness Theorem answers the questions by saying the following:

1. The solution  $x(t)$  exists if the function  $f(t, x)$  is continuous in some region  $R$  around  $(\tau, A)$  ([5],

page 24 and 70);

2. If the solution exists and if  $\frac{\partial f}{\partial x}(t, x)$  is also continuous in  $R$ , the solution is also unique ([5], page 24 and 70).

Another way to define the theorem of Existence and Uniqueness solution implies that  $f(t, x) : R \rightarrow \mathbb{R}$  must be continuous and satisfies a Lipschitz condition on a set  $R$ , where  $(\tau, A) \in R$ . This corresponds to the also called Picard-Lindelöf Theorem [20][41]. Before presenting formally this theorem, let us present first the Lipschitz condition. For the initial value problem defined by

$$\dot{x} = f(t, x), \quad x(\tau) = A, \quad (3.10)$$

$f$  satisfies a Lipschitz condition on a set  $R$  if there is a  $L \geq 0$ , called the Lipschitz constant, such that

$$|f(t, u) - f(t, v)| \leq L|u - v|, \quad \text{for all } (t, u), (t, v) \in R. \quad (3.11)$$

There is another way of writing the Lipschitz condition, presented by the following lemma.

**Lemma 1.** *Let  $D$  be the rectangle*

$$D := \{(t, p) : t \in [a, b], |p - A| \leq B\}$$

*or the infinite strip*

$$S := \{(t, p) : t \in [a, b], |p| < \infty\}.$$

*If  $f : D \rightarrow \mathbb{R}$  and  $\frac{\partial f}{\partial y}$  exists, is continuous and there is come constant  $K \geq 0$  such that*

$$\left| \frac{\partial f}{\partial y}(t, y) \right| \leq K \quad \text{for all } (t, y) \in D,$$

*then equation (3.11) holds with  $L = K$ .*

*Proof.*

$$\begin{aligned} f(t - u) - f(t - v) &= \int_v^u \frac{\partial f}{\partial y}(t, y) dy \\ |f(t - u) - f(t - v)| &= \left| \int_v^u \frac{\partial f}{\partial y}(t, y) dy \right| \\ &\leq \left| \int_v^u \frac{\partial f}{\partial y}(t, y) dy \right| \\ &\leq \left| \int_v^u \left| \frac{\partial f}{\partial y}(t, y) \right| dy \right| \\ &\leq \left| \int_v^u K dy \right| \\ &\leq K |u - v| \end{aligned}$$

□

So now the Picard-Lindelöf Theorem can be formally presented as the following:

**Theorem 1** (Picard-Lindelöf Theorem). *Let  $f : R \rightarrow \mathbb{R}$  be continuous and let  $(\tau, A) \in R$ . If there is a constant  $L \geq 0$  satisfying the Lipschitz condition in eq.(3.11), then the IVP defined in eq.(3.10) has a unique solution  $x = x(t)$  on some interval containing  $\tau$  [20][41].*

Similarly to Lemma 1, the Picard-Lindelöf Theorem can also be written in the following way:

**Corollary 1.** Let  $f : R \rightarrow \mathbb{R}$  be continuous and let  $(\tau, A) \in R$ . If  $\frac{\partial f}{\partial y}(t, y)$  exists and is continuous on  $R$  and there is some constant  $K \geq 0$  such that

$$\left| \frac{\partial f}{\partial y}(t, y) \right| \leq K, \quad \text{for all } (t, y) \in R,$$

then the IVP defined in eq.(3.10) has a unique solution  $x = x(t)$  on some interval containing  $\tau$ .

Let us now try to apply Corollary 1 to the equation (3.6), considering the effect  $u(t)$  to be constant with a large value, bigger than the other constants. So the function  $f$  becomes

$$f(t, V) = aV \left(1 - \frac{V}{K}\right) - \beta u V = f(V). \quad (3.12)$$

The derivative of function  $f$  exists, being the following

$$\frac{\partial f}{\partial V} = a - \beta u - 2 \frac{a}{K} V, \quad (3.13)$$

which is continuous in the set  $R$  defined by

$$R := \left\{ (t, V) \in \mathbb{R}^2 : t \in [a, b], \left| V - \frac{K}{2} \right| \leq \frac{K}{2} \right\}.$$

This region was created having in mind the time evolution of the function represented in figure 3.1, where the volume varies in the interval  $0 \leq V \leq K$  for  $0 \leq V(t=0) \leq K$ . For the set  $R$

$$\left| \frac{\partial f}{\partial V} \right| \leq \beta u, \quad (3.14)$$

which means that  $f$  is Lipschitz with Lipschitz constant  $L = \beta u$ . This allow us to conclude that  $\forall_{(t_0, V_0)} \exists! V(t) : V(t_0) = V_0$ . So besides the solution  $V(t) = 0$ , there are no other  $V(t) \neq 0$  such that  $V(t_0) = 0$ , for all  $(t_0, V_0) \in R$ , leading to the conclusion that it is not possible to eradicate the tumor totally by an appropriate choice of  $u$ .

## 3.2 Gompertz Growth Model

As stated in the previous section, Verhulst augmented the exponential model in order to have a model where a stable population would have a saturation value. Verhulst suggested the term  $1 - \frac{V}{K}$  and he wrote the Logistic model. Choosing a different parametrization (different term), the following model is obtained

$$\begin{cases} \frac{dV}{dt} = V(a - b \ln(V)) \\ V(t=0) = 1 \text{ mm}^3 \end{cases}, \quad (3.15)$$

where  $a$  is the initial proliferation rate (that summarizes the effect of mutual inhibition between cells and competition for nutrients) and  $b$  is a growth rate that impedes the growth for large tumor volume [3, 38]. This model is referred to as the Gompertz growth model. The fundamental property of the Gompertz model is that it exhibits an exponential decay of the relative growth rate  $\frac{1}{V} \frac{dV}{dt}$ . Solving the differential equation in (3.15), the following equation is obtained

$$V(t) = V_0 e^{\frac{a}{b}(1 - e^{-bt})}. \quad (3.16)$$

Figure 3.3 represents the tumor volume evolution computed using the Gompertz model. As it is possible to see, the volume converges to a carrying capacity  $K = V_0 e^{\frac{a}{b}}$ .

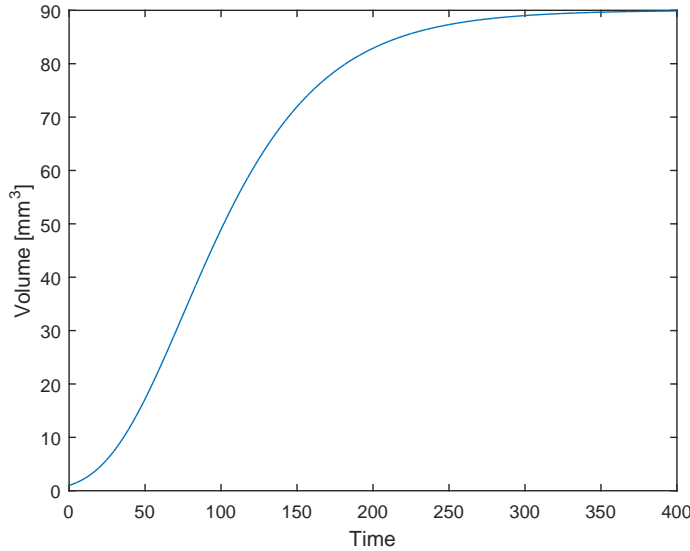


Figure 3.3: Gompertz Model, with  $b = 0.02$ ,  $a = 0.09$  and  $V_0 = 1\text{mm}^3$

### 3.3 Interacting Subsystems

This section addresses the issue of modeling subsystems that have important interactions with tumor growth. Those subsystems are the Immune System and Angiogenesis Process.

#### 3.3.1 Immune System

The Immune System (IS) is an internal mechanism of the human body that responds to infections. It is a collection of cells and molecules that are responsible for the organism defense against a wide range of microorganisms in the environment [21]. In order to fulfil this function, it needs to be able to detect a wide range of agents while distinguishing them from the healthy tissue [38]. It includes an innate immunity that is composed by cells and proteins that are immediately available to defend the organism against a wide range of pathogens [21]. It also includes an adaptive immunity subsystem which responds (or adapts) to the presence of a particular infectious microorganism, generating a powerful mechanism to neutralize and eliminate those microorganisms. The understanding of the IS allowed the creation of laboratory-produced versions to treat diseases [28]. Immunotherapy is one of these versions. Instead of targeting cancer cells directly, it enhances the intrinsic capability of the patient IS to combat cancer. So, immunotherapy has become an important way of fighting certain types of cancer cells, for instance, melanoma, prostate, kidney and others [45].

There are two types of adaptive immunity: humoral immunity, composed by antibodies that are produced by lymphocytes B (also called B cells), and cellular immunity composed by lymphocytes T (also called T cells). The antibodies protect the organism against extracellular microorganism in the blood and

tissues. On the other hand, the T cells are important in the defense against intracellular microorganisms. They act directly, killing infectious cells or activating phagocytes to kill ingested microorganisms [21].

When the IS is malfunctioning, the mechanisms that are involved in the patient defense causes injury to tissues and diseases. So it is important to maintain a balanced immune system.

The competitive interaction between the immune system and cancer cells is complex and involves nonlinear events. However, there are studies that show that the cancer therapy is only needed until the immune system is able to kill the rest of the cancer [28], and other studies that show that adaptive immunity can maintain occult cancer in an equilibrium state [38]. This is why the immune system is important in cancer therapies. The existence of such studies led to the development of a mathematical description for the tumor-immune system interaction. The simplest model is presented by Stepanova, in 1980 [38], and it has the following form

$$\begin{cases} \dot{V}(t) = \xi V F(V) - \theta V r \\ \dot{r}(t) = \alpha(1 - \beta V) V r + \gamma - \delta r \end{cases}, \quad (3.17)$$

where  $V$  is the tumor volume and  $r$  is the immunocompetent cell densities related to various types of immune cells (T-cells) activating during the reaction [38], and  $\xi, \theta, \alpha, \beta, \gamma$  and  $\delta$  are constant coefficients. In the original research, an exponential model was used for  $F_E(V) = 1$ . Other research use a Logistic model  $F_L(V) = 1 - (\frac{V}{K})$ , a Generalized Logistic model  $F_{GL}(V) = 1 - (\frac{V}{K})^\beta$  and even a Gompertz model  $F_G(V) = -\ln(\frac{V}{K})$  [38]. Depending on the parameters, the dynamical system represented in equation (3.17) can exhibit a wide range of behaviors, for example, the above example where the adaptive immunity is able to keep the cancer volume so small that it is almost undetectable.

### 3.3.2 Angiogenesis

Angiogenesis is the a physical process in which new blood vessels are formed from pre-existing vessels. The importance of the study about this phenomena is that in some studies it was verified that tumors can develop its own vasculature. In fact, the tumor stimulates and inhibits the growth of endothelial cells that form the linings of the blood vessels and capillaries that define its vasculature [38]. Those processes are complex. However, there are antiangiogenic treatments that modulate the growth of the vessels network in order to control the tumor growth. It is suggested that, instead of fighting the fast duplicating and mutating cancer cells, the antiangiogenic treatment targets the endothelial cells that form the walls of blood vessels.

The fact that there is no limiting resistance of cancer cells to angiogenic inhibitors could suggest that antiangiogenic treatment is preferable to others. However, this treatment only limits the tumor support mechanism without killing him. So, antiangiogenic treatment is not effective enough as stand alone treatment to treat cancer [38]. It has to be combined with other treatments such as chemotherapy, for example.

There is a simple mathematical model that describes the vascular phase of tumor growth. This model introduces the concept of varying carrying capacity  $q(t)$  defined as the tumor size sustainable by

the existence of vascular network.

$$\begin{cases} \dot{V}(t) = VF\left(\frac{V}{q}\right) \\ \dot{q}(t) = S(V, q) - I(V, q) \end{cases}, \quad (3.18)$$

where  $S(V, q)$  represents stimulatory effects and  $I(V, q)$  represents inhibitory effects [38]. Together they represent a balance of the dynamics of  $q(t)$ .

### 3.4 Important Remarks

Next, the most important remarks of this chapter are presented. About the Logistic model:

- Considers that the tumor volume has a saturation level;
- Non-linear model;
- By the analysis of the Logistic equation, it is possible to conclude that it is not possible to eradicate the tumor by an appropriate choice of the drug effect  $u_{max}$ .

About the Gompertz model:

- Also considers a saturation in the tumor volume;
- Non-linear model.

About the Interacting Subsystems:

- The Immune System (IS) helps reducing the tumor. However, it is also affected by the tumor, which reduces the effect that the IS has in the tumor;
- The Angiogenesis Process corresponds to the variation of the tumor volume carrying capacity (tumor saturation value), which helps the tumor to grow.



## Chapter 4

# Global Cancer Therapy Model

Remembering section 1.2, the third problem of this work is the design of the controller. In that section, this problem is divided in 3 sub-problems (3.1, 3.2 and 3.3). Problem 3.3 is studied here, using the PK model, the PD model and the Logistic model only. So the diagram block considered here is the one shown in figure 4.1.

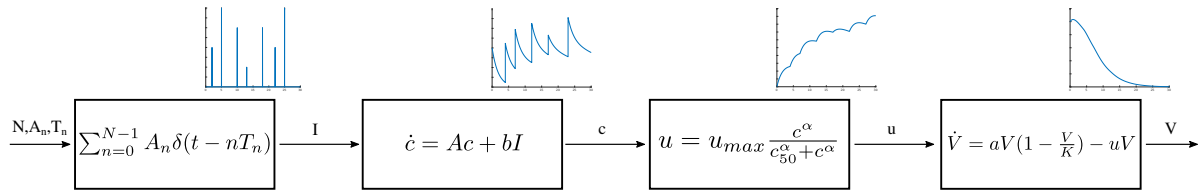


Figure 4.1: Block diagram considered in the first problem: Administration model, Pharmacokinetics, Pharmacodynamics and Logistic model

In figure 4.1, the first block corresponds to the administration model, *i.e.*, is the Dirac impulse sequence. The second block corresponds to the Pharmacokinetic model, specifically the 2 compartment model studied in section 2.1.6.2 considering the Bevacizumab as the input drug. The third block is the Pharmacodynamic model, where the Hill equation is considered, studied in section 2.2. Because there are 2 compartments, the variable  $c$  has dimension 2  $c = [c_1, c_2]$ . Compartment 2 was chosen as the effect compartment, so that the drug administered does not produce an immediate effect on the tumor. The last block corresponds to the Logistic equation, studied in section 3.1. Therefore, the inputs of this system are the three parameters – number of administrations  $N$ , drug dosage  $A_n$  and time intervals between administrations  $T_n$  – and the output is the tumor volume, given by the Logistic equation. The parameters used in each block are described in table 4.1. Note that the non-linearity of this system is given by the Hill equation and the Logistic equation, that render difficult the system control. Because of that, numeric optimization methods are considered to solve the problem.

Table 4.1: Parameters of each block used in simulations

Block	Parameter	Value	Unit	Variation Interval
PK	$K_{12}$	0.223	$day^{-1}$	-
	$K_{21}$	0.215	$day^{-1}$	-
	$K_{10}$	0.0779	$day^{-1}$	-
PD	$c_{50}$	11.4274	$mg/kg$	-
	$u_{max}$	1	-	[0.5;1.5]
	$\alpha$	1	-	[0.5;1.5]
Logistic model	$a$	0.1	-	[-0.01;0.1]
	$K$	5	$mm^3$	[-1;10]
	$V_i = V(0)$	1	$mm^3$	[0.1;10]

Also in table 4.1, some ranges are considered for values of the variables that do not depend on specific drug parameters. The main objective of each variation intervals is to show some particularities of the mathematical models that can happen (or not) in real life. In particular, negative values for the parameters  $a$  and  $K$  were considered, even if they cannot be negative in real life. However, the ranges indicated yield different mathematical responses that can have an impact on the controller behavior.

For some of these ranges, it is already possible to have an idea of what can be the impact. For instance, the variation interval of parameter  $u_{max}$  influences the effect that a same amount of drug  $c^*$  in the saturation area of the Hill Equation (as previously stated in section 2.2) has in the tumor: for small values,  $c^*$  has less impact than for higher values of  $u_{max}$ . For a controller that calculates the optimal amount of drug for each administration, this variation interval is important, since it can dictate how high/low the drug concentration can be.

The parameter  $\alpha$  dictates the variation interval of drug concentration values that causes the effect to saturate. As described in figure 2.11b, when  $\alpha$  increases, the variation interval of drug concentration, centered in  $c_{50}$ , that leads to saturation in the effect, decreases. This variation can have an important impact on the behaviour of the controller, in decreasing the dosages.

For the Logistic Model, the intervals considered can create a discontinuity in the tumor evolution. Analyzing the Logistic equation solution (without the  $-uV$  term) in equation (A.9), it is possible to see that  $V(t)$  is not defined when the denominator is zero. And there are some parameters configuration  $(a, K)$  that can lead to a zero denominator for  $t \geq 0$ . Another situation is when  $K = 0$ : the differential equation 3.2 is not defined. Figure 4.2 represents the time evolution of the Logistic equation solution denominator  $D(t) = V_0 + (K - V_0)e^{-a(t-t_0)}$  with  $a > 0$  and  $V_i > 0$ , for different values of  $K$ . It is possible to see that there are two curves that cross zero (the two circles correspond to the zeros) for  $t \geq 0$ . They correspond to values of  $K$  in the interval  $K < 0$ . The curves that do not present zero value for  $t \geq 0$  correspond to the interval  $0 < K < V_i$ .

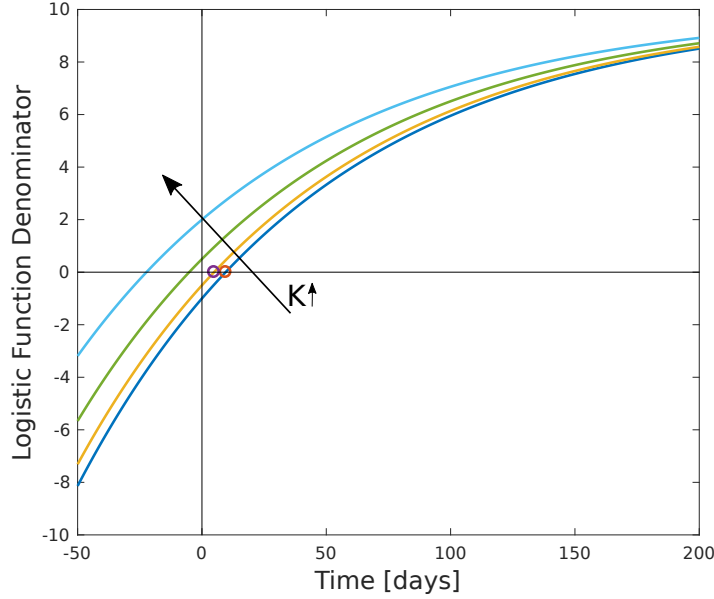


Figure 4.2: Time evolution of the logistic equation solution denominator  $D(t) = V_0 + (K - V_0)e^{-a(t-t_0)}$  for  $K = [-1, -0.5, 0.5, 2]$ , with  $a = 0.01$  and  $V_i = 10$ .

In figure 4.3, the time evolution of the Logistic Equation is represented for  $K$  in each of the intervals  $K < 0$  and  $0 < K < V_i$ . As stated, for  $K = -1$  the logistic equation response has a discontinuity, while for  $K = 9$  it does not. The similar effect also happens for  $a < 0$ , where now the discontinuity happens for  $0 < K < V_i$ , and not for  $K < 0$ .

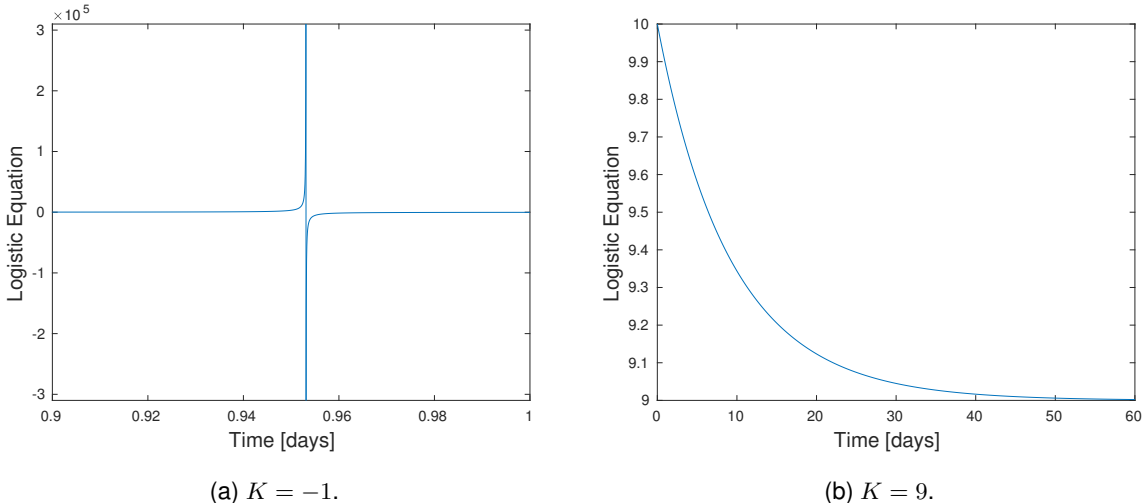


Figure 4.3: Tumor volume time evolution for different values of  $K$ , with  $a = 0.1$ ,  $V_i = 10$  and  $t \geq 0$ .

Summarizing the values that allow a continuous behavior of the Logistic Equation, the following is obtained

$$\begin{cases} a > 0 & \wedge \quad 0 < K < V_i \\ a < 0 & \wedge \quad K < 0 \end{cases} . \quad (4.1)$$

It is important to note that in a real situation, the carrying capacity does not verify  $K < V_i$ . For the tumor to grow,  $K$  needs to be higher than the initial tumor volume, otherwise either the tumor maintains its initial volume (case when  $K = V_i$ ) or the tumor dies from itself (case when  $K < V_i$ ), which is not what usually happens.

# Chapter 5

## Optimal Impulsive Control

In this work, optimal impulsive control techniques are considered to calculate optimally the three parameters of drug administration in order to minimize tumor size in cancer. But first there are some questions to be raised: what is control, what are the types of control, why optimal control is used in this work, what is impulsive control and how it is going to be used.

### 5.1 Optimal Control

Control theory, in control systems engineering, deals with the control of dynamic systems (*i.e.* systems that evolve over time). The dynamic systems can be called continuous-time systems or discrete-time systems depending on whether the time varies continuously or discretely [40]. The main goal of control is to develop models to control those dynamic systems, making actions and decisions in an optimal way, in order to ensure control stability. Many control theories were developed for this purpose. For instance, robust control, adaptive control, predictive control, optimal control, stochastic control, and others. Each of them deals with specific types of control problems and sometimes they can be combined to solve the same problem. For example, adaptive control aims at defining methods for estimations of parameters that vary or are uncertain over time. In other words, it is used in systems that have non-fixed parameters in which the controller must adapt. In the other hand, for example, predictive control aims at minimizing a cost associated to a horizon that slides in front of it. It uses current and past observations and tries to predict the horizon, based on optimization.

Optimal control is one type of control, different from others. It is a branch of mathematics that tries to find optimal ways to control a dynamic system [40]. There are several applications of optimal control: finance, economics, marketing, and many others.

Assuming a system with dimension higher than one, with  $x(t)$  being the state variable and a control variable  $u(t)$ , the so called state equation can be expressed by

$$\dot{x}(t) = f(x(t), u(t), t), \quad x(0) = x_0. \quad (5.1)$$

If both the initial condition  $x_0$  and the control trajectory  $u(t)$  are known, it is possible to integrate equation (5.1) and calculate the state trajectory  $x(t)$ . The main goal of the optimal control is to choose the control

trajectory so that the state and control trajectories maximize a cost function, called the objective function  $J$

$$J = S[x(T), T] + \int_0^T F(x(t), u(t), t) dt, \quad t \in [0, T], \quad (5.2)$$

where  $T > 0$  is a specific time horizon.  $F$  is a function of the state and control variables that describes how and what needs to be maximized during the trajectories. It generally includes terms related to the running cost during the interval for example, the effect that a drug has on the tumor dynamics, that need to be maximized [38]. Also in (5.2),  $S$  is a function of the ending state  $x(T)$  at time  $T$  that gives a value called salvage value that is a penalty term at the end of the therapy designed to introduced the desired system performance [38]. In other words, a good behaviour of the solution is needed at the end of the horizon. [40].

Usually the control and state variables have constraints associated with them. In other words, constraints only allow the control and state variable to take a set of possible values. This constraints limit the values that the ending state  $x(T)$  can take. In section 5.3 is the detailed explanation of the maximum principle for impulsive optimal control. This principle defines conditions for finding the optimal trajectories for the control variables.

## 5.2 Optimal Impulsive Control and PK model

The control types referred previously study the control of systems governed by ordinary differential equations, where the state variable evolve continuously, since the control affects only the time derivatives of the state variables [40]. However, there are some situations in which instantaneous changes are permitted by a finite amount, for instance, in management science. In this problem (called the impulsive control problem), the state variable dynamics cannot be described by ordinary differential equations. An intuitive way of representing these situations is using the Dirac impulse function, described in section 2.1.6, as previously stated. Actually, a system that has, as an input signal, the Dirac impulse sequence (eq.(2.15)), has the same solution between  $t = T_i$  and  $t = T_{i+1}$ .

Let us consider the PK state-space system for a 2 compartment model, described in equation (2.28). Consider the situation where there is a certain reference  $r$  for the concentration in compartment 1 and what is wanted is that the concentration in compartmental 1,  $c_1$ , must follow the reference, changing only the Dirac impulse amplitudes. So the problem here is the determination of amplitudes  $A_n$  that minimizes the difference between concentration in compartment 1 and the reference,  $r - c_1$ . In order to give more importance to differences higher than one, the difference is squared. This leads to an objective function described by

$$J = \int_0^T (r(t) - c_1(t))^2 dt, \quad t \in [0, T], \quad (5.3)$$

where  $T$  is the simulation horizon. Besides minimizing the difference, a cost to the impulses amplitudes is introduced in order to also minimize the drug dosage. So, the cost function is

$$J = \int_0^T (r(t) - c_1(t))^2 dt + \rho \sum_{n=0}^{N-1} \alpha_n^2. \quad (5.4)$$

where  $\rho$  is a parameter for tuning the minimization.

In a general way, the impulse optimal control problem can be stated as follows

$$\begin{cases} \min(J = \int_0^T F(x(t), u(t), t) dt + \sum_{n=0}^{N-1} G(x(t_i), v(t_i), t_i) + S[x(T)]) \\ \text{subject to} \\ \dot{x}(t) = f(x(t), u(t), t) + \sum_{n=0}^{N-1} G(x(t_i), v(t_i), t_i), \quad x(0) = x_0, \\ u \in \Omega_u, \quad v \in \Omega_v, \end{cases} \quad (5.5)$$

where  $\Omega_u$  and  $\Omega_v$  represents the constraints regions for  $u$  and  $v$ .

Figure 5.1 represents the objective function described in equations (5.3) and (5.4).

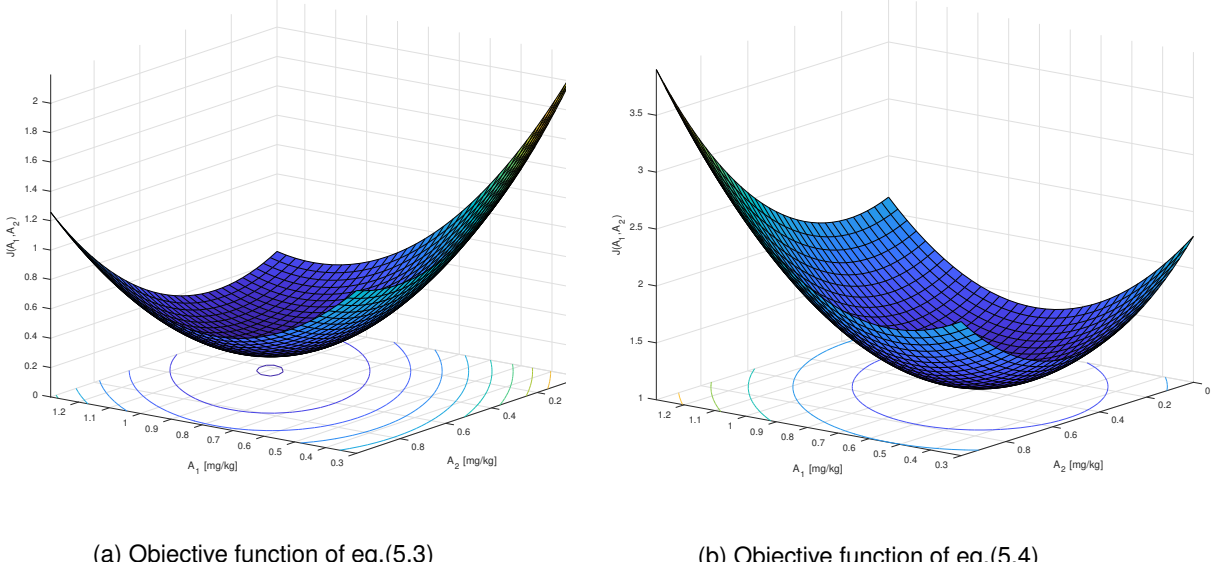
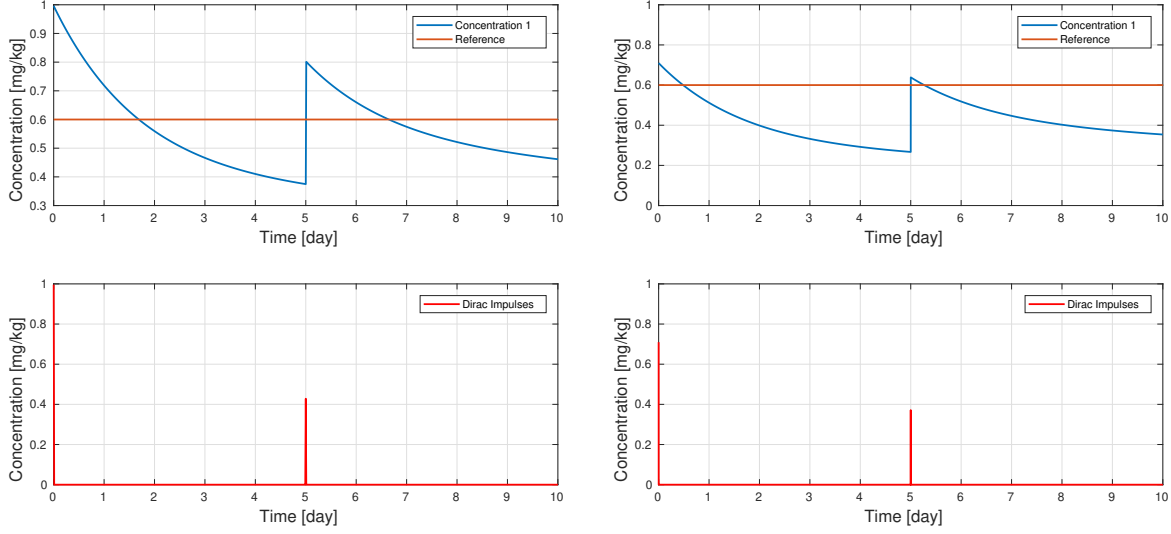


Figure 5.1: Objective functions values described in (5.3) and (5.4) for variable amplitudes, with  $N = 2$ ,  $\rho = 1$  and a constant reference  $r(t) = 0.6$

As expected, when the cost function only depends on the difference between reference and concentration in compartment 1, the amplitude values are bigger than when the cost function depends also on the amplitudes. In the objective function (5.4) there are two weights that need to be balanced in order to minimize the function. The balance is governed by the  $\rho$  parameter. If  $\rho$  increases, the objective function will give more importance to the Dirac amplitudes than the difference. In the other way around, the difference is more important. For the objective function described in (5.3) the minimum value, calculated using Quasi-Newton algorithm in the MATLAB function fminunc, is the vector of amplitudes  $A = [0.9959, 0.4282]$ . For the function described in (5.4) the minimum is the vector  $A = [0.7097, 0.3715]$ . In 5.2 the concentration variation for each of these vectors is represented.



(a) Concentration for optimal amplitudes from eq. 5.3

(b) Concentration for optimal amplitudes from eq. 5.4

Figure 5.2: Concentration variation with optimal amplitudes

Figure 5.3 represent a simulation with  $N = 10$  Dirac impulses and fixed time interval between impulses  $T_i = 5$ ,  $i = 1, \dots, N$ . The amplitudes that minimize the objective function, (5.4), using the Interior Point algorithm in MATLAB function fmincon, is  $A=[0.7603, 0.4578, 0.3215, 0.2538, 0.2194, 0.2011, 0.1897, 0.1794, 0.1648, 0.1362]$ .

Constraints were added to prevent the amplitudes from being negative. Like stated in section 2.1 , it does not make any sense the administration of a negative amount of drug.

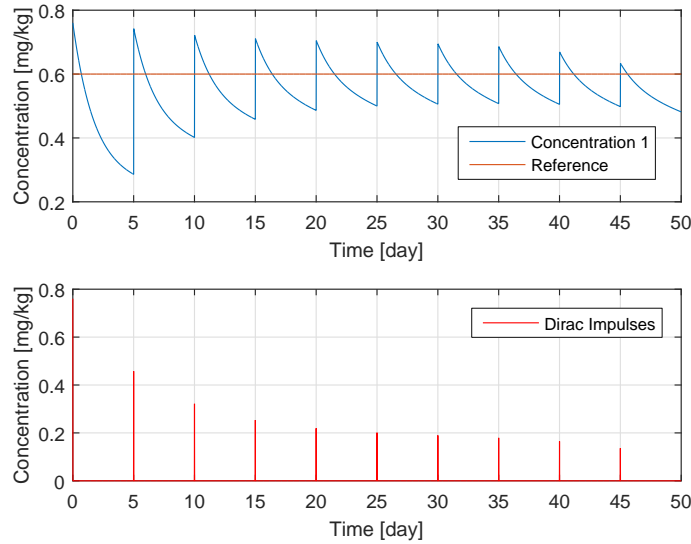


Figure 5.3: Concentration variation with 10 optimal amplitudes, with  $T_i = 5$ ,  $i = 1, \dots, N$

For the simulations in figures 5.2 and 5.3, a fixed value for the total number of impulses  $N$  and for the time interval between impulses  $T_i$ ,  $i = 1, \dots, N$  is considered. This corresponds to the problem (3.1)

defined in 1.2. The horizon is considered to be  $T = NT_i$ , where  $T_i$  is constant for all  $i = 1, \dots, N$ . Actually this assumption is not always right. The horizon can be lower or higher than that. Depending on its values, the cost function varies. If all the impulses happen during the simulation horizon, the equation (5.4) is true for all time. If that does not happen, then some or all impulses are discarded. So, the horizon must be defined a priori. Besides that, if the problem (3.2) defined in section 1.2 is considered with a certain horizon  $T$ , the variation of the time interval between impulses may lead to the same situation.

It is important to refer that if the objective functions is convex, then the minimum is a global minimum. A function  $f$  is convex if for each pair of values of  $x$ , for instance  $x'$  and  $x''$ ,  $f[\lambda x'' + (1 - \lambda)x'] \leq \lambda f(x'') + (1 - \lambda)f(x')$  for all values of  $\lambda$  that satisfy  $0 < \lambda < 1$  [17]. If the objective functions are not convex with respect to the variable parameters, then in order to find a global minimum, the problem must be rewritten. For instance, the problem, where is assumed a constant but not fixed value for the time interval between impulses, may eliminate the convexity of the objective function. However, the introduction of constraints to the maximum and minimum values of concentration can help the convexity. In [31] and [30] theorems are described to solve the optimization problem. They are different from the maximum principle, described in the next section.

### 5.3 Maximum Principle for Impulse Optimal Control

In [40] an example that explains the maximum principle for impulse optimal control is represented . This example is the following: an oil producer pumps oil from a single well; because the output rate of the well is proportional to the remaining stock, called  $x(t)$ , the output rate is  $bx(t)$ , where  $b$  is constant. So  $\dot{x}(t) = -bx(t)$ ,  $x(0) = 1$ , where 1 corresponds to the starting stock of a new oil well. When the remaining oil in the well becomes low, the oil producer abandons the well and drills a new one. So the variation of  $x(t)$  in time is similar to the variation of drug concentration in compartment 1,  $c_1(t)$ , represented in 5.3, for example. So, a convenient way of describing the process is to use the Dirac impulse, defined in section 2.1.6. It is now possible to write the state equation as follows

$$\dot{x}(t) = -bx(t) + \sum_{n=1}^{N(T)} \delta(t - t_n)[1 - x(t)], \quad x(0) = 1. \quad (5.6)$$

Considering  $v(t)$  to be the drilling control variable, where  $v = 0$  means no drilling and  $v = 1$  means the drilling of a single well, the state equation is now

$$\dot{x}(t) = -bx(t) + \sum_{n=1}^{N(T)} \delta(t - t_n)v(t)[1 - x(t)], \quad x(0) = 1. \quad (5.7)$$

To solve this problem, it is needed the determination of  $t_i$ , the magnitude  $v(t_i)$  and the number of drillings  $N(T)$ . For this problem the objective function represents the profit of the process, that needs to be maximized

$$J = \int_0^T Pbx(t)dt - \sum_{n=1}^{N(t)} Qv(t_n), \quad (5.8)$$

where  $P$  is the unit price of oil and  $Q$  is the drilling cost of drilling a well. In order to solve this optimization problem, [40] suggests the use of the maximum principle for impulse optimal control, a generalization of the Pontryagin's Principle.

In a general case where the state variables can have instantaneous changes, the objective function can be written as follows

$$\begin{cases} \min \left\{ J = \int_0^T F(x, u, t) dt + \sum_{n=1}^{N(T)} G(x(t_n), v(t_n), t_n) + S[x(T)] \right\} \\ \text{subject to} \\ \dot{x}(t) = f(x, u, t) + \sum_{n=1}^{N(T)} g(x(t_n), v(t_n), t_n), \quad x(0) = x_0, \\ u \in \Omega_u, \quad v \in \Omega_v \end{cases} \quad (5.9)$$

where  $G(x, u, t)$  represents the cost of profit associated with the impulse control,  $g(x, v, t)$  represents the instantaneous finite change in the state variable when the impulse control is applied and  $\Omega_u$  and  $\Omega_v$  are the set of possible values of the control variables  $u(t)$  and  $v(t)$ , respectively. In 1978, Blaquière developed the maximum principle optimal conditions to solve the problem stated in (5.9) [40]. To state the conditions it is necessary to define the Hamiltonian function

$$H(x, u, \lambda, t) = F(x, u, t) + \lambda f(x, u, t) \quad (5.10)$$

and the impulse Hamiltonian function

$$H^I(x, v, t) = G(x, v, t) + \lambda g(x, v, t). \quad (5.11)$$

Assuming  $x^*$  to be an optimal trajectory and  $u^*$  to be optimal controls, then there exists an adjoint variable  $\lambda$  such that the following conditions hold

$$\begin{cases} \dot{x}^* = f(x^*, u^*, t), \quad t \in [0, T], \quad t \neq t_n, \\ x^*(t_n^+) = x^*(t_n) + g(x^*(t_n), v^*(t_n), t_n), \\ \dot{\lambda} = -H_x(x^*, u^*, \lambda, t), \quad \lambda(T) = S_x[x^*(t)], \quad t \neq t_n, \\ \lambda(t_n) = \lambda(t_n^+) + H_x^I(x^*(t_n), v^*(t_n), t_n), \\ H(x^*, u^*, \lambda, t) \geq H(x^*, u, \lambda, t) \text{ for all } u \in \Omega_u, \quad t \neq t_n, \\ H^I(x^*(t_n), v^*(t_n), t_n) \geq H^I(x^*(t_n), v, t_n) \text{ for all } v \in \Omega_v, \\ H[x^*(t_n^+), u^*(t_n^+), \lambda(t_n^+), t_n] + H_t^I[x^*(t_n^+), v^*(t_n^+), t_n] = H[x^*(t_n), u^*(t_n), \lambda(t_n), t_n] + H_t^I[x^*(t_n), v^*(t_n), t_n], \end{cases} \quad (5.12)$$

where  $H_x$  denotes the partial derivative of  $H$  with respect to  $x$ , and the same is applied to the other functions with index. In the oil problem there is no variable  $u(t)$ , so the conditions in (5.12) can be adapted.

In [40] these conditions are applied to the oil driller's problems under the assumption that  $T$  is sufficiently small so that no more than one drilling will be found to be optimal. So the problem to be solved can be defined by the following

$$\begin{cases} \max \left\{ J = \int_0^T Pbx(t) dt - Qv(t_1) \right\} \\ \text{subject to} \\ \dot{x}(t) = -bx(t) + \delta(t - t_1)v(t)[1 - x(t)], \quad x(0) = 1, \\ 0 \leq v(t) \leq 1. \end{cases} \quad (5.13)$$

Defining now the Hamiltonian functions corresponding to eq.(5.10) and eq.(5.11):

$$H(x, \lambda) = Pbx + \lambda(-bx) = bx(P - \lambda), \quad (5.14)$$

$$H^I(x, v) = -Qv + \lambda(t^+)v(1 - x). \quad (5.15)$$

Let us now apply the necessary conditions of eq.(5.12) to the oil problem:

$$\dot{x} = -bx. \quad t \in [0, T], \quad t \neq t_1, \quad (5.16)$$

$$x[t_1^+] = x(t_1) + v(t_1)[1 - x(t_1)], \quad (5.17)$$

$$\dot{\lambda} = -b(P - \lambda), \quad \lambda(T) = 0, \quad t \neq t_1, \quad (5.18)$$

$$\lambda(t_1) = \lambda(t_1^+) - v(t_1)\lambda(t_1^+), \quad (5.19)$$

$$[-Q + \lambda(t_1^+)(x)]v^*(t_1) \geq [-Q + \lambda(t_1^+)(1 - x)]v \quad \text{for } v \in [0, 1], \quad (5.20)$$

$$bx(t_1^+)[P - \lambda(t_1^+)] = bx(t_1)[P - \lambda(t_1)]. \quad (5.21)$$

For  $t > t_1$ , the solution of equation (5.18) is

$$\lambda(t) = P \left[ 1 - e^{-b(T-t)} \right], \quad t \in [t_1, T]. \quad (5.22)$$

From equation (5.20), the optimal impulse control at  $t_1$  is

$$v^*(t_1) = \text{bang}[0, 1; -Q + \lambda(t_1^+)1 - x(t_1)]. \quad (5.23)$$

The bang-bang nature of the optimal impulse control stated above means that  $v^*(t_1) = 1$ . In [40] (page 329) this analysis is continued and the value for  $t_1$  is obtained  $t_1 = \frac{T}{2}$ , under the assumption that  $Q$  is relatively small and  $P, b$  and/or  $T$  are relative.

For solving the optimizations problems stated in section 1.2, the objective functions are different from the oil driller's problem but they can have the same form of equation (5.9) and, because of that, the maximum principle here stated can be used.

Using the Logistic Model (section 3.1) for describing the tumor growth, it is difficult to use analytic methods (like the maximum principle) for solving the optimization problem, since it is not easy to compute analytically the total expression of the tumor volume  $V(t)$  (see 3.1.1). So, to solve the optimization problem, numerical methods are going to be used in this work. To make a comparison, let us now try to solve the oil problem using numerical methods, in MATLAB with the optimization toolbox. Because the oil problem has only two variables, it is possible to create the curve  $J(v(t_1), t_1)$  and actually see its maximum value, as figure 5.4 suggests.

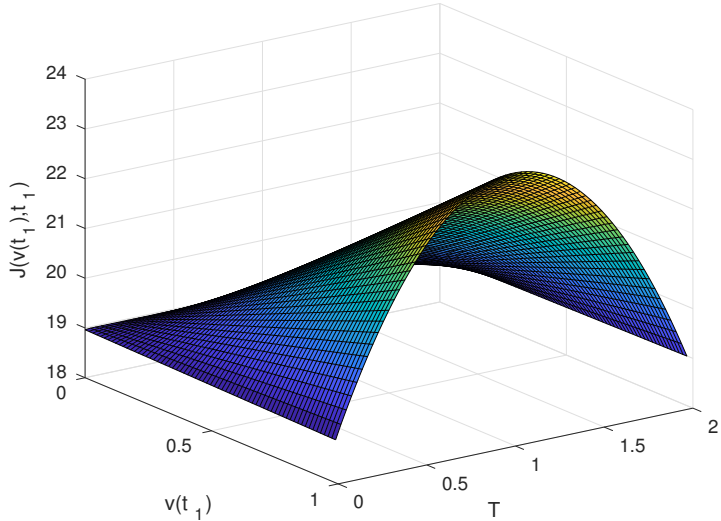


Figure 5.4: Objective function as a function of  $(v(t_1), t_1)$ , for  $T = 2$ .

As it is possible to see, the maximum value corresponds to the pair  $(v(t_1), t_1) = (1, 1)$ , for  $T = 2$ . The optimization method used for this problem was the Sequential Quadratic Programming (SQP), where the derivatives were approximated using central differences and with a maximum functions evaluations of 1200 and/or maximum iterations of 800. The parameters of the optimization method influence the solution provided by it in such a way that it could not give the real minimum of the objective function. So it is important to study the optimization method in order to know what are the best parameters configuration for each optimization problem. In this work were considered two nonlinear optimization methods: Sequential Quadratic Programming (SQP) and Interior Points methods (IP). In MATLAB, to solve nonlinear optimization problems, the function fmincon can be used, and the optimization method can be chosen.

## 5.4 Variable amplitudes and fixed time intervals

Figure 5.5 represents the signals  $I(t)$ ,  $c(t)$  and  $u(t)$  (see figure 4.1), where  $A_n = 3$  for  $n = 1, \dots, N$ ,  $T_n = 3$  for  $n = 1, \dots, N - 1$ ,  $N = 17$  and  $T = 50$  days. The drug effect, given by the Hill equation, is very similar to the concentration in compartment 2,  $c_2$ , with a scale difference. The saturation does not occur in this simulation.

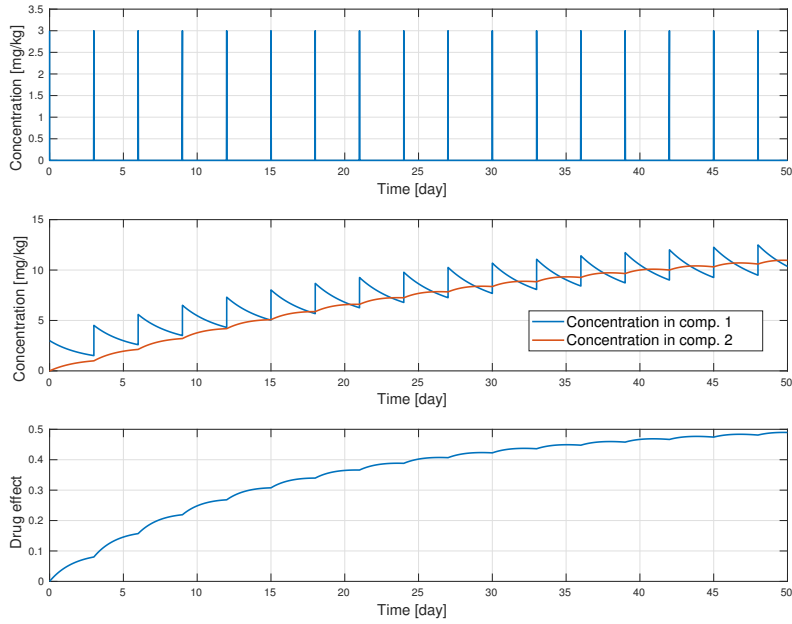


Figure 5.5: Output signals of Administration model,  $I(t)$ , Pharmacokinetics,  $c(t)$ , and Pharmacodynamics,  $u(t)$ .

It is important to notice that there is a drug accumulation effect due to the fact that the excretion rate of the compartment model is less than the drug administration rate. This accumulation is important because the determination of the optimal dosage to introduce depends on it, in order to respect all the constraints, later. Introducing now the drug effect as input to the Logistic model, the time evolution of the tumor volume is as shown in figure 5.6.

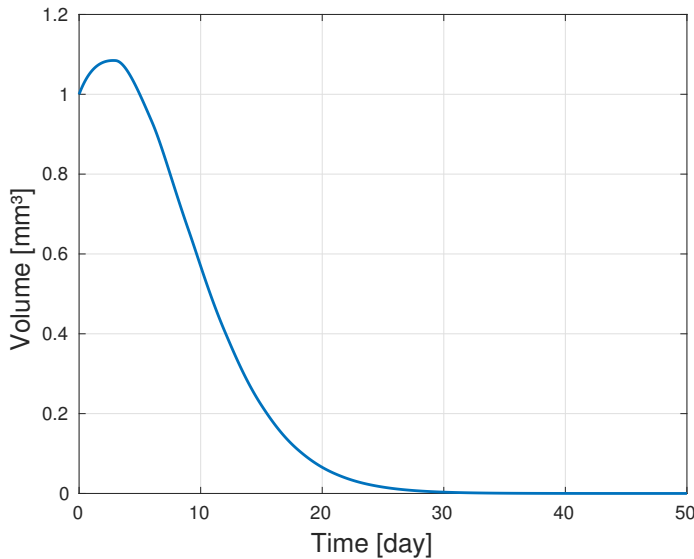


Figure 5.6: Tumor evolution over time when applied the Dirac impulse sequence described in fig.5.5.

As it is possible to see, the tumor evolution goes to zero when time goes to infinity, instead of the

behavior described in figure 3.1. For the inputs configuration of this simulations, the tumor goes to zero relatively fast. If the dosage increases, using the same time intervals, the tumor will go to zero faster. In the limit, if the dosage is very high, the tumor will disappear almost instantly. But those dosages cannot happen because there is a drug concentration limit in the human organism, above which the treatment becomes toxic to the patient. For instance, if this limit (or constraint) is  $10 \text{ mg/kg}$ , the treatment plan described in figure 5.5 is not possible, since the concentration in compartment 1 is bigger than this threshold after 25 days. Besides the existence of this limit, imposed by toxicity problems, the solution that is more reasonable is the one where the dosage of each administration is not the maximum possible, in order to reduce the drug side effects in the patient. So, the construction of the objective function has to fulfill three requirements so far:

- Minimizing the tumor volume;
- Concentration in compartment 1 and 2 less or equal to some value  $C_{max}$ , due to toxicity problems;
- Reducing side effects: not choosing the solution where the dosages are as higher as possible.

### **Minimizing the tumor volume**

For this requirement, it is necessary to use some value that can describe the time evolution of the tumor volume. Any function that describes the tumor evolution can be used. For instance, the integral of the tumor volume summarizes the entire time evolution in the interval  $[0, T]$ . The question now is should the integral of the squared volume or the integral of the absolute value of the volume be used? First of all, remember that in this problem constant and known values for the time intervals are considered, and also for the horizon  $T$  and number of administration  $N$ . The objective function only depends on the drug dosages/Dirac impulses amplitudes

$$J(A_n) = \int_0^T V^2 dt \quad \text{or} \quad J(A_n) = \int_0^T |V| dt, \quad c \in \Omega_c \quad (5.24)$$

where  $\Omega_c$  represent the constraints region for the concentrations in compartment one (which will fulfill the second requirement). It is already known for  $V(0) \geq 0$ , the  $V(t) \geq 0$ . This means that the volume will never be negative. The main difference between  $V^2$  and  $|V|$  is that the squared volume amplifies the volume when  $V > 1$  and attenuates the volume when  $V < 1$ . This difference can become very important for the optimization problem. Figure 5.7 represents the squared volume presented in figure 5.6. As it is possible to see, the squared volume amplified the values higher than one and attenuates the values smaller than one. In other words, the squared volume gives more importance to the volume when it is higher than one.

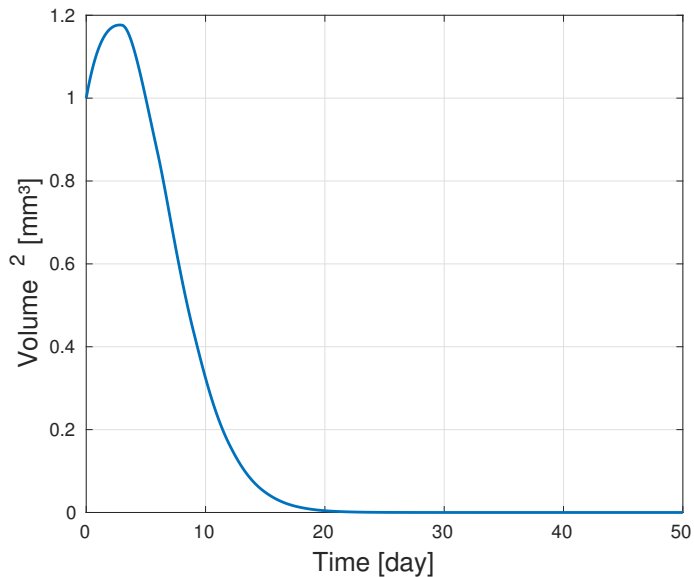
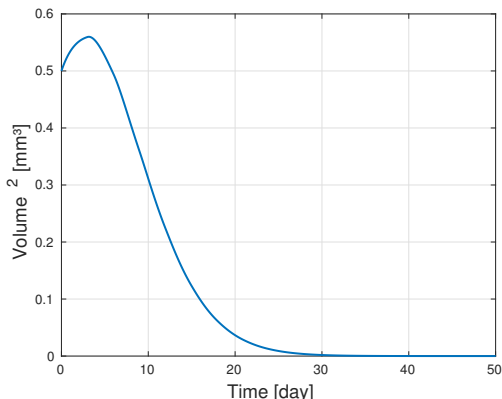
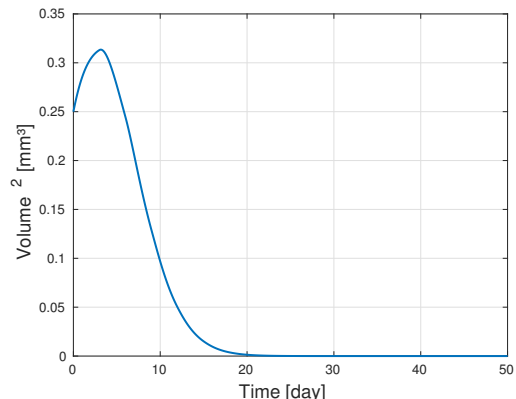


Figure 5.7: Squared Volume time evolution when applied the Dirac impulse sequence described in fig.5.5

Figure 5.8 represents the tumor volume evolution and the squared volume evolution with a initial condition of  $V(0) = 0.5 \text{ mm}^3$ ,



(a) Tumor volume



(b) Tumor volume squared

Figure 5.8: Tumor volume and squared volume for  $V(0) = 0.5 \text{ mm}^3$ , when applied the Dirac impulse sequence described in figure 5.5

Figure 5.8 represents the tumor volume evolution and the squared volume evolution with a initial condition of  $V(0) = 2 \text{ mm}^3$ ,

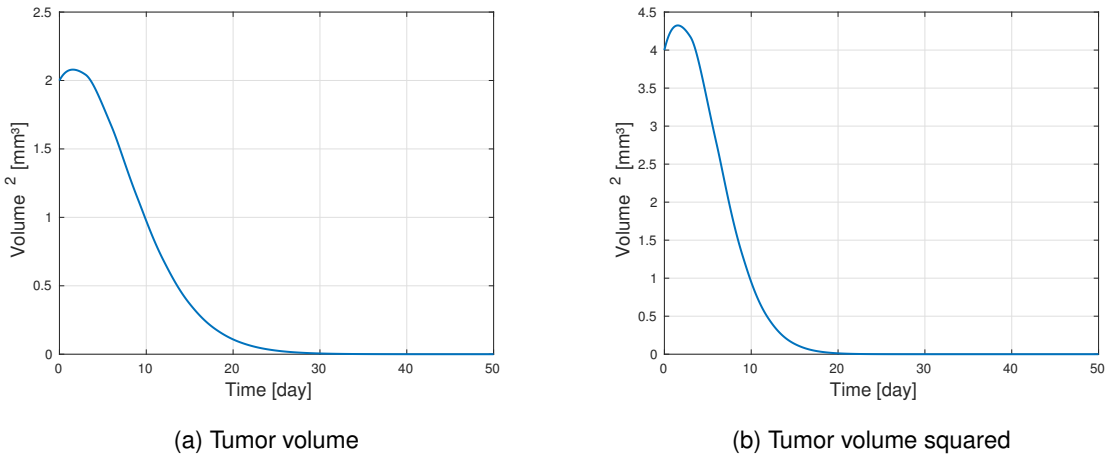


Figure 5.9: Tumor volume and squared volume for  $V(0) = 2 \text{ mm}^3$ , when applied the Dirac impulse sequence described in figure 5.5

So the squared volume besides shrinking the tumor volume evolution in time, its integral can have very different values depending on the initial condition. Another way of analyzing the difference here stated is by observing the surface and contour of both integrals. Figures 5.10 and 5.11 represent the surfaces and contours of  $V^2$  and  $|V|$ , respectively, considering the concentration constraint that constraint some amplitudes configurations, in order to not have concentrations in compartment one above  $C_{max} = 10mg/kg$ .

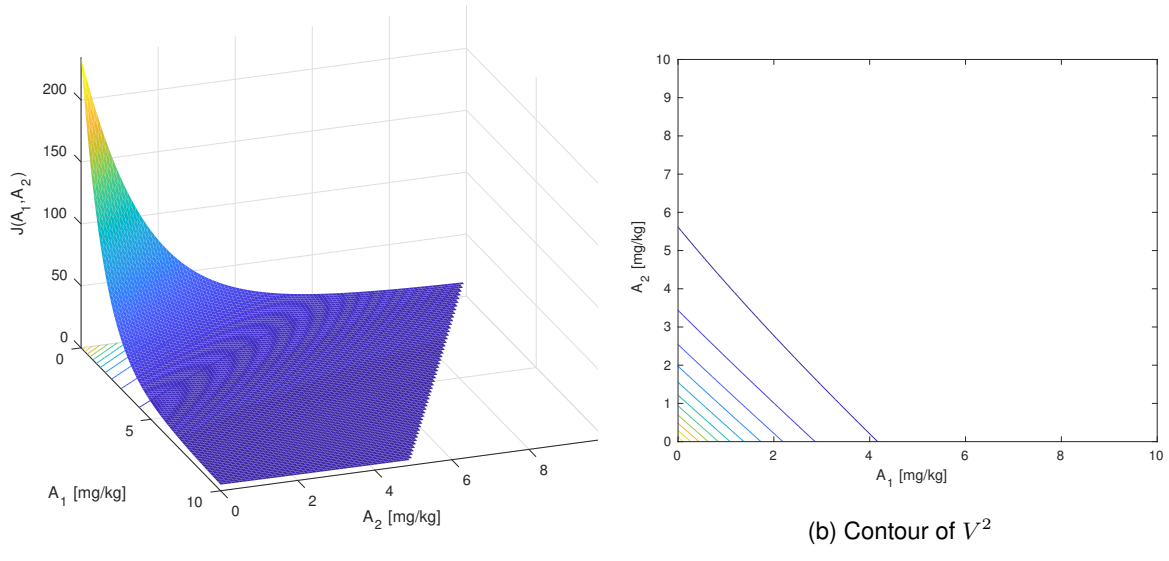


Figure 5.10: Surface and contour of  $V^2$  considering  $N = 2$ ,  $T_1 = 3$  days,  $\rho = 0.5$  and  $T = 30$  days.

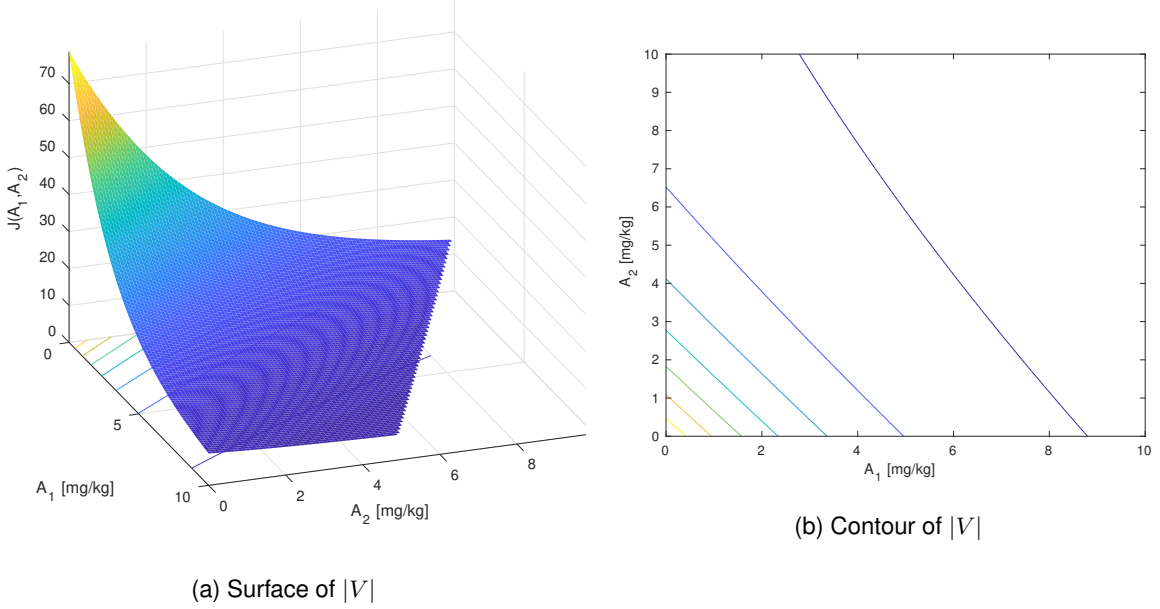


Figure 5.11: Surface and contour of  $|V|$  considering  $N = 2$ ,  $T_1 = 3$  days,  $\rho = 0.5$  and  $T = 30$  days.

By observing the scales of the Z-axis of both surfaces, it is possible to conclude that the surface of  $|V|$  is smoother than the surface of  $V^2$ . It also important to say that, for instance,  $A_1, A_2 \geq 5$ , the  $V^2$  presents an almost flat surface, which can difficult the optimization process. This is due to the fact that, for those amplitudes (also for the time interval considered  $T_1 = 3$  days), the tumor volume time evolution is already close to zero, in addiction to the fact that a value lower than 1 squared is even smaller. Again, this leads to the conclusion that the  $V^2$  does not give importance to the tumor volume when it is close to zero. The following table 5.1 resumes some important advantages and disadvantages of  $V^2$  and  $|V|$ .

Table 5.1: Advantages and Disadvantages of  $V^2$  and  $|V|$ .

	Advantages	Disadvantages
$V^2$	<ul style="list-style-type: none"> <li>For <math>V(0) &gt; 1</math>: rapid tumor volume reduction;</li> <li>For situations where what matters is reducing the tumor, regardless its final value.</li> </ul>	<ul style="list-style-type: none"> <li>For <math>V(0) &lt; 1</math>: slow tumor volume reduction; Does not care about small volume values;</li> </ul>
$ V $	<ul style="list-style-type: none"> <li>Reduces the tumor volume to its minimum value possible.</li> </ul>	<ul style="list-style-type: none"> <li>For <math>V(0) &gt; 1</math>: slower tumor volume reduction than with <math>V^2</math>.</li> </ul>

## Reducing Side Effect

For the third requirement, it is necessary to add a new term to the objective function that penalizes all the Dirac amplitudes. Actually this term is similar to the term added in equation (??) to also minimize the drug dosages. Similarly to the previous section, squared amplitudes or absolute value of amplitudes can be used. So now there are four different objective functions that can be considered, considering the integral of  $V^2$  or  $|V|$  and the sum of  $A_n^2$  or  $|A_n|$ .

Simulating the system with  $N = 2$ ,  $T_n = 3$  for  $n = 1$ ,  $T = 30$ ,  $\rho = 0.5$ ,  $C_{max} = 10 \text{ mg/kg}$  and  $N$  variable amplitudes, the figure 5.12 is obtained, considering all four possibilities for objective functions.

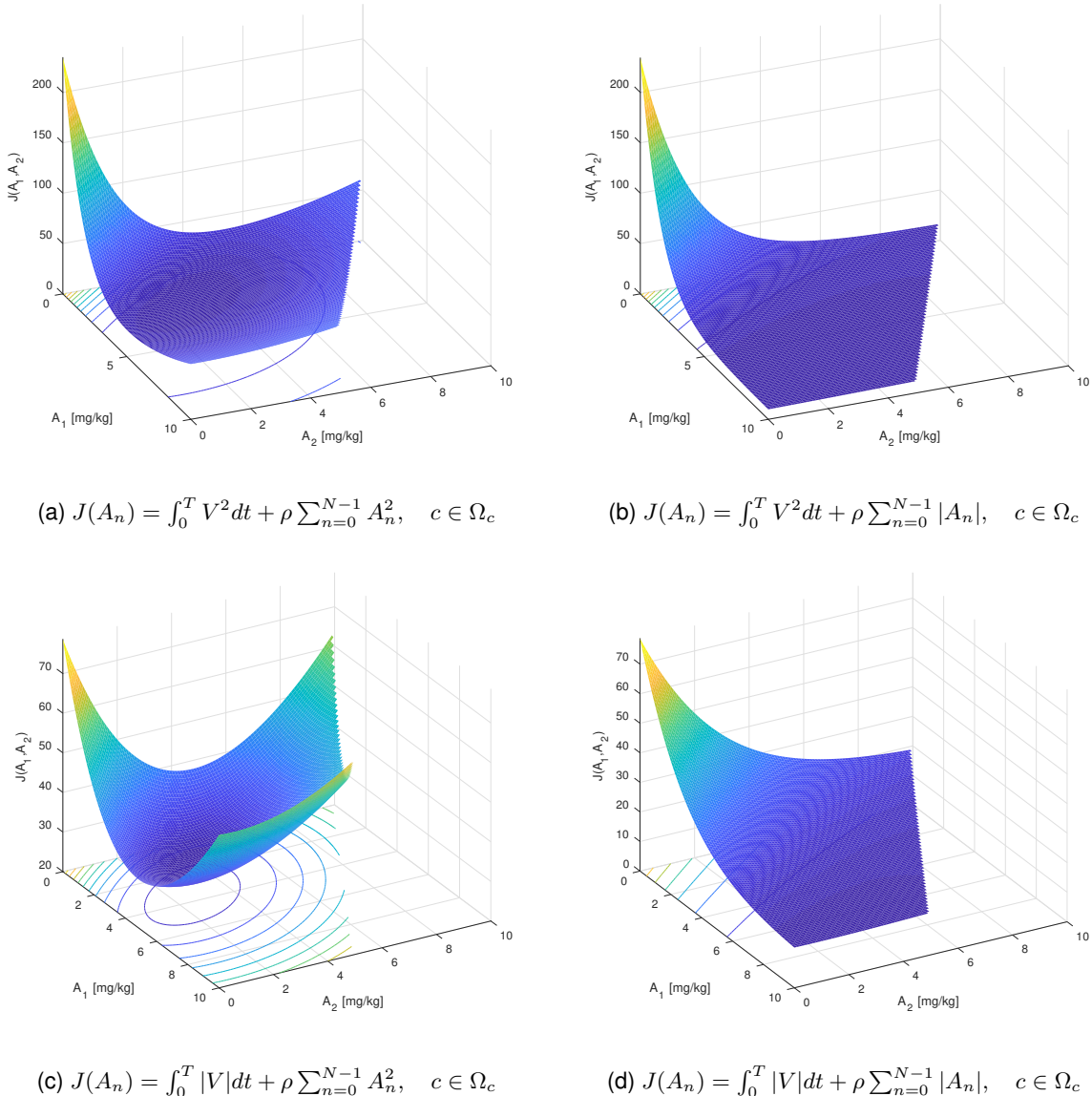


Figure 5.12: Surface and contour of different objective functions considering  $N = 2$ ,  $T_1 = 3 \text{ days}$ ,  $\rho = 0.5$  and  $T = 30 \text{ days}$ .

The amplitudes found to be optimal for each of the objective function presented in figure 5.12 and the corresponding tumor volume final value are presented in the following table.

Table 5.2: Amplitudes found to be optimal for each objective function presented in figure 5.12 and the corresponding tumor volume final value.

	$A_n^2$	$ A_n $
$V^2$	$[3.6346, 2.438], V(30) = 0.347$	$[10, 0], V(30) = 0.0532$
$ V $	$[3.5141, 2.609], V(30) = 0.3339$	$[10, 0.95], V(30) = 0.0359$

Note that the contour presented in figures 5.12a and 5.12c suggest a convex objective function. The convexity is more clear in figure 5.12c.

As previously stated, regardless of which objective function is considered, the two terms in this equation need to be balanced depending on what kind of solution we are looking for. If  $\rho$  increases, the term that corresponds to the sum of the amplitudes will be bigger than the term that corresponds to the time evolution of the tumor volume. Because of that, the most important thing for the controller is minimizing the amplitudes, independently if the tumor is minimized or not. In the other way around, in the limit where  $\rho \rightarrow 0$ , the controller will choose to increase amplitudes at maximum possible, respecting the constraint. So, choosing the parameter  $\rho$  influences the solution of the problem, as it can be demonstrated below.

#### 5.4.1 Influence of parameter $\rho$

Independently of the  $\rho$  value, the values for the optimal amplitudes will decrease  $A_1^* > A_2^* > \dots > A_N^*$ . This happens because the values of the initial amplitudes cause higher impact in the tumor volume evolution, as stated at the end of section 5.4. In order to counteract this effect, it is possible to separate the amplitudes in the objective function and apply different weights for each amplitude. So, the weight of the first amplitude must be higher than the weight of the second amplitude, and so on and so forth, creating a decay, which can be done in many ways. For instance, a percentage decay can be used, meaning that, the weight applied to the amplitude  $n$ ,  $w_n$ , is a percentage of the weight applied to the previous amplitude:  $w_n = \alpha w_{n-1}$ , where  $\alpha$  is the percentage decay, with  $w_0 = \rho$ . Another possibility is to use the parameter  $\rho$  as the decay rate, meaning that,  $w_n = \rho w_{n-1}$ , with  $w_0 = \rho$ . Besides the decay, it is important to study the case when the tumor initial volume change. If  $V(0)$  increases, the average value of the integral term in the objective function will also increase. In the limit, the balance between the integral term and the amplitudes penalization term can be affected, decreasing the importance of minimizing the amplitudes. Because of that, let us consider that all the amplitudes weights are proportional to the initial tumor volume  $w_n \propto V(0)$ .

The toxicity constraint can also be fulfilled by adjusting the value of  $\rho$  and not just by the constraints in the concentration compartments. To do that, it is necessary to answer the following question: what are the values of  $\rho$  that give different optimal solutions for different maximum constraints. In other words, if  $\rho$  is small, the amplitudes penalization is also small, which means that the amplitudes are allowed to have higher value, probably reaching their maximum value, given by the toxicity constraint. So the question is from which  $\rho$  values the optimal amplitudes do not reach their maximum value? The answer to this question is given by the analysis of the minimum value of the objective function as a function of

$\rho$ . Each curve in figure 5.13 represents the minimum value of the objective function for different values of  $\rho$ , for a specific constraint value  $C_{max}$ , considering squared amplitudes and the absolute value of the amplitudes. For this figure the parameters  $N = 10$ ,  $T_n = 3$  for  $n = 1, \dots, 9$ ,  $T = 30$  days and  $C_{max} = 10$  mg/kg are considered.

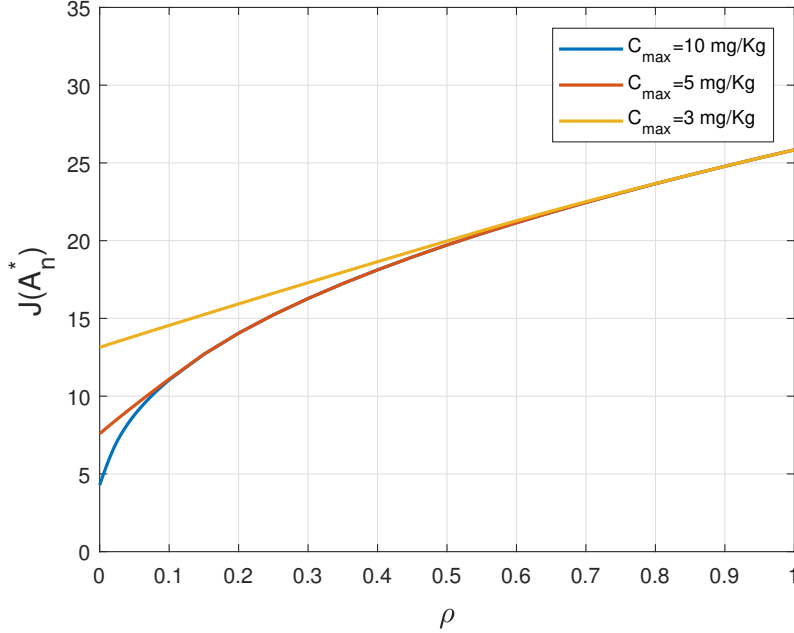


Figure 5.13: Optimal solutions depending on  $\rho$ , for different values of  $C_{max}$ , with  $\alpha = 0.9$

It is possible to analyze several things:

- The minimum value of the objective function increases when  $\rho$  increases. This is due to the fact that for small values of  $\rho$ , the amplitudes can have higher values, respecting the constraints, and for higher dosages, smaller the tumor gets;
- When  $\rho$  decreases and the constraint value increases, the minimum value of the objective function decreases. This is due to the fact that for higher constraints, the amplitudes are allowed to have higher values, which will have more effect in the tumor;
- For  $\rho \in [0.6, \infty]$ , the three curves have the same value. This means that, for  $\rho$  in that interval, the minimum value of the objective function is independent of the constraint value. In other words, it means that the drug concentration in the organism is less than 10, 5 or even 3 mg/kg.

Using the information provided by figure 5.13, it is also possible to verify the values of  $\rho$  that fulfill the toxicity constraint. For instance, as stated before, for  $\rho = 0.6$ , the minimum value of the objective function becomes independent from the toxicity constraint  $C_{max} = 3$  mg/kg. So, if  $\rho \geq 0.6$ , the drug concentration in the organism will be less or equal than 3 mg/kg. The same applies to the constraint  $C_{max} = 5$  mg/kg, where now  $\rho$  must be higher than  $\rho \geq 0.15$  and constraint  $C_{max} = 10$ , where  $\rho \geq 0.02$ .

The choice of the appropriate value for parameter  $\rho$  translates the robustness of the controller. For values of  $\rho$  in the region  $[0, 0.2]$ , the minimum value of the objective function has a larger variation

than for the region  $[0.2, \infty]$ . In other words, if  $\rho$  is in the first region  $[0, 0.2]$ , any small variation  $\Delta\rho$  will have a higher impact on the minimum value of the objective function than if  $\rho$  is in the second region  $[0.2, \infty]$ . Because of that, less impact means more robustness. However, for  $\rho$  in the second region, the amplitudes will decrease and, consequently, the tumor evolution will increase. So, there is a parallelism between robustness and performance. In figure 5.14 is possible to verify the parallelism. In figure 5.14a the optimal outputs of the Administration model, Pharmacokinetics and Pharmacodynamics are represented, with  $\rho = 0.5$ . Note that the tumor volume at  $t = 30$  days is higher than if  $\rho = 0.002$ , in figure 5.14b.

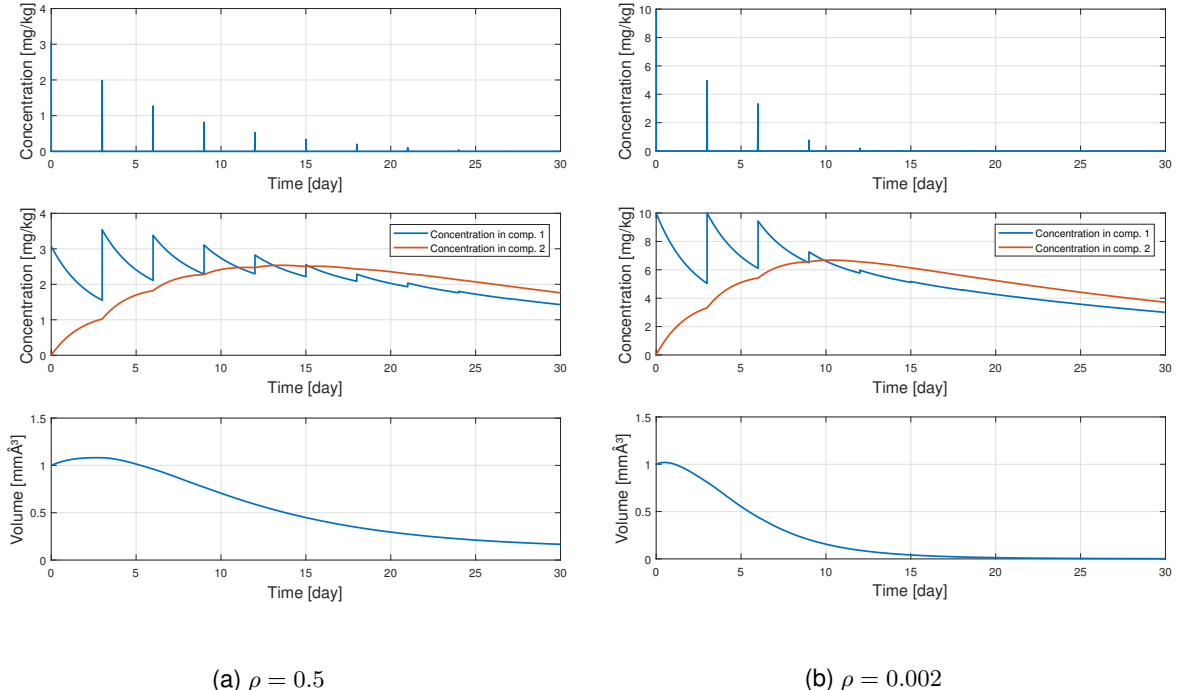


Figure 5.14: Optimal output signals of Administration model,  $I(t)$ , Pharmacokinetics,  $c(t)$ , and Pharmacodynamics,  $u(t)$ , using a percentage decay with  $\alpha = 0.9$ ,  $N = 10$ ,  $T_n = 3$  for  $n = 1,..,N - 1$  and  $C_{max} = 10 \text{ mg/kg}$ .

### 5.4.2 Influence of parameter $T$

In the previous section, the influence of the parameter  $\rho$  was analyzed, in terms of constraints fulfillment, performance and robustness. However, the time horizon  $T$  also influences the optimal solution in such a way that for high  $T$ , the optimization will have more information about the tumor volume time evolution. In the ideal case  $T = \infty$ , which is not possible for computations. So the question arises: how large the time horizon must be in order to have a more conscious (about the tumor volume time evolution) optimal solution? To answer the question, one must analyze the minimum value of the objective function for different values of  $T$ .

There are two ways of describing the  $T$  variation. One of them is to fix the time intervals between administrations,  $T_n$ , to a certain value, and increase  $T$ . The other one is to maintain a certain relation

between  $T$  and  $T_n$ , while increasing  $T$ . Figure 5.15 represents the evolution of the objective function minimum value depending on parameter  $T$ , using fixed time intervals (figure 5.15a) and fixed relation between time intervals and time horizon (figure 5.15b) with  $\frac{T}{T_n} = 10$  for  $n = 1, \dots, N - 1$ .

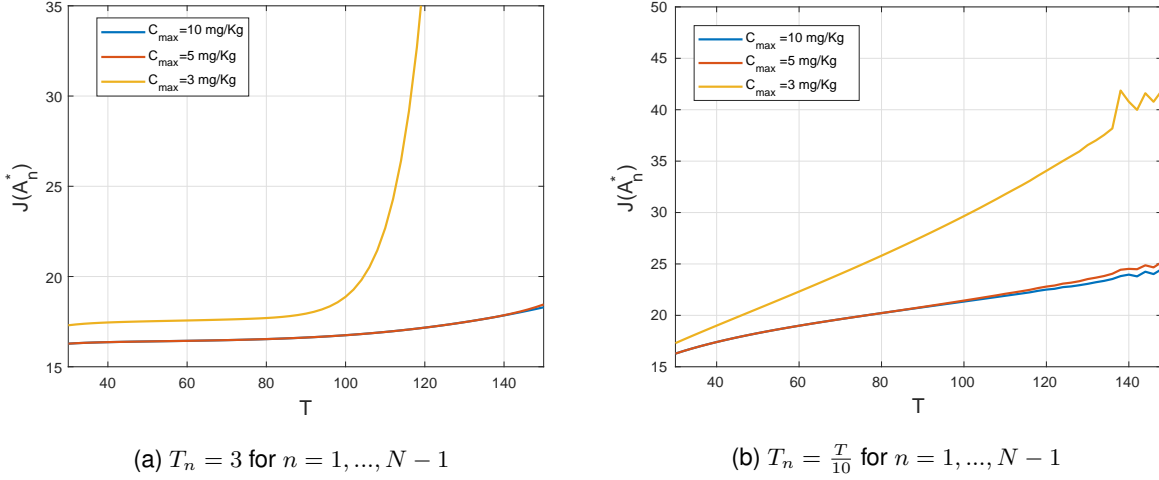
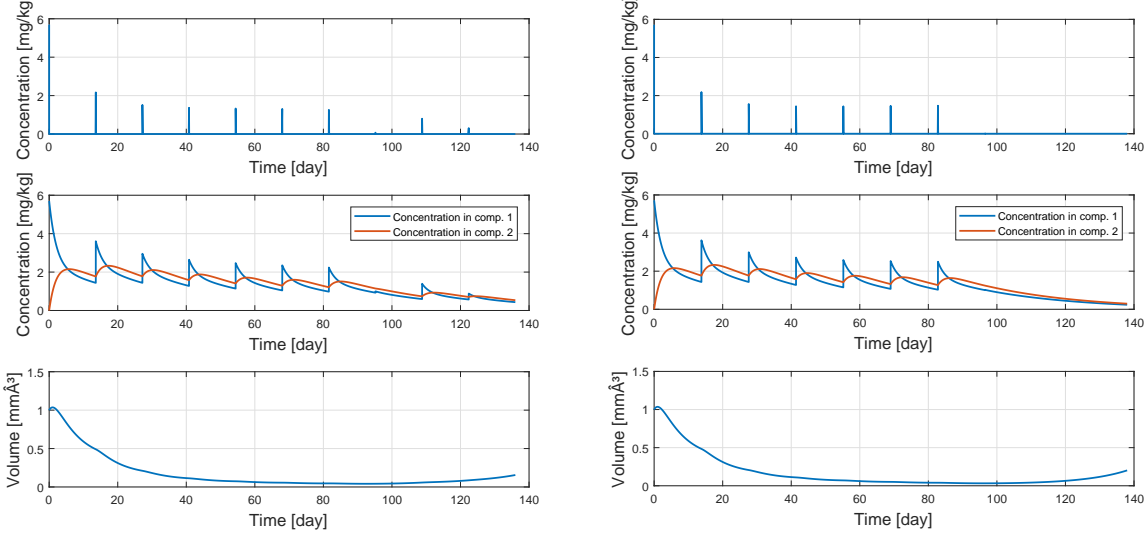


Figure 5.15: Optimal solutions depending on  $T$ , for different values of  $C_{max}$ , with  $\alpha = 0.9$ ,  $N = 10$  and  $\rho = 0.3$

As it is possible to see, the minimum value of the objective function increase when  $T$  increases. This is due to the fact that, when  $T = T + \Delta T$ , there is more area considered in the integral of the volume squared term of the objective function, even if the tumor volume decreases.

For the case where fixed time intervals are considered (figure 5.15a), when  $T = T + \Delta T$ , because there is more information about the tumor volume time evolution and the Dirac impulses are applied in the same place, its amplitudes will have to increase in order to continuously minimize the volume. This leads to the reason why the minimum value of the objective function evolution differ when different constraints are considered. Furthermore, for instance, for the constraint  $C_{max} = 3 \text{ mg/kg}$  and for relatively large  $T$ , the curve has a large increase because the amplitudes have reached its maximum value and, because of that, the tumor volume starts to increase. As previously concluded, there is also values of  $T$  that allow the amplitudes to not reach its maximum values. Those values also correspond to the values of  $T$  where the curves separate.

For the case where there is a fixed relation between time intervals and time horizon, the analysis is similar. However there is an important detail to be discussed. Note the different behavior of the curves in figure 5.15b, when  $T \geq 130$ . This is due to the fact that, for the past administrations, the impact that the dosages have in the tumor versus their amplitude, in the objective function, lead to very small amplitudes, depending on the time interval. In figure 5.16 it is possible to see this effect. In figure 5.16a it is possible to see all the 10 amplitudes and in figure 5.16b the last three amplitudes have very small positive amplitudes.



(a)  $T = 136, T_n = 13.6$  for  $n = 1, \dots, N - 1$

(b)  $T = 138, T_n = 13.8$  for  $n = 1, \dots, N - 1$

Figure 5.16: Optimal solutions for  $T = 136$  and  $T = 138$ , with  $\alpha = 0.9$ ,  $N = 10$  and  $\rho = 0.3$

This aspect is important in such a way that it tells us that, when the tumor volume gets small, the impact of the amplitudes is also small and, because the parameter  $\rho$  for those amplitudes is not zero, the controller prefers to decrease the dosage instead of continuously minimizing the tumor. This may not be the ideal solution, but for the objective function described above this is what happens. One possible solution is to put  $\rho = 0$  from amplitude  $A_m$ , where  $1 \leq m \leq N$ , until  $A_N$ .

### 5.4.3 Receding Horizon Control

In the previous section, it was concluded that  $T$  must be a finite parameter. Also, when  $T$  increases, the information that the controller has about the tumor volume evolution also increases. However, it is important to notice that the mathematical models used in the model described in chapter 4 were developed based on knowledge of biochemical, physiological and/or physical processes and not based on actual experimental data. This means that their behavior can introduce error between what they predict and what is really happening in the human organism. The longer the time horizon  $T$  (simulation time), the greater this error can become. So, there is a parallelism between information and error.

Receding Horizon Control (RHC), also known as Model Predictive Control (MPC), is a control technique in which the system input (for instance, the treatment plan for the patient) is determined in different recalculation instants, by solving an optimal control (OC) problem (in this case, optimal impulsive control (OIC) problem), over a finite prediction horizon into the future [24]. Consider the following example: imagine a driver in his car, that can only see the road once. After knowing all the information about the road ahead, the driver applies the exact controls to the car in order to reach a certain point. Note that the driver can only see until a certain distance ahead. This is what the OC problem tries to solve: in a finite time horizon, calculate the exact input in order to fulfill some goal. The RHC is what allows the driver to re-open his eyes and see again the road, after a certain blind period  $\Delta T$ . In other words, with

RHC the driver is able to open his eyes and close them almost instantaneously, allowing him to see what he already saw plus  $\Delta T$ , which also allow the driver to adapt the previously calculated input to what he already saw and the new information. In a more general way, RHC introduces feedback which allows the controller to consider perturbations, when the time horizon is moved in time.

Applying this concept to the problem of this work, the following is done: for a finite horizon  $0 \leq t \leq T$ , solve the OIC problem and select, for instance, just the first drug administration to be applied to the patient; next, move the time horizon into the future, for instance  $T_1 \leq t \leq T = T + T_1$ , and solve the new OIC problem, where the new initial conditions correspond to the final conditions of the previous OIC problem in  $t = T_1^-$ ; repeat the process (iterate the process) by moving the time horizon.

Figure 5.17 illustrates the RHC process for three iterations. In iteration two, there is one drug administration already selected for the treatment, and the OIC problem corresponds to  $0^2 \leq t \leq T^2$ , where  $0^i$  and  $T^i$  are the time horizon limits for iteration  $i$ . In the figure, the dislocation time considered  $\Delta T$  is  $\Delta T = T_n$ , with  $T_n = \text{constant}$  for  $n = 1, \dots, N - 1$ . Depending on the dislocation time parameter, the number of selected drug administrations in each iteration can vary. When  $\Delta T$  increases, the number of selected administration also increase, which means that the receding horizon evolves faster. However, this is not necessarily good. For instance, if  $\Delta T > T_1 + T_2$ , the number of selected administrations in each iteration is  $\#s^i = 2$ . This means that a new piece of information is added to the OIC problem in every two time intervals, which can lead to more sudden changes in the selected administrations. If, between two time intervals, the tumor increases, the Receding Horizon Control will only adapt to that change after two administrations.

Because each selected drug administration have more information about the tumor volume time evolution, this technique creates the idea of feedback to the optimal controller. Each time the time horizon moves, the previous optimal solution re-adapts to the new information, even if the tumor suddenly

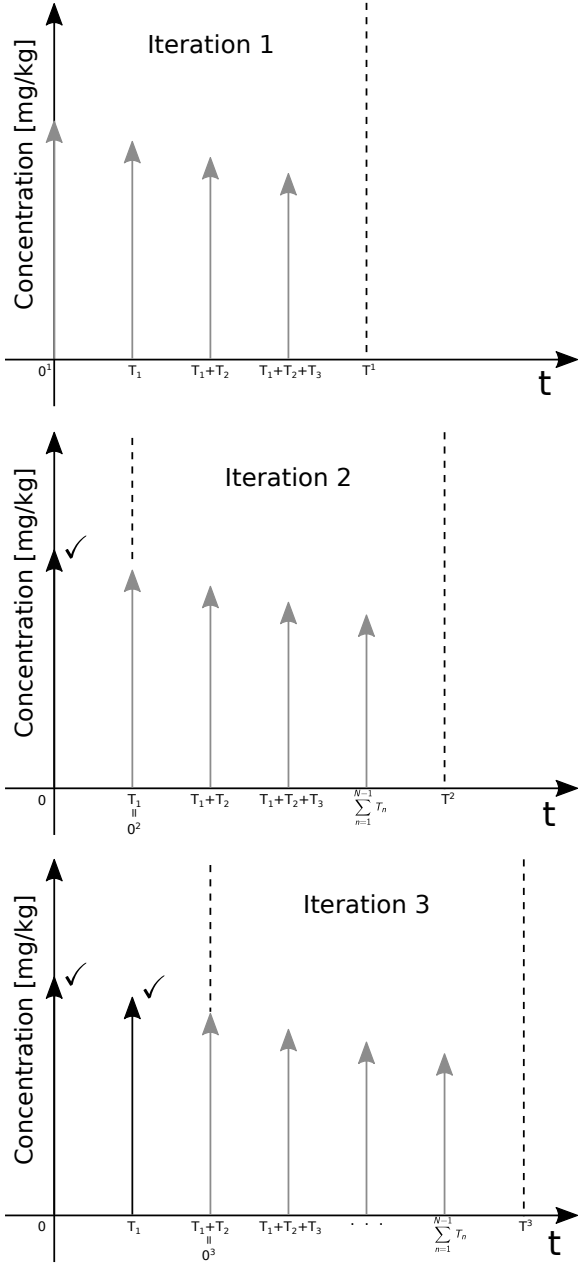


Figure 5.17: Receding Horizon illustration of three iterations, with  $N = 4$ .

increases, just like the driver re-adapts to any change in the region that he already saw but also in the new region that he can see, now that he has driven a certain distance. This being said, it is also important to say that RHC is more suitable for slow linear and nonlinear systems since constrained optimization problems takes time to be solved online [24].

There is another aspect to be discussed. We now know that in each iteration, a constrained OIC problem is solved. But remember that in the OIC problem discussed in section 5.4, a percentage decay rate with  $\alpha = 0.9$  is considered. It means that for a certain time horizon  $T$ , all the dosages weight decrease 10%. In the other hand, for instance, if  $\Delta T = T_n$ , in iteration  $i$  the weights applied to each drug dosage correspond to the same weights applied to the drug dosages in iteration  $i - 1$ . In other words, the weight applied to the drug dosage  $s(i)$  is the same weight applied to  $s(i - 1)$ . So, there can be two variants of the RHC for the problem considered in this work. Variant one where the parameter  $\rho$  is the same in each iteration and, in that case, the situation explained before happens, and variant two where the parameter  $\rho$  decreases the same 10% in each iteration.

Figure 5.18 represents the model simulations considering the two variations explained above. Comparing the two variations, it is possible to conclude that using variation one (figure 5.18a) the dosages are smaller than using variation two (figure 5.18b). Because  $\rho$  is constant between iterations, the weight applied to each dosage is higher than the weight applied using variation two. The consequence of this is that, for a same period of time considered, the tumor volume presents lower values when variation two is considered, as figure 5.18 suggests.

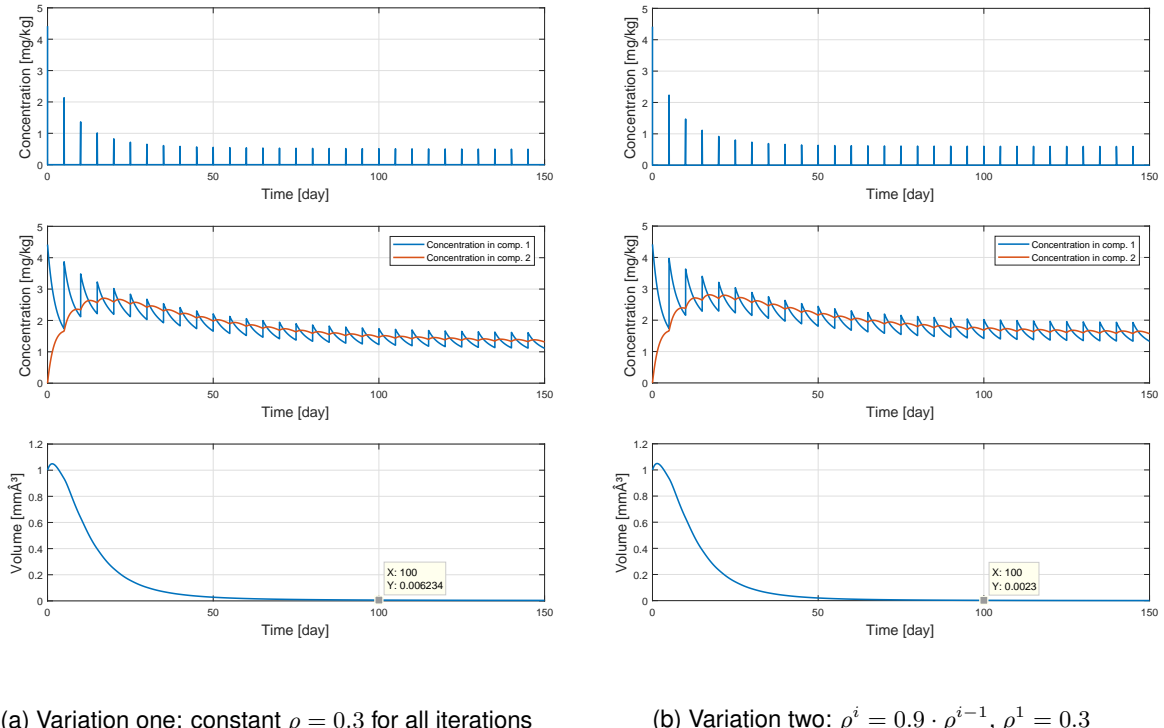


Figure 5.18: Receding Horizon Control simulation considering the two variations

In order to compare RHC to OIC, it is possible to simulate the model considered in this work as the

following figure suggests.

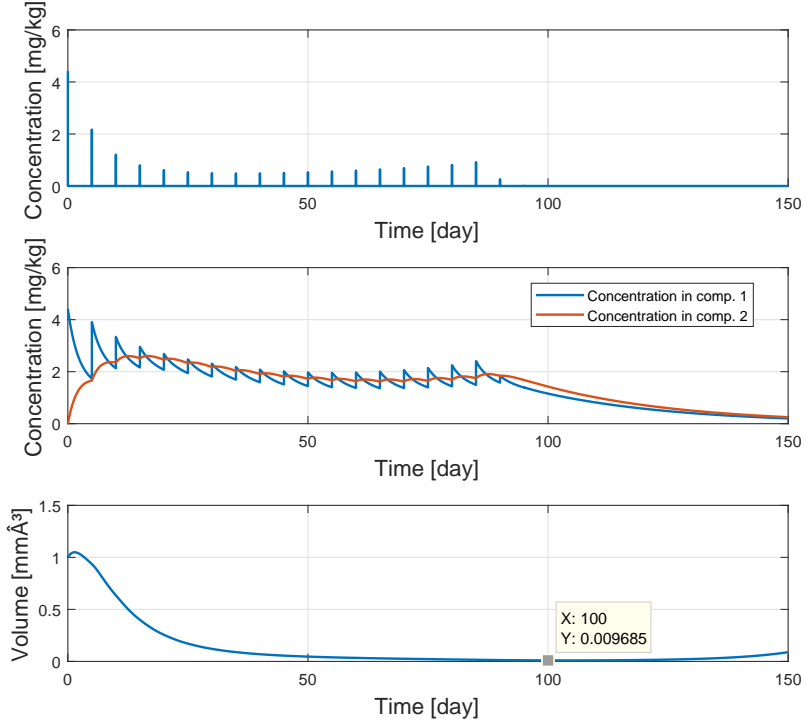


Figure 5.19: Optimal solution for  $T = 150$ ,  $N = 30$ ,  $T_n = 5$  for  $n = 1, \dots, N - 1$  and  $\rho = 0.3$ .

As previously stated, when the tumor volume is too small, the controller chooses to decrease the amplitudes, since their impact is almost null in the volume evolution. Besides that difference between RH and OIC, the other difference is the amplitudes themselves. The reason for that is that the controller does not know anything about the future volume evolution. Actually is possible to see that, in the end of the simulation the tumor volume starts to increase again. Another important aspect is the tumor volume for  $t = 100$  days. Comparing that information with figure 5.18, it is possible to verify that the RCH provides lower values for the tumor volume, independently of the variation considered.

The difference between RH and OIC can be more clear with the introduction of perturbations in the model. The perturbation can be introduced in many different ways: resetting the tumor volume integrator with a different initial condition, introducing an instantaneous change in the tumor volume; change the maximum effect of the drug in the tumor by changing the  $u_{max}$  parameter of the PD model, as stated in chapter 4; or even changing any other parameter of the total model described in chapter 4. In a real case scenario, resetting the integrator with different initial condition correspond to an instantaneous increase of the tumor volume during the treatment which could not be a real phenomenon. Changing the maximum effect of the drug in the human organism could represent a real situation: in a certain period of the treatment, the human organism could react differently to the drug, causing different effects in the tumor volume, for the same drug concentration. Figure 5.20 represents the RHC applied to the model, considering this perturbation occurring twice, at  $t = 45.5$  and  $t = 100.5$  days, where for  $t \in [0, 45.5[$ ,  $u(t) = 1$ , for  $t \in [45.5, 100.5[$ ,  $u(t) = 0.6$  and for  $t \in [100.5, 150]$ ,  $u(t) = 1.4$ , and also considering the

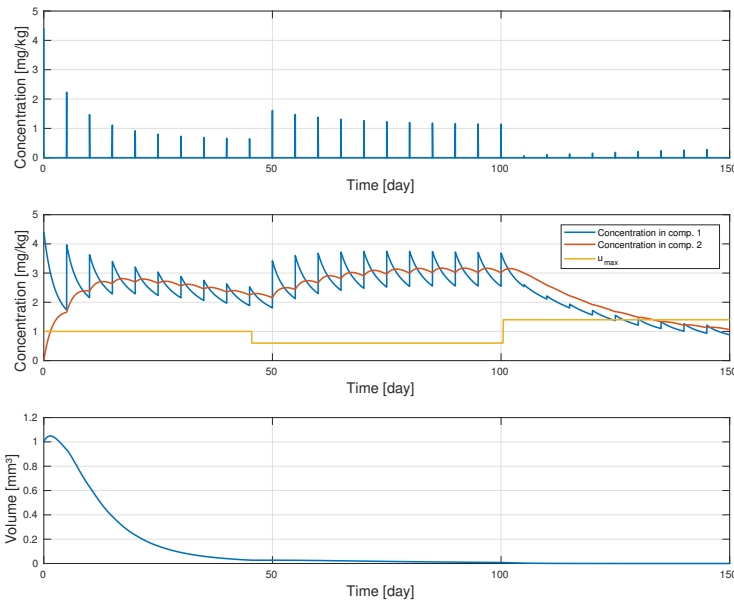


Figure 5.20: Receding Horizon Control simulation considering the variation two, with changes in the parameter  $u_{max}$  as perturbation.

variation two where  $\rho^i = 0.9 \cdot \rho^{i-1}$ ,  $\rho^1 = 0.3$ .

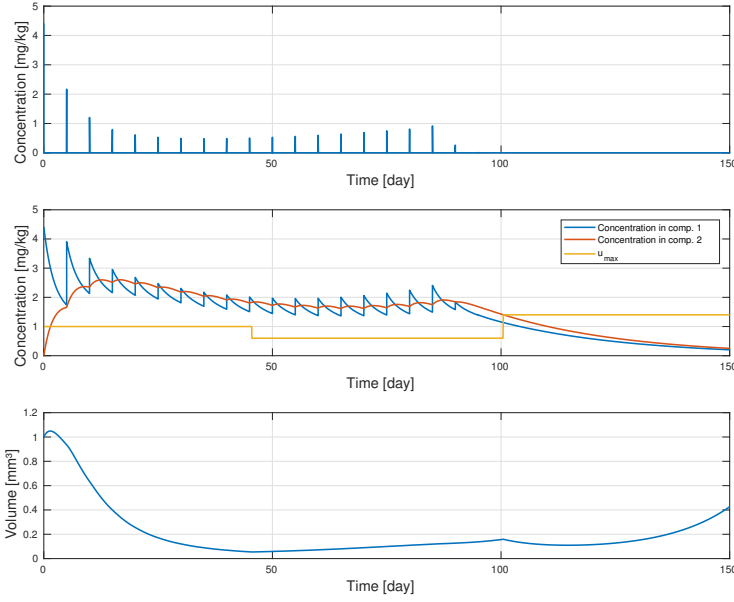


Figure 5.21: Optimal Impulsive Control Simulation with changes in the parameter  $u_{max}$  as perturbation.

For  $t \in [45.5, 100.5]$  the drug has less effect on the tumor volume, so the RHC increases the amplitudes in order to compensate for the loss of effect. For  $t \in [100.5, 150]$  the drug has more effect in the tumor volume, so the RHC decreases the amplitudes in order to reduce the unnecessary side effects

of the drug. Locking to the tumor volume time evolution, it is similar to the evolution presented in figure 5.18b. Simulating now the model using OIC method, figure 5.21 is obtained.

As it is possible to see, the OIC cannot adjust the solution to the perturbations because it does not have feedback, like RHC.

## 5.5 Variable amplitudes and periodic time intervals

In this section, besides having variable amplitudes, a periodic but unknown value for the time interval is considered. Figure 5.22 represents the objective function described in figure 5.12a considering only two amplitudes, with the first amplitude  $A_1$  fixed and the second amplitude  $A_2$  and the time interval  $T_1$  are variables.

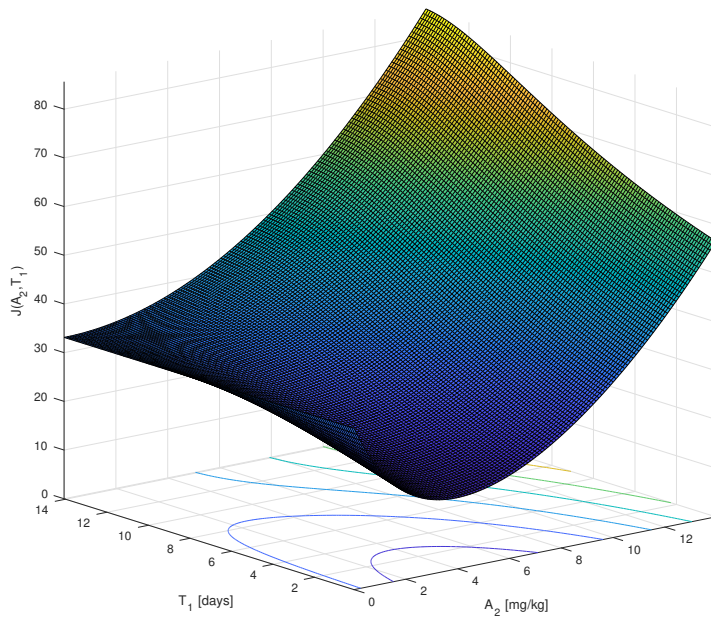


Figure 5.22: Objective function as a function of the second amplitude and the time interval, considering  $T = 15$  days,  $N = 2$  and  $A_1 = 1$  mg/kg.

As it is possible to see in the contour of the curve, the objective function does have a minimum value for small values of the time interval. But when the time intervals increases, the objective function becomes more flat, for  $A_2 = 4$  for instance. These flat areas are problematic because, for initial points in this area, the optimization methods will not be able to find a good search direction in which the objective function decreases. Doing some simulations with this objective function, and increasing the number of amplitudes  $N$ , it is possible to conclude that the function is not convex because considering different initial points (for the optimization algorithm), different minimums where found (local minimums), which suggests the non convexity. Figure 5.23 represents the tumor volume time evolution using different solutions that came from different initial conditions in the optimization method. Initial condition two and six are the ones that give a faster decrease in the tumor volume initially. Those correspond to the

solutions where the time interval is near zero, in which the objective functions presents a lower value. This means that, for all the initial conditions considered in figure 5.23, the solutions two and six could represent the best local minimums to be chosen as the real solution of the problem. Because of that the following question is raised: in a real scenario, is acceptable or satisfactory having the periodic time interval near zero? If yes, then the problem is solved. If not, then the next question is: what can be done to look for a different solution? One possible answer is to change the objective function (add a new term) in order to penalize small time intervals. This new term must be a function of the periodic time interval that if the time interval is, for instance, near zero, the term must output a large value so it can change the total objective function in order to contradict the best local minimum. There are many different functions that can do so.

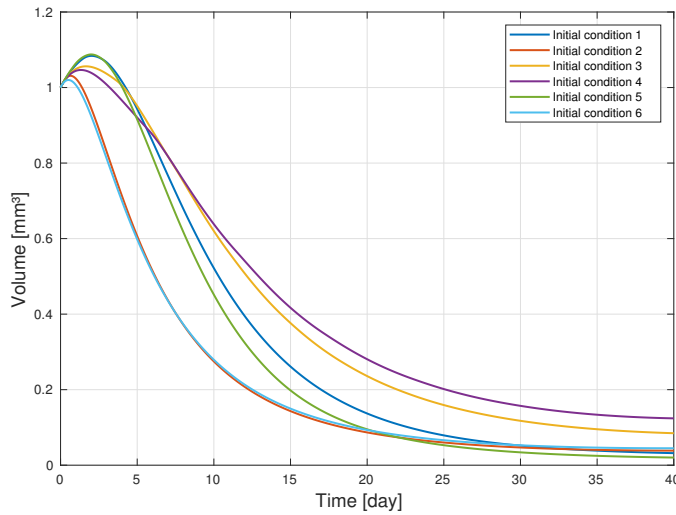


Figure 5.23: Tumor volume time evolution considering solutions from different initial conditions in the optimization method

The function  $\frac{1}{T_1}$  could be used for that sake. Another function could be the negative and translated exponential function  $e^{-T_1+\tau}$ , where  $\tau$  is the translation parameter. For  $T_1 \gg 0$ , the exponential function presents a higher range of variation than the function  $\frac{1}{T_1}$ . In other words considering  $T_1 \gg 0$  and  $\delta > 0$ ,  $|e^{-T_1+\tau} - e^{-(T_1+\delta)+\tau}| > \left| \frac{1}{T_1} - \frac{1}{T_1+\delta} \right|$ . This fact represents an advantage for the exponential and a consequential disadvantage of the  $\frac{1}{T_1}$  function, in the problem considered. This is due to the fact that if the range of variation increases, the difference between choosing  $T_1$  or  $T_1 + \delta$ , in terms of optimality, also increase allowing the optimal controller to make a more clear choice.

Considering the exponential function as the new term of the objective function, there are two parameters to be defined: the translation parameter  $\tau$  and the weight  $\omega$  applied to the exponential term. The final expression of the new term is  $\omega \cdot e^{-T_1+\tau}$ . Similarly to the parameter  $\rho$  applied to the amplitudes term in the objective function, the definition of these two news parameters can influence the optimal solution to the problem. The parameter  $\tau$  must be such that when the time interval goes to zero, the term must go to infinity or, at least, must present very high values. So it can be  $\tau = 2$ . Concerning the parameter  $\omega$ , its effect can be analyzed by simulating the system with different initial conditions for each different

value for  $\omega$ . Using three different values for  $\omega$ , the following figure is obtained.

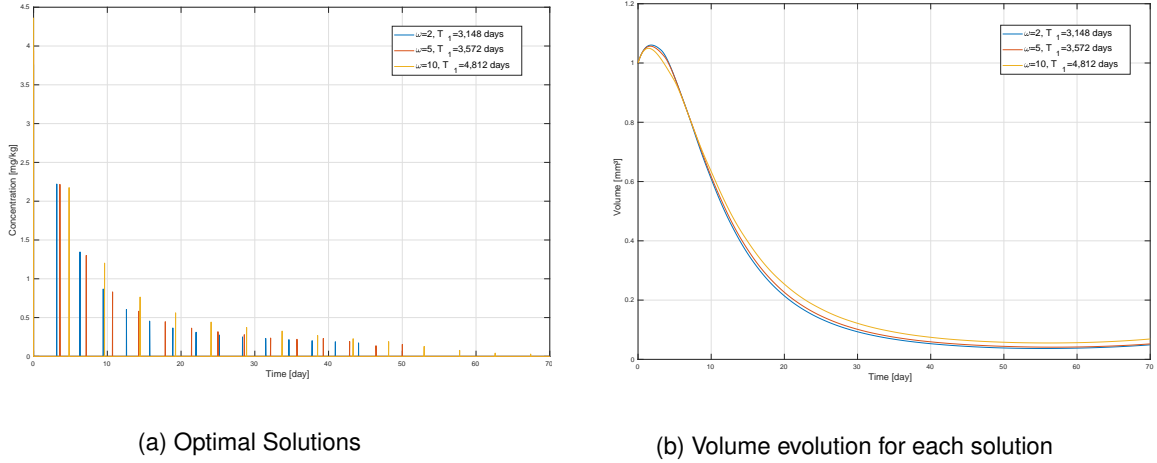


Figure 5.24: Optimal solutions and tumor volume evolutions for each solution, for  $\omega = 2$ ,  $\omega = 5$  and  $\omega = 10$ .

As it is possible to see in figure 5.24a, when  $\omega$  increases, the time interval  $T_1$  also increases. It is also possible to verify that when  $\omega$  increases, the final value of the tumor volume also increases. This means that when  $\omega$  increases, the new term becomes more important than the other terms, in particular the term that corresponds to the minimization of the tumor volume (the integral of the squared tumor volume) that tries to decrease the time interval.

So far, the weight applied to the exponential term corresponds to a constant value. This becomes a disadvantage when different initial conditions of the tumor volume are considered. If the initial tumor volume decreases, then the integral term in the objective function also decreases, since the area under the tumor volume curve also decreases. If the weight applied to the exponential term maintains its constant value, this term will always be more important to the minimization methods. So if the initial tumor volume decreases, the time interval will increase, considering a constant value of the weight  $\omega$ . In order to contradict this effect, the weight applied to the exponential term can be proportional to the initial tumor volume, so the weight applied is  $\omega_N = V(0)\omega$ , where  $\omega_N$  is the new weight.

As previously stated, the purpose of the new exponential term in the objective function is to penalize small values of the time interval. Also depending on the parameter  $\omega$ , the importance of this penalization can be higher or lower. Besides this penalization, there is another solution for the problem considered here, that considers a new parameter  $T_1^C$ . This parameter, called the central value of the time interval, corresponds to a value around which solutions will be found. In other words, the goal here is to find solutions by specifying a region where the time interval must be, around  $T_1^C$ . This can be accomplished by replacing the exponential term with a quadratic term, where its minimum is in  $T_1^C$ . So the objective function expression becomes the following

$$J(A_n, T_1) = \int_0^T V^2 dt + \rho \sum_{n=0}^{N-1} A_n^2 + \omega_N(T_1 - T_1^C)^2, \quad c \in \Omega_c. \quad (5.25)$$

Using optimization methods (SQP) to minimize the objective function, the figure 5.25 is obtained.

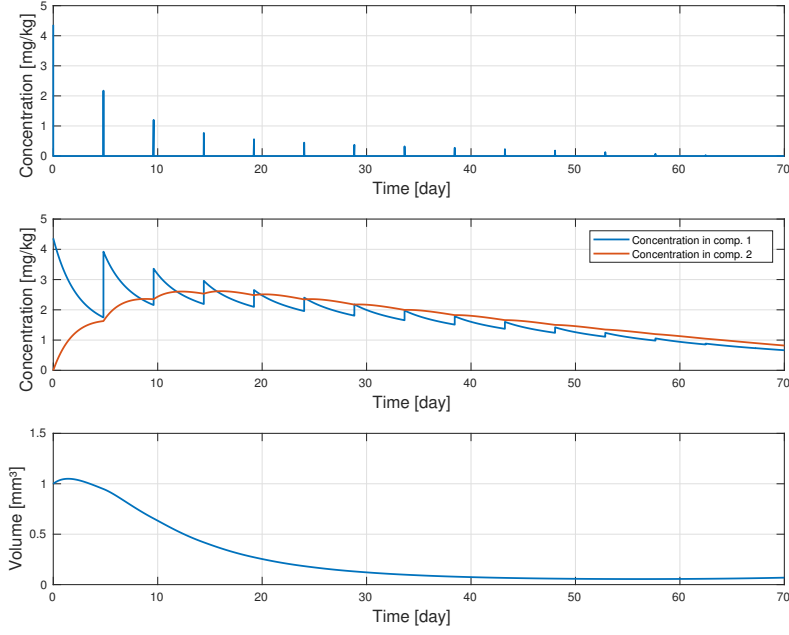


Figure 5.25: Optimal solution considering periodic time interval, with  $N = 10$ ,  $T_1^C = 5$  and  $\omega_N = 2$ . The optimal time interval is  $T_1^* = 4.8049$  days.

The solution found to be optimal does not correspond to the case in which the time interval is equal to the central value of the time interval parameter. Actually the optimal time interval is  $T_1^* = 4.8049$  days. This shows that using a quadratic function in the objective function in order to "force" a solution continues to be an optimal control problem, since the solution can vary depending on the other terms of the objective function.

As previously stated, when the time intervals are considered to be also an optimization variable, the objective function loses its convexity, presenting flat areas and more than one minimum. The introduction of the time interval penalization function does not turn the objective function convex. It only penalizes small time intervals. So the approach used in this work to find the best solution is running the optimization algorithms using ten different initial points and then choose the solution that gives the lowest objective function value. This approach takes a considerable amount of time. Each optimization takes about one and a half hour to be completed, which must be multiplied by ten to give the amount of time used to find the best solution (among all ten solutions).

### 5.5.1 Influence of the Immune System

As stated previously in section 3.3, the Immune System plays an important role in the case in which the patient is diagnosed with cancer. It can help killing the tumor and, consequently, decreasing the total amount of drug administrated to the patient, reducing the side effects of the treatment. Mathematically, the influence of the IS corresponds to the addition of a new differential equation  $\dot{r}(t)$ , where  $r$  is the immunocompetent cell densities related to various types of immune cells, that influence the tumor volume

differential equation through also the addition of a new term  $-\theta Vr$ , where  $\theta$  is a constant coefficient and  $V$  the tumor volume. So the total expression of the tumor volume differential equation, considering also the effect of the treatment, is

$$\begin{cases} \dot{V}(t) = aV(1 - \frac{V}{K}) - \beta uV - \theta Vr \\ \dot{r}(t) = \alpha(1 - \beta V)Vr + \gamma - \delta r \end{cases}, \quad (5.26)$$

where  $u$  is the treatment effect on the tumor. Figure 5.26 represents the solutions found to be optimal with and without the influence of the Immune System.

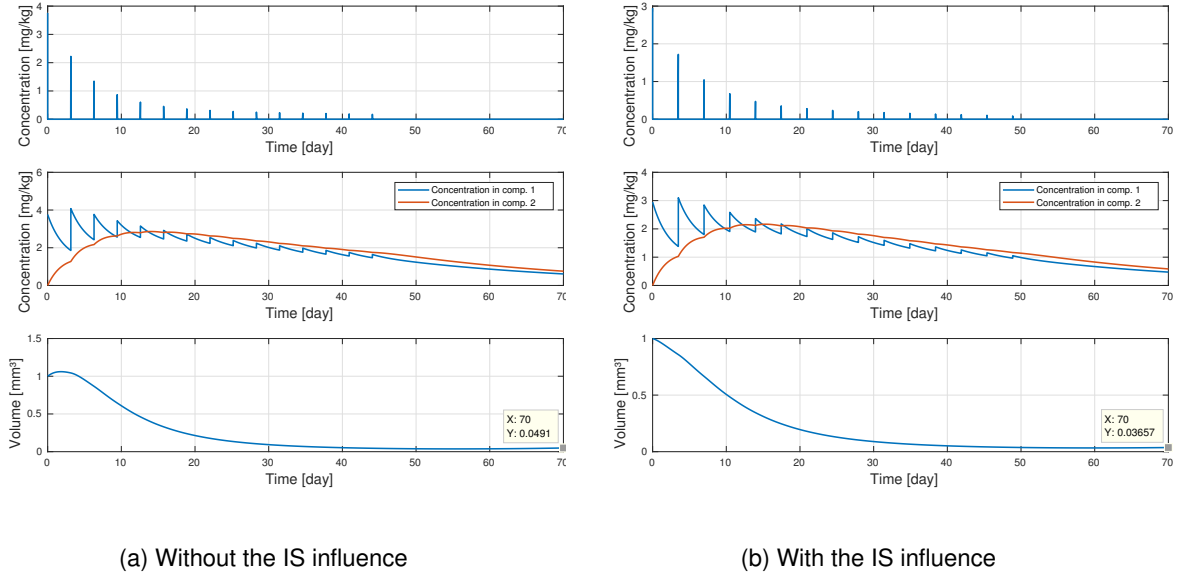


Figure 5.26: Optimal solutions considering the influence of the Immune System.

As it is possible to verify, the IS helps reducing the tumor volume time evolution. This effect can be shown in the first 10 days of treatment, for instance. After that, the tumor evolution is quite similar to the one where the influence of the IS is not considered. Actually this happens because there is also an influence of the tumor in the IS, as it is possible to see in the system of differential equations (5.26), in the equation  $\dot{r}(t)$ . This influence may be more noticeable in figure 5.27, where the immunocompetent cell densities and the tumor volume is represented, without the consideration of the treatment effect  $u(t)$ . Instead of the behavior shown in figure 3.1, the tumor starts to decrease due to the immune system. After that, the tumor affects the immunocompetent cell densities and the immune system starts to weaken. Due to that fact, the tumor increases. Because the immunocompetent cell densities never goes to zero, the tumor will not be able to reach its carrying capacity. This analysis implies that considering the immune system, the tumor presents a weaker behavior in terms of growth. This means that the dosages needed in the treatment can be decreased (as figure 5.26 suggests), allowing the patient to not be so affected by the drug toxic effect.

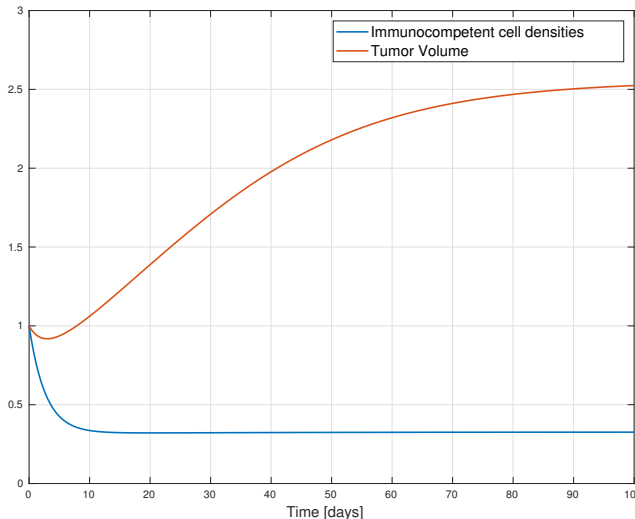


Figure 5.27: Relationship between the tumor volume and the immune system.

### 5.5.2 Influence of the Angiogenesis Process

The proliferation of cancer cells depends on an adequate supply of oxygen and nutrients. This is why the study of the vascular network is important. As previously stated, angiogenesis is the process in which new blood and lymphatic vessels form. Through these new vessels the tumor can obtain the required oxygen and nutrients, and because of that, the angiogenesis process helps the tumor to grow. As in the previous section, mathematically the angiogenesis process corresponds to the addition of a new differential equation  $\dot{q}(t) = S(V, 1) - I(V, q)$ , where  $q$  corresponds to the carrying capacity of the tumor. The functions  $S(V, q)$  and  $I(V, q)$  represent the stimulatory effects that allow the tumor to grow and the inhibitory effects, respectively. These functions can have different expressions. In [12] these functions are defined as follows, considering also the treatment

$$\begin{cases} \dot{V}(t) = aV \left(1 - \frac{V}{q}\right) - \beta u V \\ \dot{q}(t) = \phi V - \varphi q V^{\frac{2}{3}} \end{cases}, \quad (5.27)$$

where  $\phi$  and  $\varphi$  are positive constant rates of the angiogenesis stimulation and inhibition, respectively. Figure 5.28 represents the variation of the carrying capacity as well as the tumor volume, described by the differential equations above.

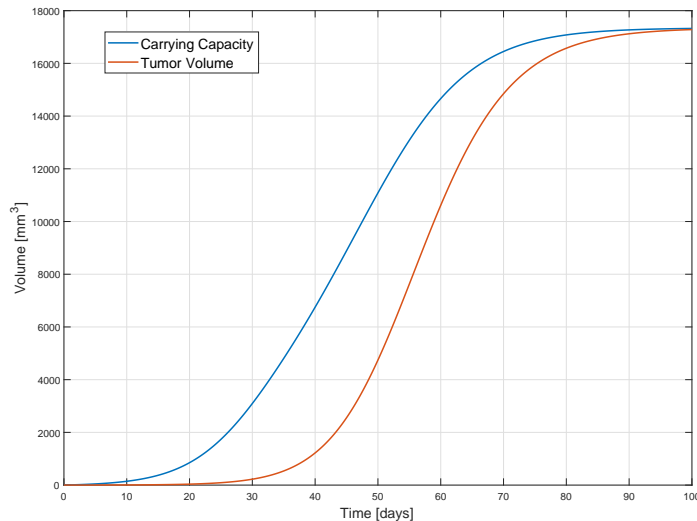
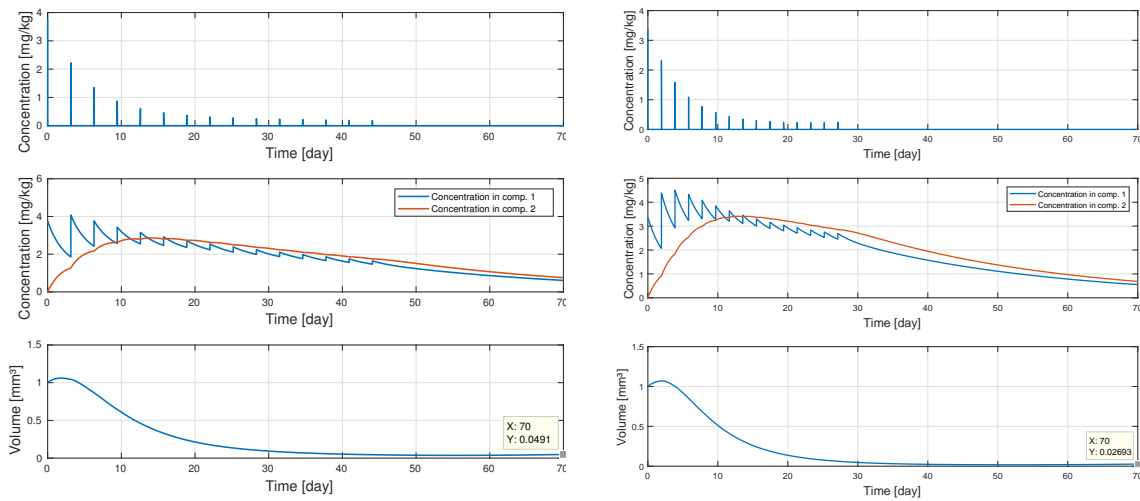


Figure 5.28: Relationship between the tumor volume and the angiogenesis process.

Comparing this behavior with figure 3.1, the angiogenesis helps the tumor to grow faster. Figure 5.29 represents the solutions found to be optimal with and without the consideration of the angiogenesis process.



(a) Without the angiogenesis process influence

(b) With the angiogenesis process influence

Figure 5.29: Optimal solutions considering the influence of the angiogenesis process.

In order to reduce the tumor, the controller decided to decrease the periodic time interval to increase the amount of drug in the human organism at the beginning of the treatment.

As discussed previously, the immune system helps the tumor reduction while the angiogenesis process helps the tumor to grow faster. The question now is what happens when both IS and angiogenesis

process are considered. This question leads to a system of differential equation as follows

$$\begin{cases} \dot{V}(t) = aV \left(1 - \frac{V}{q}\right) - \beta u V - \theta V r \\ \dot{r}(t) = \alpha(1 - \beta V)Vr + \gamma - \delta r \\ \dot{q}(t) = \phi V - \varphi q V^{\frac{2}{3}} \end{cases}. \quad (5.28)$$

Simulating now this system of equation, figure 5.30 is obtained. The tumor starts to decrease due to the influence of the immune system and after that, it starts to increase.

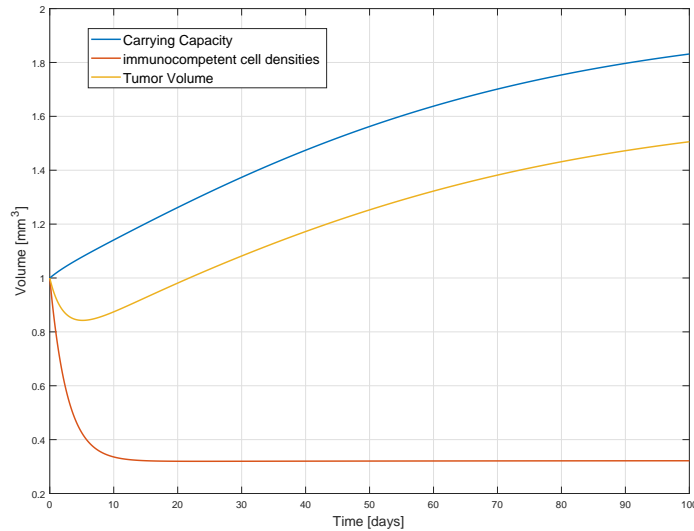


Figure 5.30: Relationship between the tumor volume, the immune system and the angiogenesis process.

The solution found to be optimal is represented in figure 5.31.

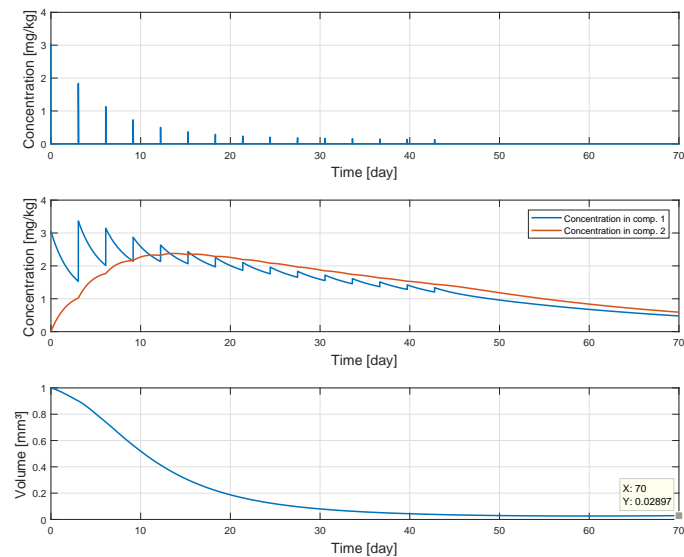


Figure 5.31: Optimal solutions considering the influence of the angiogenesis process and the immune system.

So, minimizing the objective function is actually minimizing the area under the tumor volume curve (minimizing the integral of the tumor). In order to do that, the controller chooses to decrease the time interval in order to apply drug at the beginning of the treatment, where the tumor is higher. In the limit, if the time interval is zero, that would correspond to the case where all the drug is administered at once at  $t = 0$ . But by doing this, the side effects could be worst. This is why new terms were added in order to push the time intervals to be higher. In this section two different terms were considered: the exponential term that penalizes small time intervals; and the quadratic term that forces the optimal time interval to be near some parameter  $T_1^C$ .

## 5.6 Variable amplitudes and time intervals

In this section non periodic and unknown time intervals and amplitudes are considered. If  $N$  is the number of amplitudes, the number of time intervals is  $N - 1$ . In total, the number of variables in this problem is now  $2N - 1$ . When this number increases, the number of possible configurations of the variables also increases which means that the objective function could have more flat areas and local minimums, leading to a more complex problem. As in the previous section, if small time intervals are not penalized, the controller will opt to choose them, in order to minimize the area under the tumor volume curve, since that with small intervals and high amplitudes, the drug concentration on both compartments increases. Many possible solutions can be implemented, but none of them will be best than the other only because when such a complex objective function is considered there is no algorithm to solve it. The new terms added in the last section can be also implemented in this problem but now, each time interval will have its own weight and exponential or quadratic function associated. Besides those solutions, a new objective function is considered, where the main goal now will not be minimizing the area under the tumor volume curve but minimizing the final value of the tumor volume.

### 5.6.1 Minimum Attention Control

As stated in the beginning of section 5.5, the problem of choosing the number  $N$  of impulses and the time intervals  $T_n$  between them is what turns the optimization problem more complex. If  $N$  and  $T_n$  are known, then the adjustment of the amplitudes is simple, as section 5.4 suggests. In this section, Minimum Attention Control is studied in order to understand how can  $N$  and  $T_n$  be determined or, at least, in order to specify an optimization problem that is more simple to solve.

Nowadays, in control engineering, several controller implementations are done in embedded micro-processors and using shared communications networks, in which control tasks share computational and communication resources with other tasks [11]. Typically controllers are still implemented in a time-triggered form, meaning that the control task is executed periodically, where the already developed theory on sample data systems can be used. However over-utilization and over-provisioned hardware can occur, since it might not be necessary to execute the control task every period. This leads to the development of several control strategies in order to reduce computations and communications resources to execute control tasks. Minimum Attention Control (MAC) is one of those strategies, in which the objec-

tive is to minimize the attention the control loop requires. In other words, MAC maximizes the next time instant, while guaranteeing a certain level of closed-loop performance [11]. So the MAC problem is to find a function  $F_{MAC}$  and a function  $h$  such that  $A_n \in F_{MAC}(c(\sum_{i=0}^n T_i))$  and  $T_{n+1} = T_n + h(c(\sum_{i=0}^n T_i))$ , where  $T_n$  corresponds to the time intervals and  $c(T_n)$  correspond to the drug concentration in both compartment at the time instant  $\sum_{i=0}^n T_i$  for  $n = 1, \dots, N$ , with  $T_0 = 0$ .

As previously stated, when the time intervals are also considered to be variable, the objective function becomes non convex. However, this fact motivated the investigation about separating the amplitudes optimization from the time intervals calculation. Different ways were considered in this work: constant areas  $\xi_n \cdot A_n \cdot T_n$ , where  $\xi_n$  corresponds to different weights applied to each area; time intervals depending on the tumor volume evolution  $T_n \propto \log(V(t_{n+1})) - \log(V(t_n))$ , where  $t_n$  correspond to the time instant of the administration  $n$ ; considering a different objective function for the time instants and other for the amplitudes. So the amplitudes are optimized using a certain combination of time intervals. When one of the above ways is used to calculate the time intervals, the amplitudes will no longer be optimal, since the time intervals has changed. Even considering an iterative approach, no equilibrium between the amplitudes optimization and the time intervals calculation was reached. This means that more investigation about this problem is needed. However, in order to continue this work, the amplitudes and time intervals are optimized together using ten different initial point in the optimization algorithm. The minimum that presents the lowest objective function value is then chosen.

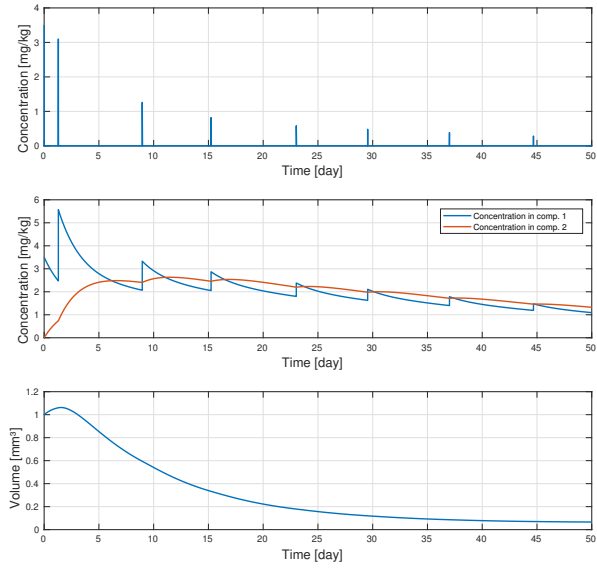
The adaptation of the MAC concept to this work problem is simple, since the control task corresponds to the Dirac impulses and what is needed is to maximize the time intervals between them, maintaining a certain performance that corresponds to the tumor volume minimization.

It is already known that the tumor volume integral term in the objective function (independently if it is the integral of  $V^2$  or  $|V|$ ) will force the concentration to increase when the volume is high, which consequently increases the amplitudes and decreases the time intervals. So the goal is to find a way to maximize the time intervals in such a way that when the volume decreases, the intervals increase. This can be done by using, once more, the exponential penalization or pair of exponentials or even a negative linear or quadratic function, for instance.

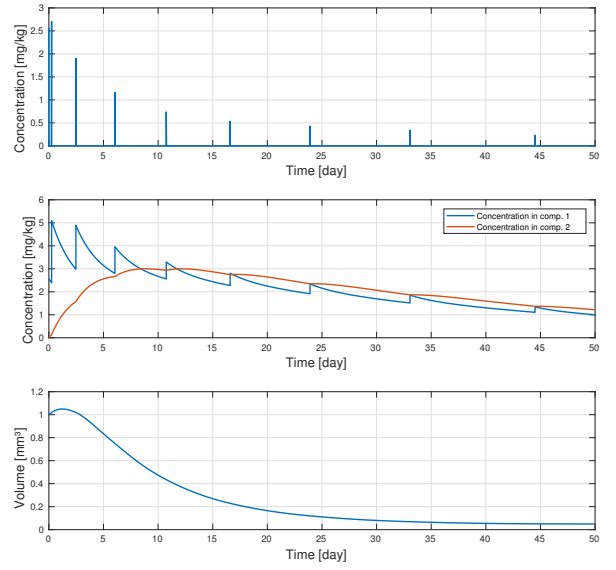
Independently of the penalization function used, the total expression is the following

$$J(A_n, T_n) = \int_0^T V^2 dt + \sum_{n=0}^{N-1} \rho_n A_n^2 + [\omega_1, \omega_2, \dots, \omega_{N-1}] [f(T_1), f(T_2), \dots, f(T_{N-1})]^T, \quad c \in \Omega_c, \quad (5.29)$$

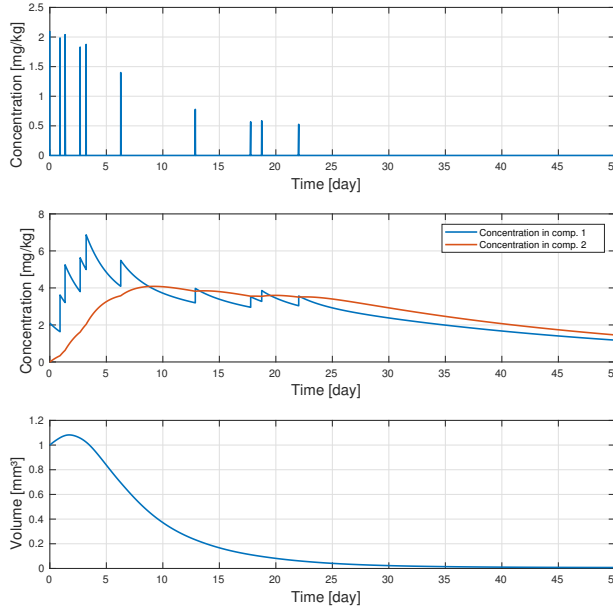
where  $f(T_i)$  with  $i = 1, \dots, N - 1$  corresponds to any function that penalizes the intervals as a function of each time intervals, and  $\omega_i$  with  $i = 1, \dots, N - 1$  corresponds to the weight applied to each function  $f(T_i)$ . Figure 5.32 represents the optimal solutions considering exponential penalization(fig. 5.32a)quadratic penalization(fig.5.32b), negative linear penalization and also negative quadratic penalization, for constant weight  $\omega_i$ , with  $N = 10$  administrations and time horizon  $T = 70$  days. In this simulation instead of using a quadratic function, two exponentials were used to simulate a quadratic function,  $f(T_i) = e^{T_i - (T_i^C + \delta)} + e^{-T_i + (T_i^C - \delta)}$ . This pair of exponentials grow faster than the quadratic, imposing the ideal solution to be near the centre of them. It is remarked that each pair of exponentials are centered in different increasing values  $T_{i+1}^C > T_i^C$ .



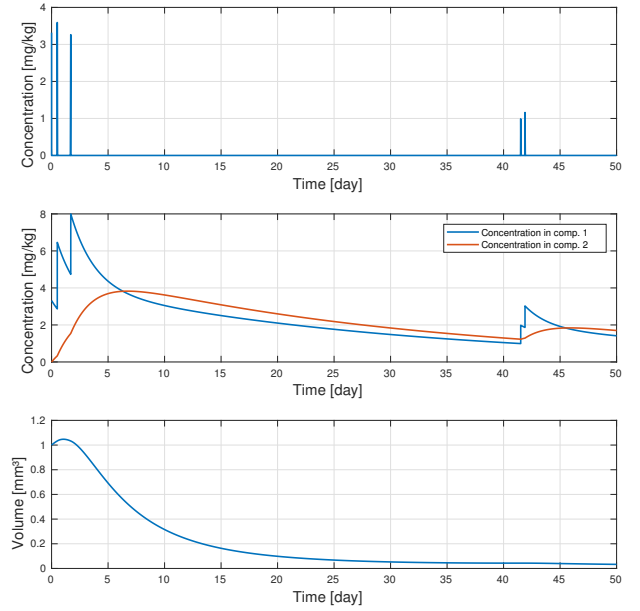
(a) Considering the exponential penalization



(b) Considering the par of exponentials penalization



(c) Considering the negative linear penalization



(d) Considering the negative quadratic penalization

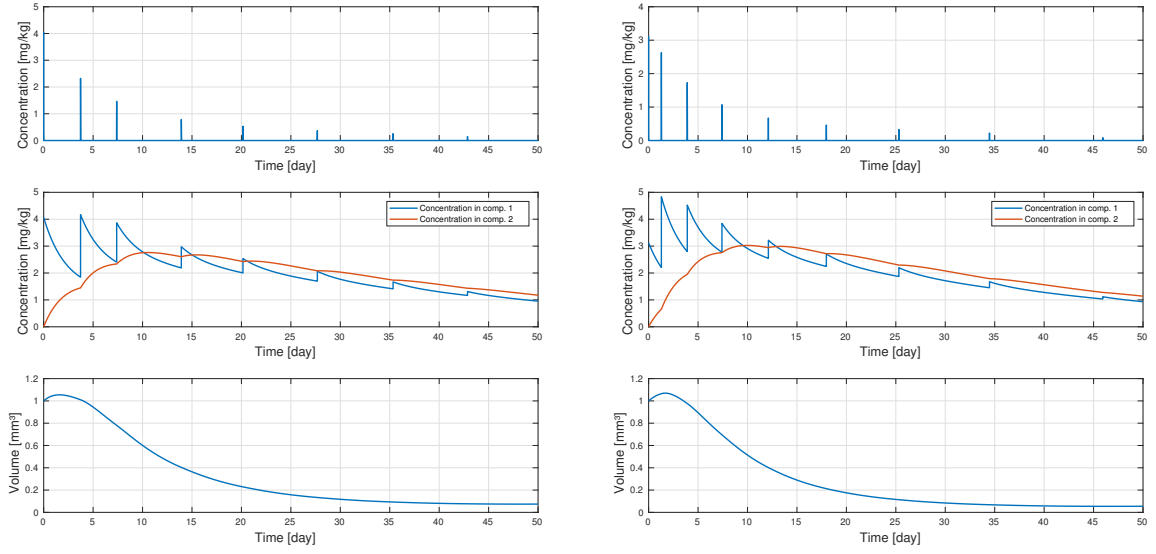
Figure 5.32: Optimal solutions considering exponential, pair of exponential, negative linear and negative quadratic penalization functions with constant weights. It is also considered the integral of  $|V|$  and the sum of squared amplitudes in the objective function.

Depending on the penalization weights, the situation where the sum of all time intervals is bigger than the time horizon can happen. This situation implies that it is possible to have Dirac impulses that do not appear during the treatment session. This leads to the variation of the total number of administrations. In other words, as it is possible to see, in figure 5.32a it is only possible to count eight administrations and

in figure 5.32b, nine administrations, when actually the number of administrations was  $N = 10$ . So this means that the weight applied to the exponential or quadratic functions works as a tuning button in terms of the number of administrations  $N$ . If the weight increases,  $N$  decreases and if the weight decreases,  $N$  will increase, never going higher than the number of administrations defined at the beginning of the optimization.

As stated previously in the amplitudes case, the weights applied to each of them needed to be different in order to penalize the first amplitudes more than the latest ones due to the fact that the minimization of the area under the tumor volume curve needed more drug in the firsts administrations than the lasts. In another perspective, the last amplitudes have less impact on the area under the curve. To contradict this effect, it was introduced a decay rate of 10% in the weights applied. In this problem, the time intervals have the same issue. That is why in figure 5.32 the first time intervals are very small even when they are penalized by the exponential or quadratic functions. So one possible way of defining the weights is saying that they depend only on the tumor volume at the time instant that the administration is applied. For instance, the weight applied to the first time interval  $T_1$  corresponds to a function  $\omega(V(T_1))$ ; the weight applied to the second time interval  $T_2$  corresponds to a function  $\omega(V(T_1 + T_2))$  and so on and so forth. The question now is how could be this function defined. Remember that the main goal of this function is to provide a higher weight when the tumor volume is high and a low weight when the tumor volume is low. Any function that fulfills this goal can be used. The simplest function is the linear function  $\omega_i(V(\sum_{n=1}^i T_n)) = aV(\sum_{n=1}^i T_n) + b$ , where  $\omega_i$  correspond to the weight applied to the exponential or quadratic function of the time interval  $T_i$ , and  $a$  and  $b$  are constant parameters of the linear function. Choosing properly these parameters, the new optimal solutions considering, for instance, exponential and pair of exponentials penalization are the ones described in figure 5.33.

Comparing figure 5.33 with figure 5.32, the first time intervals are now increased. In a general way, what is important to retain is that the weight applied to the penalization function, either if it is constant or if it is described by a linear relationship with the tumor volume, works like a tuning button of the number of administrations  $N$  considered during the treatment duration: if the weight increases (in the linear case, if the parameter  $b$  increases),  $N$  decreases and vice versa. It is also important to say that the integral term in the objective function will force the intervals to be small. In order to introduce the MAC concept in this problem, a penalization function is added, which will force the intervals to be in their maximum value possible, reaching an equilibrium between the integral term and the penalization function. This equilibrium can be changed by changing the weight  $\omega_i$ .



(a) Considering the exponential function

(b) Considering the par of exponentials as function

Figure 5.33: Optimal solutions considering both exponential and par of exponentials functions with linear weights.

## 5.6.2 Fixing N

In the previous section,  $N - 1$  time intervals were considered, where small values were penalized by a function. This penalization leads to an indirect variation of the total number of administrations considered for treatment. There is a simple way of saying that all the administrations must be inside the treatment period considered. This procedure consists in the addition of one more time interval: the interval  $T_N$  between the time horizon  $T$  and the time instant of the last administration. With this new variable, is possible to add a new constraint to the optimization problem (as it is done in [36]) which is

$$\sum_{n=1}^N T_n = T. \quad (5.30)$$

Since the controller looks at all time intervals equally, this constraint will force the controller to choose an optimal solution where the time intervals are more evenly distributed in the time horizon  $T$ . This means that it is not necessary to use a penalty function. Establishing a minimum value for the time intervals of  $T_n^{min} = 0,25$  days and optimizing the objective function without any penalization function on the time interval, the solutions represented in figure 5.34 was found to be optimal, considering also the integral of the absolute value of the volume in the objective function, with  $C_{min} = 0$  and  $C_{max} = 10$  mg/kg. As it is possible to see, even without any interval penalization, the solution has increasing intervals when the tumor size decreases, similar to a minimum attention behavior.

Since the intervals are now better distributed in time (due to the restriction), it is possible to introduce some variations in the objective function, in order to obtain some different results, using different perspectives. So far what is done is the following: the mathematical model considered in this work

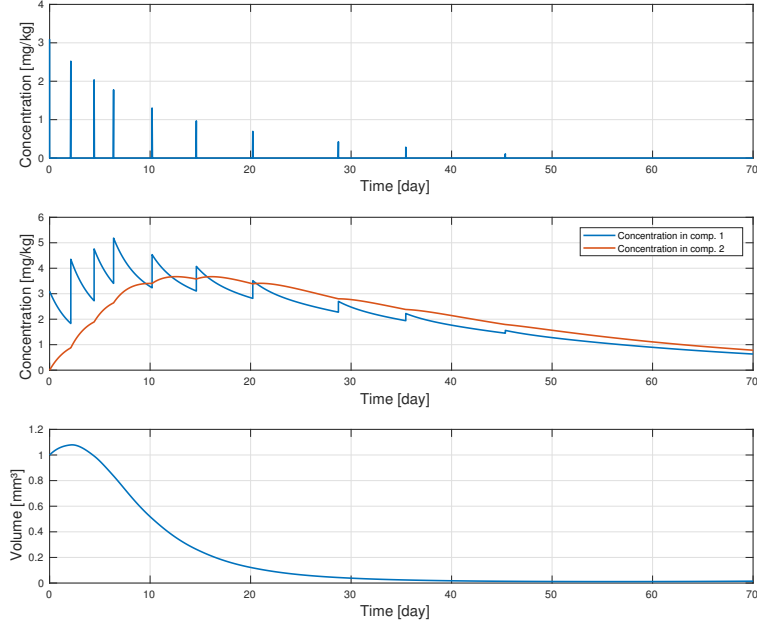


Figure 5.34: Optimal solution considering restriction 5.30.

is adapted to the patient, a time horizon and weights (for the objective function) are chosen and the controller gives us the optimal solution that minimizes the tumor volume time evolution and the drug dosages. Let us consider now that, instead of minimizing the tumor volume time evolution, what is minimized is the final tumor volume  $V(T)$ . So the objective function is now

$$J(A_n, T_n) = V(T) + \sum_{n=0}^{N-1} \rho_n A_n^2, \quad c \in \Omega_c, \quad \sum_{n=1}^N T_n = T \quad (5.31)$$

considering  $N = 10$  administrations. The minimization of the amplitudes is always important, otherwise the amplitudes will have their maximum value, depending on the restrictions. Remember that the percentage decay in the weight  $\rho$  was considered because the integral term forced the first amplitudes to present high values. In this perspective, that will not happen, so the weight  $\rho$  can now be a constant, leading to the following objective function

$$J(A_n, T_n) = V(T) + \rho \sum_{n=0}^{N-1} A_n^2, \quad c \in \Omega_c, \quad \sum_{n=1}^N T_n = T. \quad (5.32)$$

Figure 5.35 represents the solution found to be optimal considering the above objective function, with  $N = 10$  administrations,  $C_{max} = 10 \text{ mg/kg}$ ,  $C_{min} = 1.5 \text{ mg/kg}$ ,  $\rho = 0.003$  and  $T = 70$  days. Comparing this figure with figure 5.34, the intervals are now more distributed since that what is important to minimize is the volume final value instead of the volume behavior in time. This solution shows a more interesting impulse distribution in time that leads to a more constant concentration behavior in the human organism, as well as a lower variation of the concentration, which is an important aspect in order to reduce side effects. Maybe there is an equilibrium between the first perspective (that led to figure 5.34) and this new perspective represented by equation (5.32).

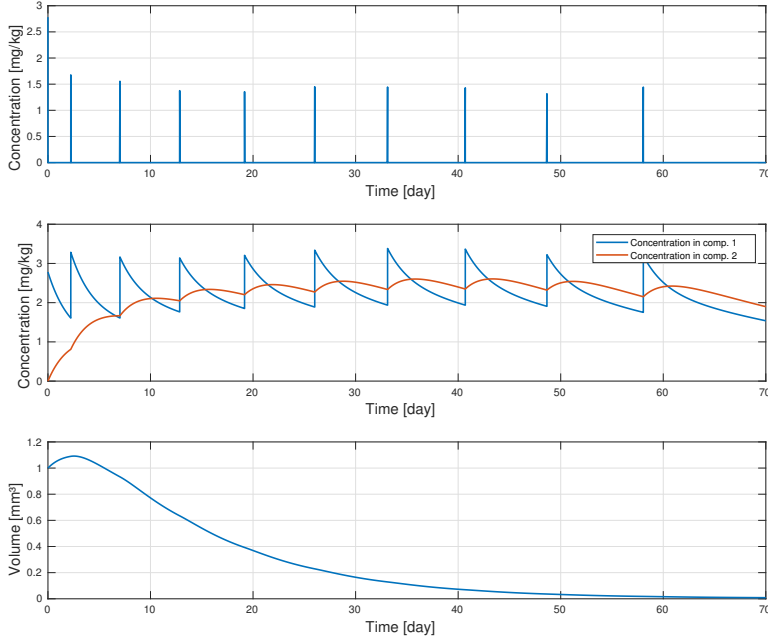


Figure 5.35: Optimal solution considering the objective function presented in equation (5.32).

Let us consider that besides minimizing the final tumor volume and the amplitudes, the tumor volume evolution is also minimized, leading to the following objective function

$$J(A_n, T_n) = V(T) + \rho \sum_{n=0}^{N-1} A_n^2 + \Omega \int_0^T V dt, \quad c \in \Omega_c, \quad \sum_{n=1}^N T_n = T. \quad (5.33)$$

Let  $\Omega \in [0, 3]$ . Figure 5.36 represents the value of the objective function in the optimal solution  $(A_n^*, T_n^*)$  as a function of the parameter  $\Omega$ . As  $\Omega$  increases, the importance that the controller gives to the minimization of the tumor volume evolution also increases. It is expected that the drug concentration in the organism starts to increase in the beginning of the treatment, which means that the amplitudes increase and the tumor final value decreases. So when  $\Omega$  increases, the amplitudes will also increase, which explains the behavior of the curve in the above figure.

Figure 5.37 represents the variation of the behavior of the tumor volume during the treatment (represented by the integral  $\int_0^T V dt$ ) and the tumor volume final value as a function of the parameter  $\Omega$ . As it is possible to verify, when  $\Omega$  increases, both tumor evolution and final value decrease.

Let us consider now a different perspective, where the main objective is to minimize the impulse amplitudes subject to the constraint  $V(T) = V^*$ , where  $V^*$  corresponds to a certain desired final tumor volume value, besides the other constraints. This could correspond to a real scenario, where what is wanted is the final tumor volume to have a specific value, while minimizing the drug dosages. So the objective function is now the following

$$J(A_n, T_n) = \rho \sum_{n=0}^{N-1} A_n^2, \quad c \in \Omega_c, \quad \sum_{n=1}^N T_n = T, \quad V(T) = V^*. \quad (5.34)$$

Since there is only one term in the objective function, there is no need for the existence of a weight  $\rho$ . So

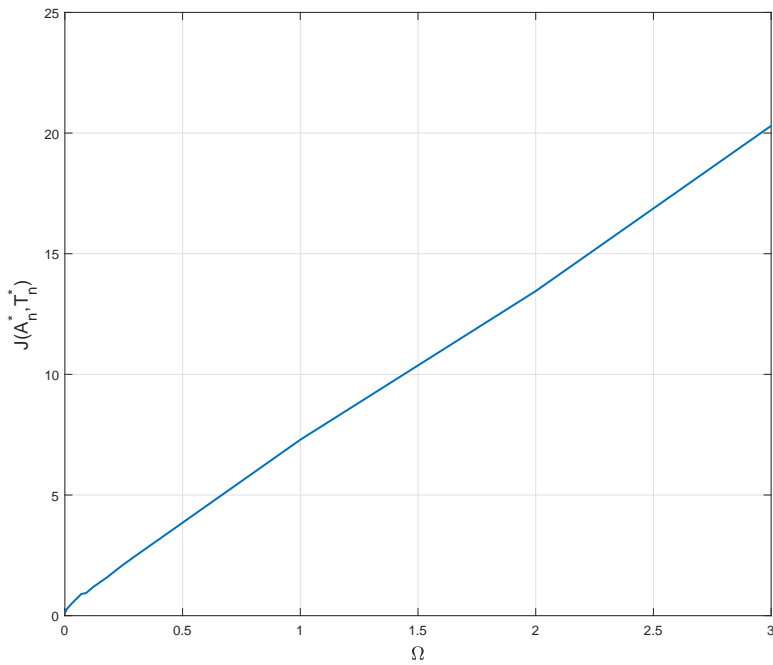


Figure 5.36: Objective function values of the optimal solutions considering different  $\Omega$  values.

suppose that  $\rho = 1$ . Note that the objective function is now convex, due to the fact that it corresponds to a linear combination of convex functions. However the problem, as a whole, is not convex. The problem here is to respect the constraint  $V(T) = V^*$ . Figure 5.38 represents the solution found to be optimal considering the problem in equation (5.34).

Because now the goal is to have a specific final tumor volume value, there are many different possible configurations that can respect that goal. If the problem were to minimize the tumor volume final value, the number of configurations would be lower. However, in this perspective it was possible to find an objective function that is convex, leaving the problem to the constraints where an optimization method as IP method can be used to solve, since it uses the barrier function concept in order to maintain the solution inside the feasible area.

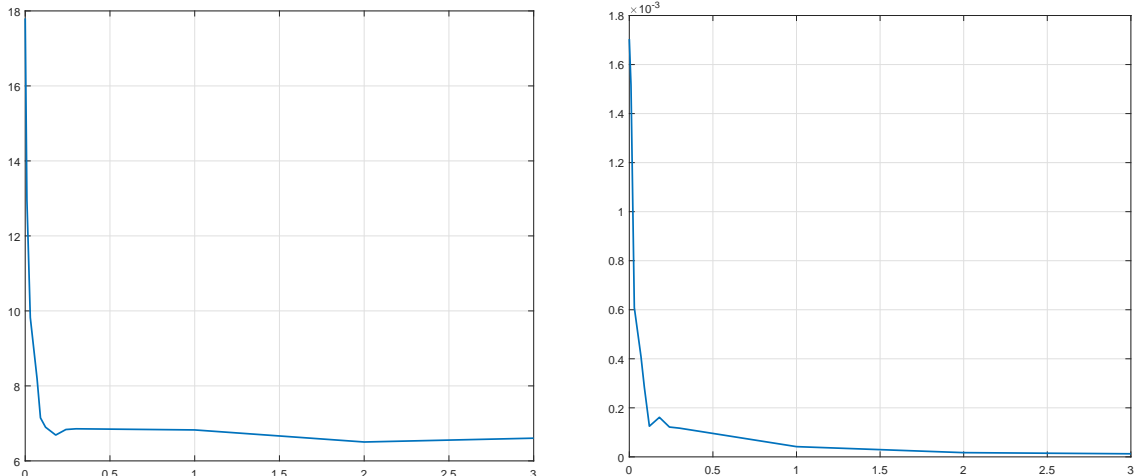


Figure 5.37: Behavior of the tumor volume during treatment and its final value considering the optimal solutions for different  $\Omega$  values.

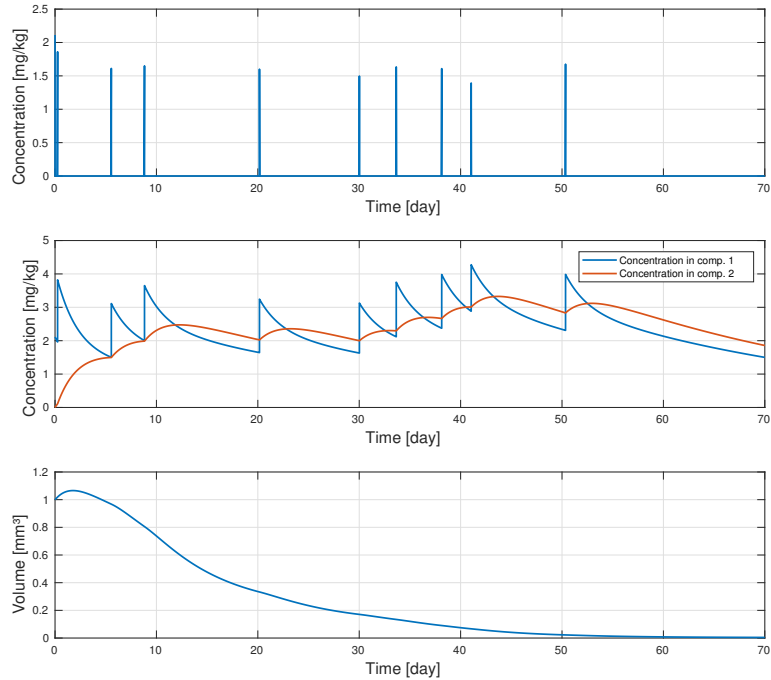


Figure 5.38: Optimal solution considering the objective function presented in equation (5.34).

### 5.6.3 Pseudo-spectral Analysis

So far it is known that what makes the optimization problem difficult is the fact that the impulse time instant can also change in time. Actually many impulse control design techniques proposed in the

literature consider fixed time instants and only the Dirac impulse amplitudes can be varied, since that this problem is less complex to solve [36]. In order to consider the situation where the impulse time instants are also treated as decision variables, the need of developing computationally efficient algorithms is increasing. This is what is discussed in [36], where a pseudo-spectral approach is proposed. In this approach, the state variables are represented in terms of standard orthogonal polynomials of time, where the idea is to project the nonlinear high dimensional state variables (in a general case) into a low dimensional and easier problem to solve. In other words, the optimal control problem is projected into a low dimensional nonlinear problem by the selection of grid points where the solution is forced to be exact, and then this problem is solved using a computationally efficient optimization algorithm. The fact that the pseudo-spectral method requires a low number of grid points, that leads to a low dimensional optimization problem, which is a faster method than the methods used above in this work, computationally speaking.

There are several different polynomials that can be used to represent the state variables. For instance, Chebyshev polynomials with Chebyshev-Gauss-Radau (CGR) or Chebyshev-Gauss-Lobatto (CGL) grid points can be used.

In order for this technique to be applied, first the problem needs to be re-written in terms of the normalized time, where each time interval value must be in the interval  $[-1, 1]$ , where  $-1$  correspond to the initial time instant and  $1$  correspond to the final time instant, as figure 5.39 suggests.

Chebyshev polynomials are given by  $\phi_N(\tau) = \cos(N\cos^{-1}(\tau))$ , where  $N$  is the degree of the polynomial,  $\tau = \cos(\theta)$ ,  $\tau \in [-1, 1]$  and  $\theta \in [0, \pi]$ . So the first terms of the polynomial are  $\phi_0(\tau) = 1$ ,  $\phi_1(\tau) = \tau$  and the next terms are given by the recursive relationship

$$\phi_{N+1}(\tau) = 2\tau\phi_N(\tau) - \phi_{N-1}(\tau). \quad (5.35)$$

The corresponding relationship in differential form is given by

$$\dot{\phi}_{N+1}(\tau) = 2\phi_N(\tau) + 2\dot{\phi}_N(\tau) - \dot{\phi}_{N-1}(\tau). \quad (5.36)$$

Considering, for instance, the CGR grid points, the  $N + 1$  points are given by  $\tau_c = \cos(\frac{\pi c}{N})$ , for  $c = 0, 1, 2, \dots, N$ . Note that the computation of the grid points and the polynomials is fast due to the existence of the recursive relationships.

Next, in the objective function, the state differentiation is approximated by taking the differentiation of

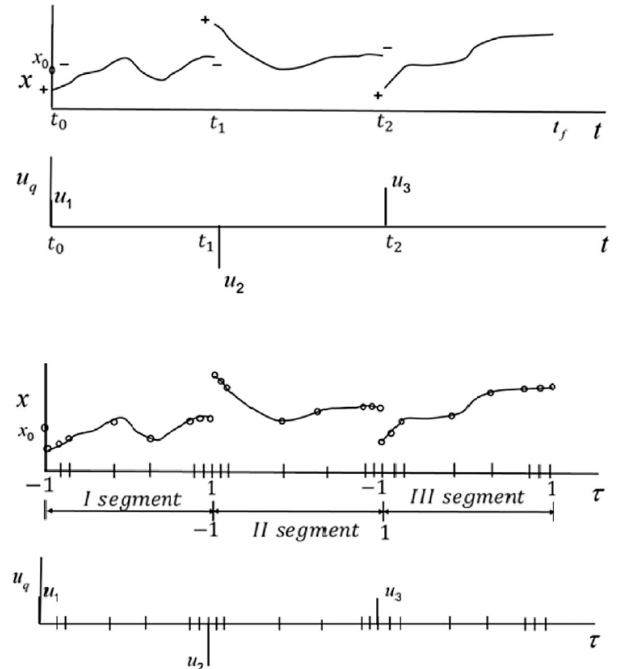


Figure 5.39: Normalization of time  $t$  in  $\tau \in [-1, 1]$  for each of the time intervals  $t_0 \geq t \geq t_1$ ,  $t_1 \geq t \geq t_2$ ,  $t_2 \geq t \geq t_f$ , where  $x$  correspond to the state variable and  $u_q$  correspond to the Dirac impulse sequence considered [36].

the approximating polynomials

$$x_{iq}^\tau \approx \sum_{k=0}^{N-1} a_{iq}^k \phi_k(\tau), \quad \dot{x}_{iq}^\tau \approx \sum_{k=0}^{N-1} a_{iq}^k \dot{\phi}_k, \quad (5.37)$$

where  $x_{iq}^\tau$  is the  $i$ th state variable at  $q$ th interval (segment in the figure 5.39) for the normalized time  $\tau$ ,  $N$  is the number of the Chebyshev polynomials used to approximate the state variables and  $a_{iq}^k$  is the weight applied to the polynomial  $k$  of the segment  $q$  of the state variable  $i$ . So in matricial form, the nonlinear impulse system  $\dot{X} = f(X)$ , where  $f$  is a nonlinear function of the state vector  $X = [x_1, \dots, x_i]$ , can be written as  $A_q \dot{\phi}(\tau_c) = \frac{\Delta T_q}{2} f(A_q \phi(\tau_c))$  for  $\tau_c \in (-1, 1)$ , with jump condition  $A_q \phi(-1) = g(A_{q-1} \phi(+1), u_q)$ , where the term  $\frac{\Delta T_q}{2}$  appears from the time normalization in each  $q$  interval,  $A_q$  is the weight matrix and  $\phi(\tau_c)$  correspond to the vector of polynomials. These two equations correspond to constraints of the optimization problem, along with the intervals constraint  $\sum_{q=1}^{S_q} \Delta t_q = t_f$ ,  $\Delta t_q \geq 0.25$  and the impulse amplitude constraint  $C_{max} = 10$  and  $C_{min} = 1.5 \text{ mg/kg}$ . The algorithm presented in [36] is considered. See [36] for more details.

In the model considered in this work, there are two states variables: concentration in compartment one,  $c_1$ , and two,  $c_2$ . However, what is wanted to optimize is the tumor volume. So this work proposes to add one more state that corresponds to the tumor volume  $V$  that depends on the  $c_2$ , which depends on  $c_1$ . So the three states are needed for the optimization problem formulation. The main idea here is approximating each of the three states using  $N$  weighted Chebyshev polynomials. By approximating the states, the differentiation of the states is done by the differentiation of the polynomials. The weights, that are also optimization variables, are chosen such that the differential equality is maintained. The time intervals and the impulse amplitudes are also optimization variables. The parameters needed to be defined correspond to the total number of administrations and the number of polynomials used to approximate the states. Figure 5.40 represents the solution found to be optimal for 10 administrations and 10 Chebyshev polynomials and considering also the constraints already considered in the above optimizations, along with the final tumor volume constraint  $V(T) \leq V^*$ . This solution is similar to the solution presented in figure 5.35, since what is aimed is to minimize the impulse amplitudes and also the tumor volume, even if this last goal is inserted in the constraints, besides finding the right polynomials weights.

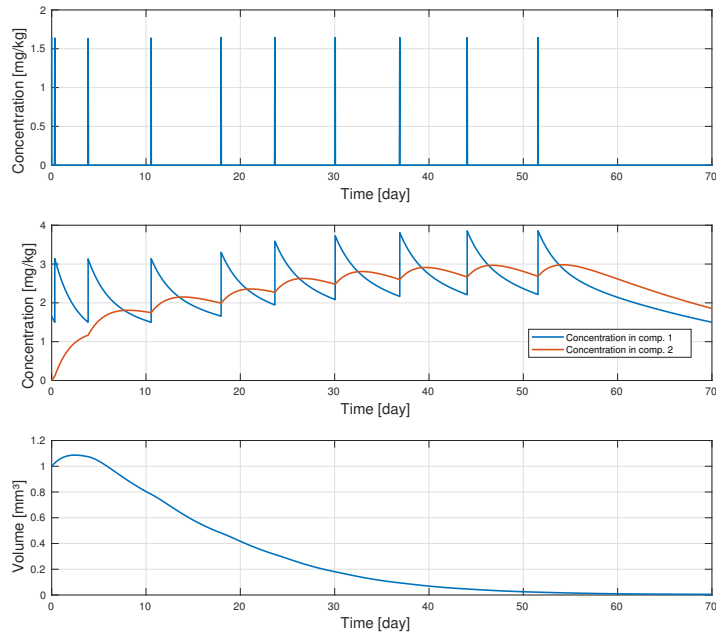


Figure 5.40: Optimal solution using a pseudo-spectral method, considering the objective function presented in equation (5.32).

Is important to say that the computational time used for the optimization algorithms to find the optimal solution of this problem is relatively lower than the time used for the other problems. This is due to the fact that what is being solved does not correspond to the real problem but to an approximation. If the number of polynomials used increases or, in the limit, if it is infinity, there will be no difference between the real and the approximate problem and it would take the same time.

As previously stated, in order to find the best solution, the optimization problem is solved using ten different initial points and then the solution that gives the lowest objective function is considered the best solution (among all ten solutions). Considering the parameters configuration used for finding the solution presented in figure 5.40, all ten solutions were exactly the same. This suggests that, using  $N = 10$  polynomials, the approximated problem is convex.

## 5.7 Important Remarks

Table B.1 summarizes the most important aspects of this chapter.



# Chapter 6

## Results and Discussion

In the previous chapter, a study about different perspectives and objective functions was made, considering the parameters described in the table 4.1. However the parameters may not have always those values. Their variation can affect the controller performance. This chapter starts with a Sensitivity analysis, where the variation of some parameters is considered. Afterwards, the Gompertz model is used instead of the Logistic model and a comparison is made.

### 6.1 Sensitivity Analysis

The process of designing a controller to control a system passes through choosing the proper controller type, depending on the system and the goals. Independently of the chosen controller type, all controllers models have parameters that need to be tuned for a desired performance. After the tuning process, the controller will consider those parameters for the system. However, it is possible to have variations on the parameters due to spontaneous physical events or others. After the controller design, these variations can affect the controller performance, leading to situations where the goal is not reach or even catastrophic events. Sensitivity Analysis is an area of Control Theory that study the behavior of the controller when parameters variation is considered. The goal of this analysis is to prevent undesired behaviors.

#### 6.1.1 Parameter Variation

In this section, the solutions found to be optimal are presented for different parameters. The controller consider the model described in chapter 4, where the objective function is the following

$$J(A_n, T_n) = \int_0^T |V| dt + \sum_{n=0}^{N-1} \rho_n A_n^2, \quad c \in \Omega_c, \quad \sum_{n=1}^N T_n = T, \quad (6.1)$$

where  $C_{min} = 1.5 \text{ mg/kg}$ ,  $C_{max} = 10 \text{ mg/kg}$  and  $T = 70 \text{ days}$ .

The parameters considered in this section are the initial tumor volume value  $V(0)$ , the maximum effect of the drug concentration  $u_{max}$  and the carrying capacity of the Logistic model  $K$ . These parameters are considered since they have more impact in the controller performance. In the previous chapter

the parameters values considered were  $V(0) = 1 \text{ mm}^3$ ,  $u_{max} = 1$  and  $K = 5$ . The optimal solution considering this values is

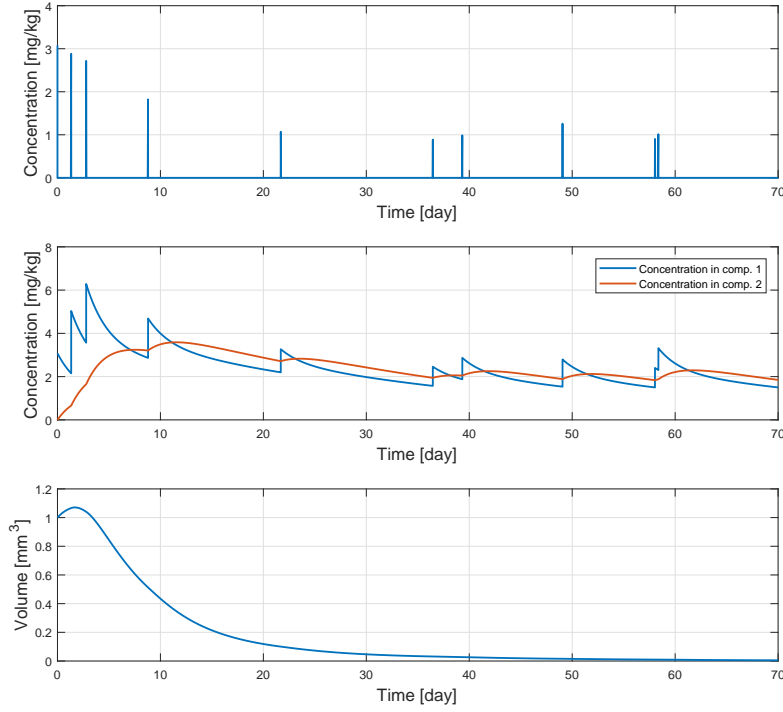


Figure 6.1: Optimal solution considering the objective function 6.1.

Changing the initial tumor volume to  $V(0) = 5 \text{ mm}^3$ , maintaining the other parameters constant, the optimal solution is as shown in figure 6.2.

Comparing figure 6.2 to the solution presented in figure 6.1, higher amplitudes would be expected since the initial volume is higher. However, note that now  $V(0) = K$ , which means that the tumor is at his maximum volume. In other words, if no treatment is considered, the volume derivative is zero, according to the Logistic equation. This means that when the treatment is applied, the tumor will start to decrease immediately, allowing the amplitudes to be small.

Considering now  $V(0) = 3 \text{ mm}^3$ , the optimal solution is the one shown in figure 6.3.

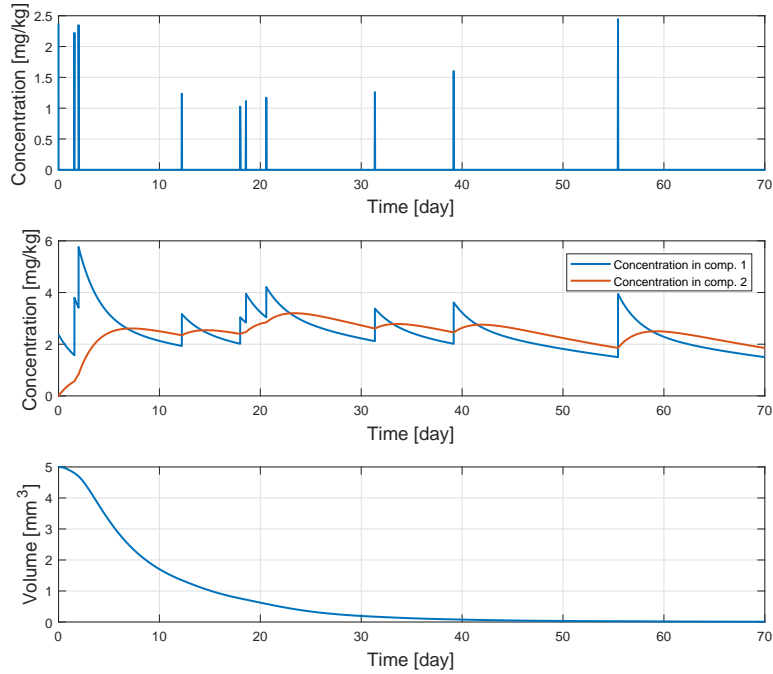


Figure 6.2: Optimal solution considering the objective function 6.1, for  $V(0) = 5 \text{ mm}^3$ .

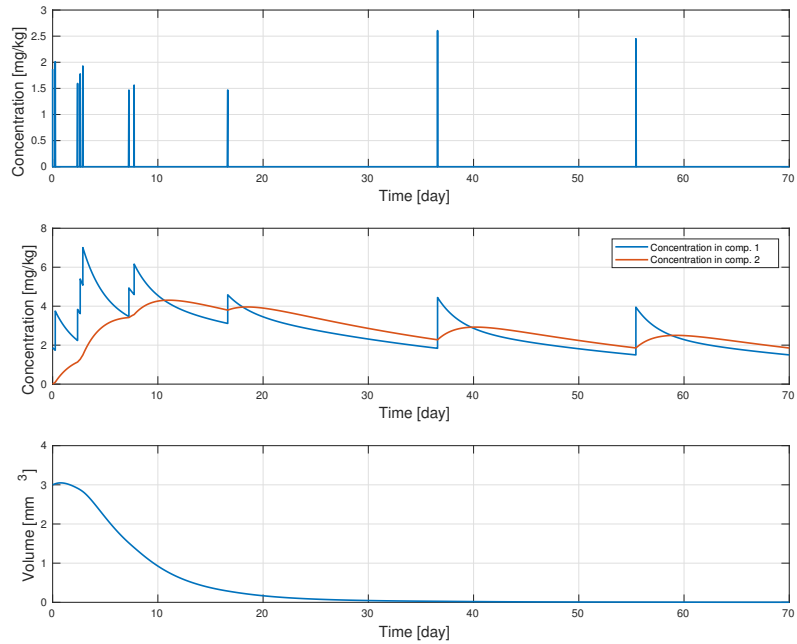


Figure 6.3: Optimal solution considering the objective function 6.1, for  $V(0) = 3 \text{ mm}^3$ .

Note that now the previous situation does not occur. The derivative of the volume is not zero for  $t = 0$ . Because of that, the drug concentration, for instance, in the period  $0 \leq t \leq 10 \text{ days}$  is higher than the concentration in simulation 6.2 for the same period, even for a lower initial volume. It is possible

to conclude that treat a tumor that is already at his maximum size takes less drug concentration at the beginning of the treatment, for this particular study.

Remember that the amplitudes weights are proportional to the initial volume, as explained in section 5.4.1. This detail is very important for the balance between the integral term and the amplitudes term in the objective function. Figure 6.4 represents the same situation above described but considering the amplitudes weights to be non proportional to the initial volume. As it is possible to see, the amplitudes

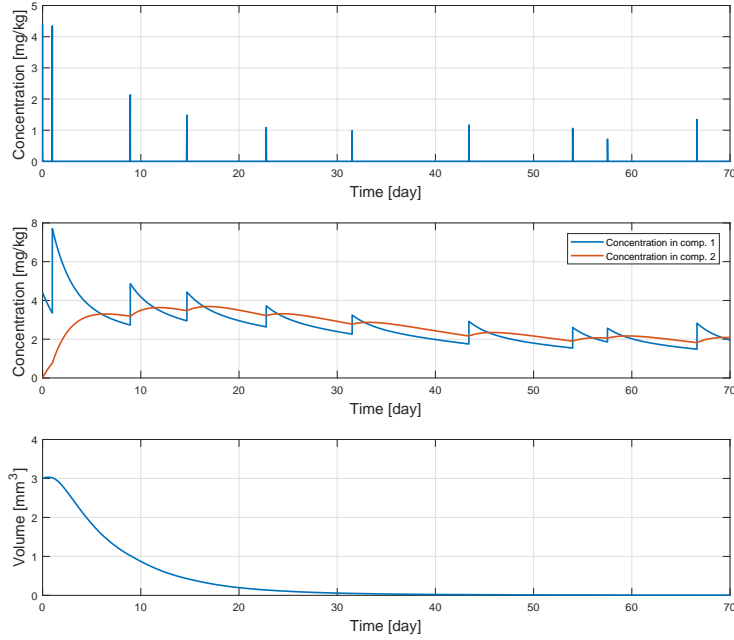


Figure 6.4: Optimal solution considering the objective function 6.1, for  $V(0) = 3 \text{ mm}^3$ , considering non proportional amplitudes weights to the initial volume.

are now allowed to be higher since their penalization weight has decreased. Because of that, the time intervals are also allowed to have higher values, since the drug concentration can be increased by the drug dosages (amplitudes values).

Considering now the following parameter configuration  $u_{max} = 0.5$ ,  $V(0) = 1 \text{ mm}^3$  and  $K = 5$ , the solution found to be optimal is represented in figure 6.5.

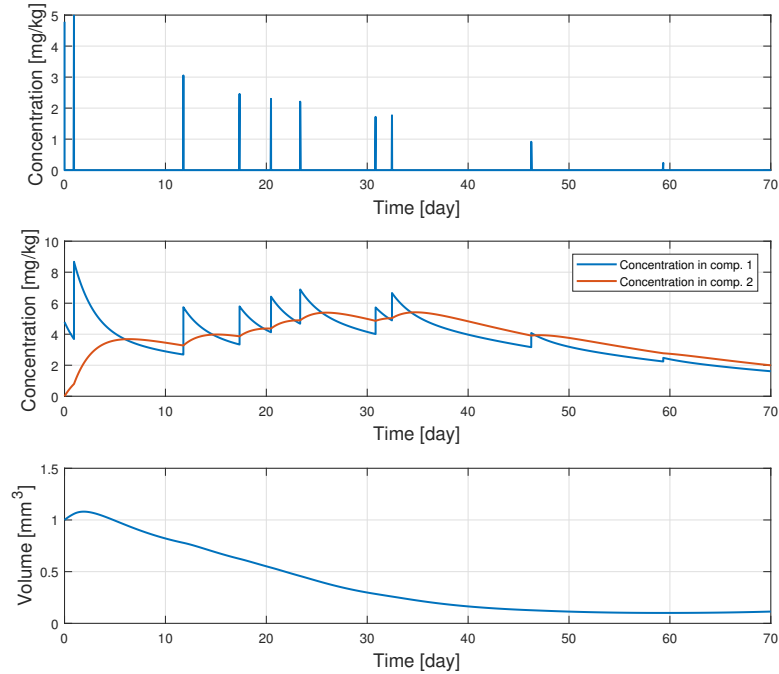


Figure 6.5: Optimal solution considering the objective function 6.1, for  $u_{max} = 0.5$ .

Because the drug concentration has now less impact/effect in the tumor evolution, the amplitudes were forced to increase in order to minimize the tumor volume. However, because of the amplitudes weights, the maximum concentration restriction was not reached. An equilibrium between minimizing tumor volume and toxicity effect was reached. This study can actually be used to test new drugs in order to improve their performance during treatment.

Increasing the drug maximum effect to  $u_{max} = 1.5$ , the optimal solution is the one represented in figure 6.6. As it is possible to verify, the amplitudes have decreased and the time intervals have, in average, a higher value, comparing to the situation where  $u_{max} = 0.5$ . This comparison show that the variation of this parameter can influence substantially the optimal solution, allowing a better solution in terms of attainability and toxicity. The amplitudes did not present lower values due to the minimum concentration restriction  $C_{min} = 1.5 \text{ mg/kg}$ .

Let us consider now  $K = 10 \text{ mm}^3$ , maintaining the other parameters with their original values. The optimal solution is represented in figure 6.7.

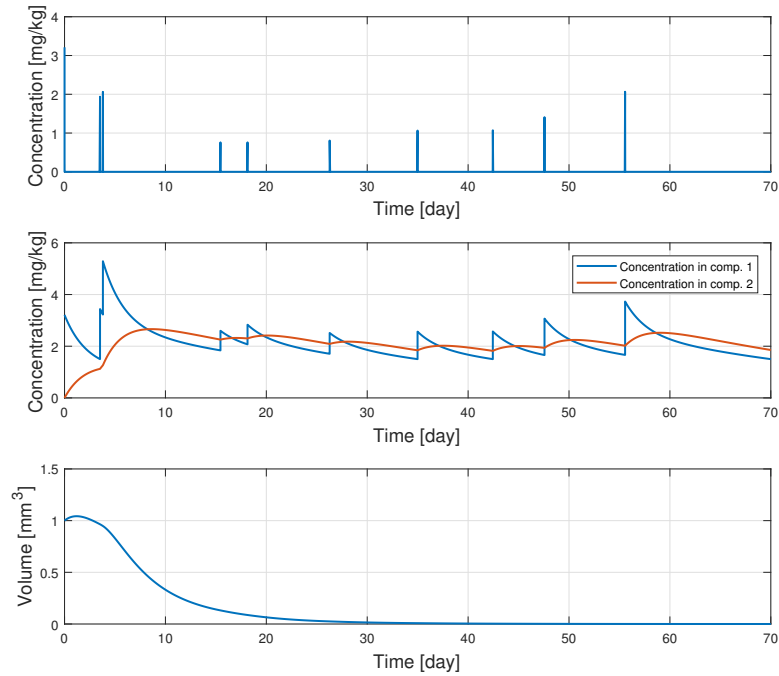


Figure 6.6: Optimal solution considering the objective function 6.1, for  $u_{max} = 1.5$ .

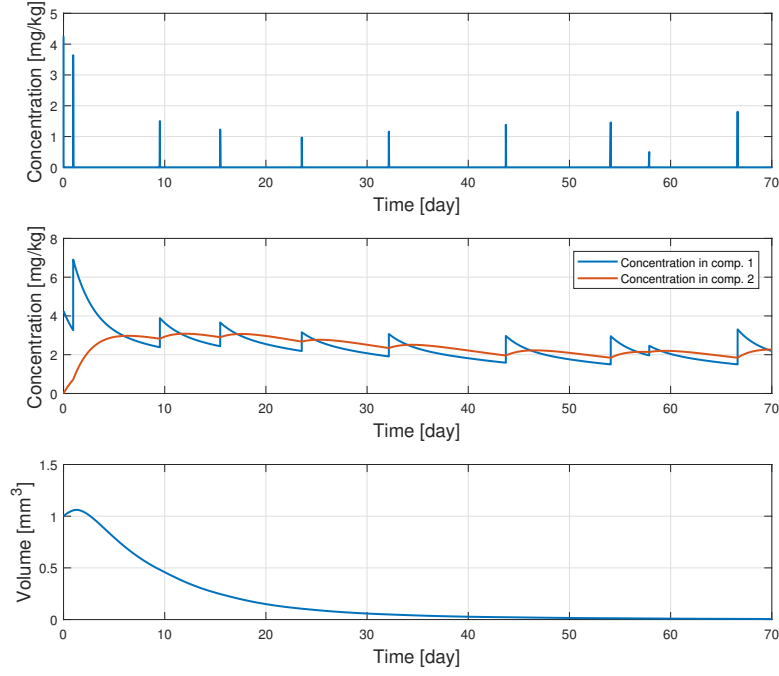


Figure 6.7: Optimal solution considering the objective function 6.1, for  $K = 10$ .

Comparing this solution with the solution presented in figure 6.1, it is possible to verify that the amplitudes have higher values in this solution than in the solution in figure 6.1. This is due to the fact

that when  $K$  increase, the volume derivative also increase, since the difference between  $V(0)$  and  $K$  increase (remember the logistic equation (3.2)).

### 6.1.2 Modelling Errors

In this section, the behavior of the controller solution is studied when errors are considered in some of the general model parameters. The error considered correspond to the same parameters previously considered:  $V(0)$ ,  $u_{max}$  and  $K$ . In order to analise the controller behavior, it is necessary to define a criteria that can describe the performance of an optimal solution of a certain problem when those parameters are not the ones that the controller consider. The chosen criteria correspond to the tumor volume time evolution  $\int_0^T |V|dt$  and the tumor final volume  $V_f$ . Considering the optimal solution presented in figure 5.34, and changing the parameter  $V(0)$ , the following results are obtained

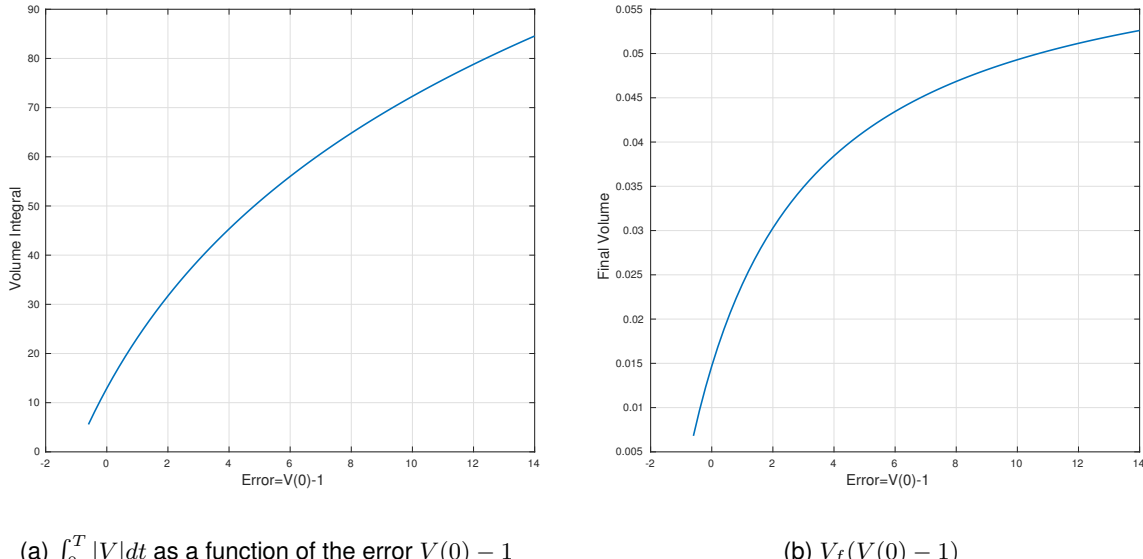


Figure 6.8: Tumor volume time evolution and tumor final value as functions of the error  $V(0) - 1$ , where  $V(0) \in [0.4, 15] \text{ mm}^3$  and the value 1 correspond to the initial volume used for the optimal solution considered.

As it is possible to verify, using the same optimal solution, when the initial volume is lower than the original (which is  $1\text{mm}^3$ ), both tumor volume evolution and final value decrease and vice versa. Also, both curves suggest that there is a certain error value from which the variation of both tumor evolution and final value decrease, suggesting a saturation. Remember that the tumor carrying capacity remains constant at  $K = 5 \text{ mm}^3$ . So when the initial volume  $V(0) < K$ , the volume derivative is positive, meaning that the tumor did not reached its maximum volume yet (as previously stated, the controller will have to compensate the fact that it needs to force the derivative to be zero, first, and then to be negative, which lead to an increase of the amount of administered drug). When  $V(0) = K$ , the derivative is zero, meaning that the tumor already reached its maximum value (the controller just need to force the derivative to be negative). For  $V(0) > K$ , the derivative is already negative, meaning that the tumor

volume is higher than its final value (in this situation, the amount of administered drug is much less than in the previous situations). So when the error is equal to four (meaning that the initial volume considered is equal to five), the derivative changes its signal to a negative value. This is why the variation of both curves decreases.

Considering now the variation of the parameter  $u_{max}$ , the tumor volume evolution and final value behaves as shown in figure 6.9.

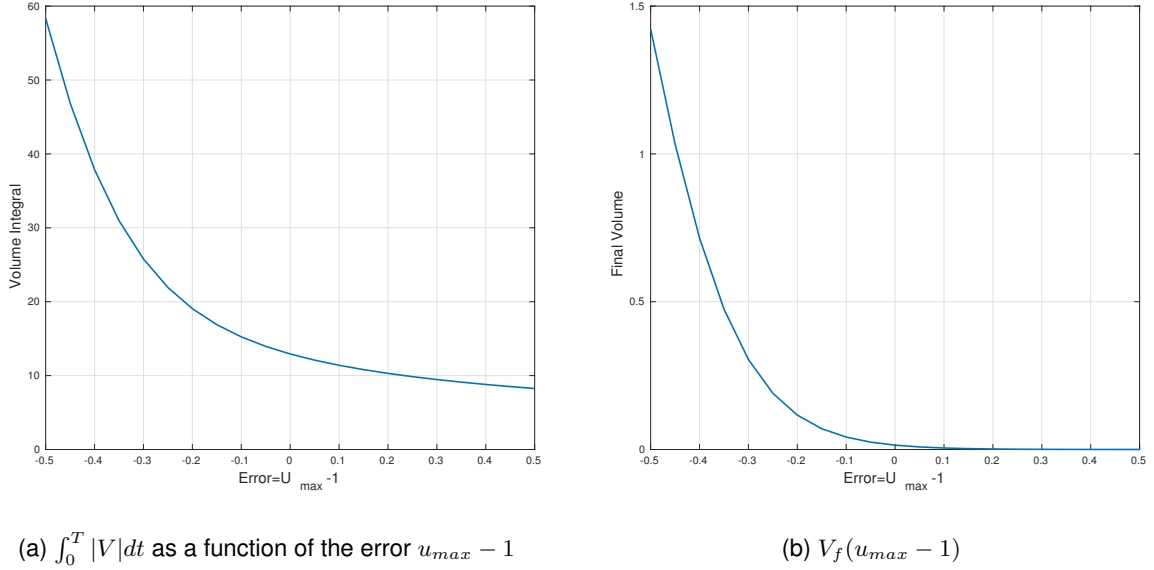


Figure 6.9: Tumor volume time evolution and tumor final value as functions of the error  $u_{max} - 1$ , where  $u_{max} \in [0.5, 1.5] \text{ mm}^3$  and the value 1 correspond to the initial  $u_{max}$  value used for the optimal solution considered.

The parameter  $u_{max}$  corresponds to the maximum effect that a certain drug concentration has in the tumor. When this parameter increase, the same amount of drug has higher effect in the tumor evolution, leading to the decrease of the both tumor volume evolution and final value curve. As previously stated, it is also possible to verify in figure 6.9b that increasing the treatment effect in the tumor does not lead to a zero tumor final volume., as it is shown in section 3.1.2.

Considering the variation of the parameter  $K$ , the tumor volume evolution and final value behaves as shown in figure 6.10. Note that when  $K$  increases, the initial volume derivative also increase, since the difference between the initial volume and its maximum value (final value) increase. The behaviour is similar to figure 6.9.

### 6.1.3 Quantization

In this section, quantization is considered in the control variables. In other words, the values of the control variables are quantized using different resolutions. For instance, if the resolution is 0.5, the control variables can only have values that are multiples of 0.5.

In order to study the quantization issue, the optimal solution considered in figure 5.34 is again used

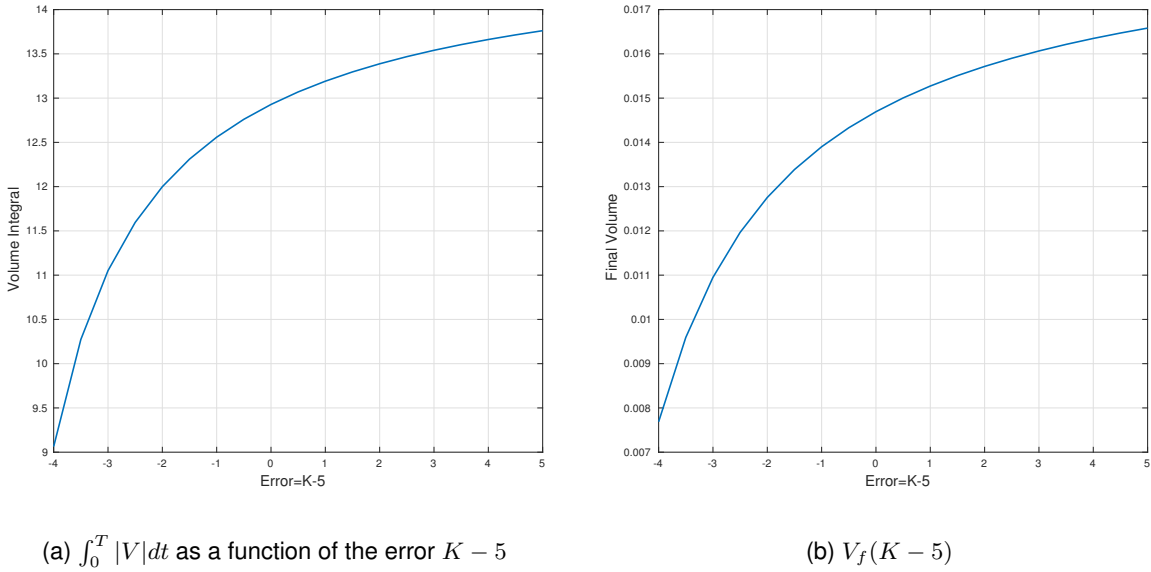


Figure 6.10: Tumor volume time evolution and tumor final value as functions of the error  $K - 5$ , where  $K \in [1, 10] \text{ mm}^3$  and the value 5 correspond to the initial  $K$  value used for the optimal solution considered.

and its objective function is evaluated for different quantization values.

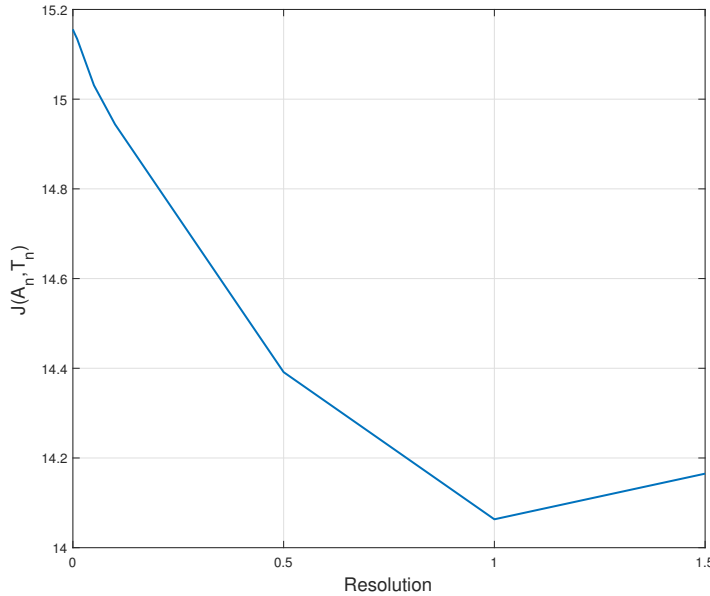


Figure 6.11: Objective function considered in figure 5.34 evaluated for different quantization values

What is actually happening is that when the quantization increase, a value that is really  $A_1 = 2.643$ , for instance, becomes  $A_1 = 2.60$  when the quantization is 0.05,  $A_1 = 2.5$  when the quantization is 0.5 and so on and so forth. So the quantized value decrease when the quantization increase. This means that the amplitudes and time intervals will start to decrease. Remember that the objective function considered only penalizes the amplitudes. Because the amplitudes decrease, due to the quantization, the objective

function value in the optimal solution also decreases. However when the amplitudes decrease there will be less administered drug which could increase the tumor volume evolution (leading to the integral term increase). But the time intervals also decrease, which will allow the accumulation of drug in the human organism, leading to the decrease of the tumor volume evolution. And so, in the end, the objective function value in the optimal solution decreases as it is shown in figure 6.11 due to the amplitudes decrease.

Figure 6.12 represents the original optimal solution and the solution considering a quantization of 1 in the control variables.

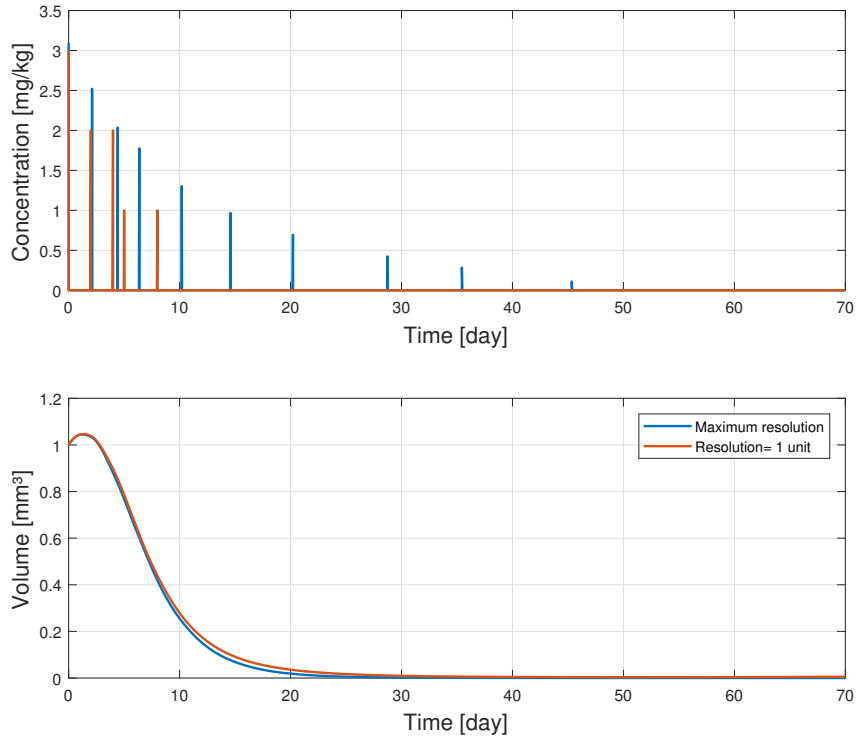
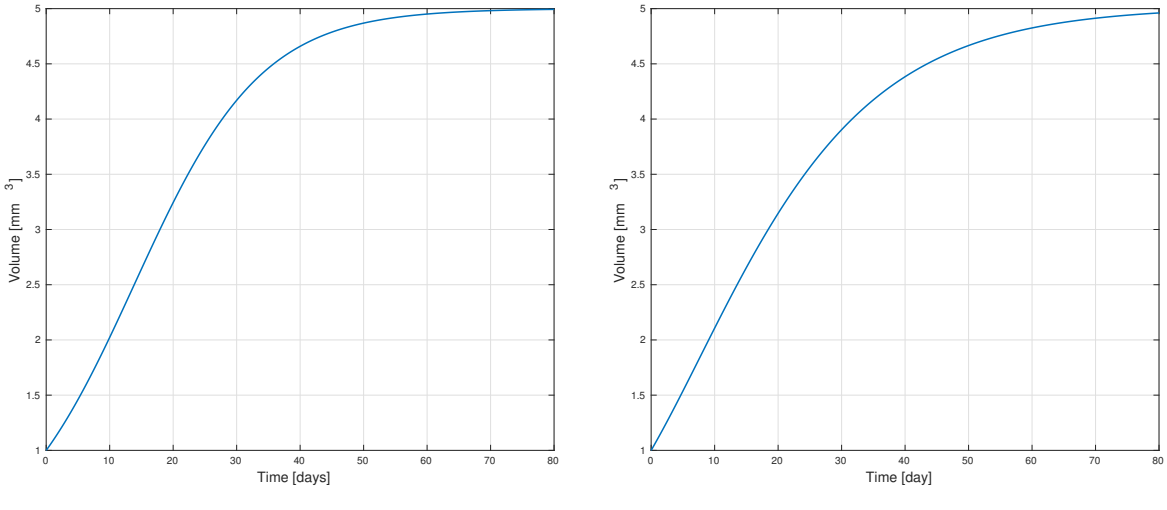


Figure 6.12: Original solution and solution considering quantization of 1.

Note that the tumor volume evolution is almost the same, comparing both original and quantized solutions.

## 6.2 Using the Gompertz Growth Model

In this section the Gompertz growth model is considered. While the carrying capacity in the Logistic model corresponds to the  $K$  parameter, in the Gompertz model, the carrying capacity is not visible in the differential equation. However, taking the limit of the differential equation solution, it is possible to verify that in the Gompertz model the carrying capacity is  $K_G = V_0 e^{\frac{a}{b}}$ . In order to compare both models, it is necessary, at least, the same carrying capacity. Considering  $K = 5$ ,  $V(0) = 1$ ,  $a = 0.1$  and  $b = 0.062$  the tumor volume evolution in time for both models is as shown in figure 6.13.

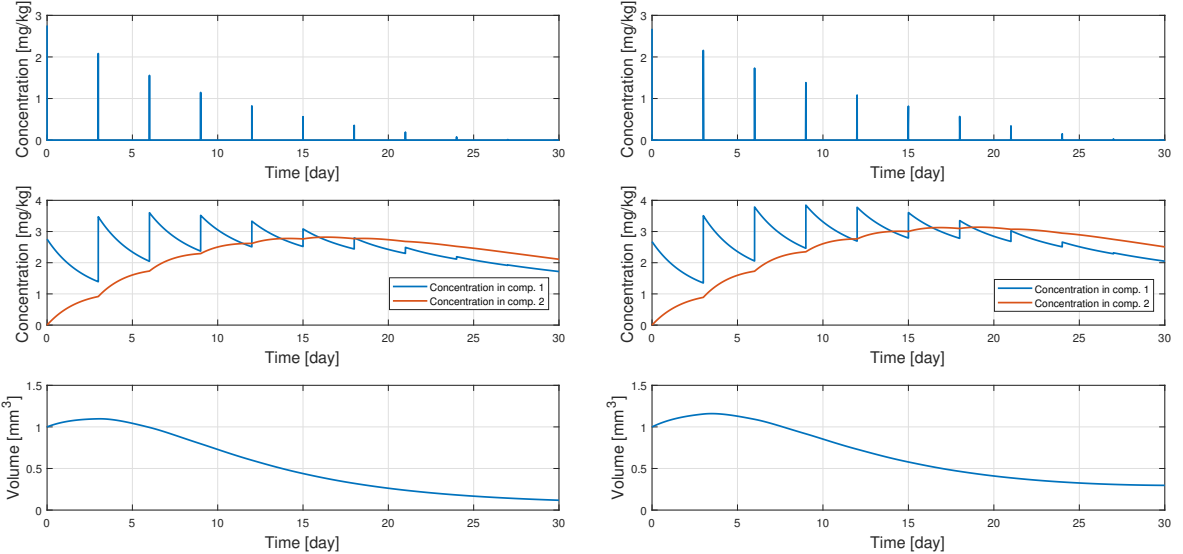


(a) Considering the Logistic growth model

(b) Considering the Gompertz growth model

Figure 6.13: Tumor volume time evolution considering both Logistic and Gompertz growth models.

As it is possible to verify, for the chosen parameters the curves for both models are very similar. However, note that the curve in figure 6.13a reaches its final value faster than the curve in figure 6.13b. Using those same parameters and considering constant time intervals  $T_n = 3 \text{ days}$  for  $n = 1, \dots, N - 1$ , the optimal solutions for both models are



(a) Considering the Logistic growth model

(b) Considering the Gompertz growth model

Figure 6.14: Optimal solutions considering constant time intervals  $T_n = 3$ ,  $N = 10$  and  $T = 30 \text{ days}$ .

It is remarked that it is necessary more drug concentration when using the Gompertz model. Observing the curves in figure 6.13 it is possible to verify that in the beginning, the tumor growth using the Gompertz model is faster than the one using the Logistic model. Between  $10 < t < 20$ , the growth is

faster using the Logistic model, which only happens when the volume is between 2 and  $3\text{ mm}^3$ . When treatment is considered, this does not happen. So the reason why the drug concentration is higher when using the Gompertz growth model is that, for volume values around  $1\text{ mm}^3$ , the Gomperz models presents a faster volume growth, forcing the amplitudes to increase.

# Chapter 7

## Conclusions

This dissertation aims at designing an optimal controller with impulsive action to plan a therapy to minimize tumor size in cancer, while reaching a compromise with also minimizing the therapy toxic effects, taking into account subsystems that can influence tumor growth. This work started by the problem formulation (chapter 1), where mathematical models were presented and combined in order to create model that can describe the problem.

Chapter 2 started by the study of compartmental models, where the conclusion that their positivity, mass conservation and stability is reached. It was also possible to conclude that reseting and changing the initial condition of the system is the most accurate way of using the Dirac impulse sequence as input to the system. A two compartmental model was considered in this work, with constant flows and output functions ( $K_{12}$ ,  $K_{21}$  and  $K_{10}$ ), and the Dirac impulse sequence as input function. The Hill Equation was used as Pharmacodynamical model, which introduced a saturation in the concentration of compartmental two evolution.

Chapter 3 studied two tumor growth models: Logistic and Gompertz. Each of them introduces a saturation effect in the tumor volume evolution. The Logistic equation was solved and it was possible to conclude that it would not be possible to eradicate the tumor for tumor volume initial conditions different from zero, considering the way that the treatment is inserted in the Logistic equation (eq.(3.6)). Two subsystems that influenced the tumor volume evolution were presented: Immune System and Angiogenesis. They were represent by the addiction of new differential equations that also depend on the tumor volume. As stated in sections 5.5.1 and 5.5.2, the Immune systems starts to attack the tumor, reducing the volume. Because the immune system is also affected by the tumor, its strength also decreases, leading to an equilibrium, where the tumor will continue to growth, depending on the initial tumor volume and the initial immunocompetent cell densities related to various types of immune cells (T-cells). The Angiogenesis process represents the variation of the tumor carrying capacity in time, that allows the tumor to grow faster and to reach a much higher volume, also depending on the initial volume, carrying capacity and some others parameters.

In chapter 4, the global model used in this work was presented and variation intervals for some variables were considered. The situation where the Logistic equation is not continuous was studied,

leading to continuity conditions presented in 4.1.

Chapter 5 started by the introduction of optimal control theory. An optimal impulsive control problem is presented, where the objective was to compute the Dirac impulse sequence amplitudes that minimizes the difference between the concentration in compartment one and a certain reference value. The results suggested that the objective function presented is convex. The Maximum Principle was then presented using the oil drilling problem as example of application. A comparison between analytical and numerical solvers was made and it was possible to conclude that the accuracy of the solutions presented by the numerical methods depend on the tolerance values defined before the optimization process, comparing to the analytical solution which is supposed to be more accurate.

The first problem of this work was presented, where only the impulse amplitudes were considered to be variable. Different objective functions were studied in order to address different possible situations, considering constraints in the drug concentration. The influence of the parameters  $\rho$  and  $T$  was then studied and it was possible to conclude that there are some regions for those parameters that allow the controller to have a more robust behaviour. Still in the first problem, Receding Horizon techniques were considered as a possible solution for the case when perturbations to the model occur during the treatment that, otherwise, were not be possible to consider.

Considering now the second problem, where besides the variable amplitudes, unknown but periodic time intervals were also considered, it was possible to conclude that the previous objective function became clearly non convex, since for different initial conditions, different solutions (local minimums) were found to be optimal. An understanding about the influences that each term in the objective function have in the optimal solution led to the addition of a new term that penalized small time intervals. The influence of the Immune System and the Angiogenesis process was studied and the conclusions were already discussed above.

The third and last problem considered in this work was discussed afterwards. In this problem variable amplitudes and time intervals were considered. Minimum Attention Control techniques were used in order to vary the number of impulses (number of treatment sessions) considered for treatment. Exponential, par of exponentials, negative linear and negative quadratic penalization functions were used for that sake. Different weights were then applied to the penalization functions in order to minimize the attention given to beginning of the treatment. It was possible to conclude that when the penalization weight increases, the number of treatment sessions decrease and vice versa. After that, a new approach was presented, where the total number of sessions is forced to be constant by the introduction of a new time intervals restriction. With the addiction of this new restriction, it was possible to eliminate any time interval penalization function, since the time intervals were more distributed in the time horizon considered. Using this restriction, different perspectives were proposed where new objective functions and restriction were considered (some terms in the objective function were passed to the optimization restrictions and vice versa). In the first of three perspectives (eq.(5.32)), it was possible to conclude that minimizing only the final tumor volume, besides the amplitudes, led to a more lower and constant drug concentration in the human organism. The disadvantage is the fact that the tumor volume evolution is not minimized. In the second perspective, besides minimizing only the tumor final value, the tumor

evolution (the addition of the integral term) is also minimized. Different weights for the integral term are considered and it was possible to conclude that when the weight increases, the tumor final value and evolution decreases. In the third and last perspective it was possible to specify the tumor volume final value, which led to a more complex problem to solve. However it could correspond to a realistic scenario.

Still in the third problem of this work, a Pseudo-spectral approach was considered, which had the objective of simplify/decrease the dimension of the space states. The approach was adapter to this work. The results using 10 polynomials suggested that the approximated problem was convex. The method showed itself to be powerful.

In the last chapter (chapter 6), a sensitivity analysis was made. It started with an analysis about parameter variation, where families of responses were analyzed. First, considering the variation of the initial tumor volume, it was possible to conclude that when the initial volume increase, the amount of administered drug also increase. However the increasing depends also on the carrying capacity value. It was also concluded that the balance between the terms of the objective function can vary if the amplitudes penalization weights are not proportional to the initial volume. Considering the variation of the maximum drug effect on the tumor, it was possible to conclude that when the maximum effect decrease, the amplitudes penalization did not allowed the amplitudes to be higher enough to minimize tumor volume evolution. In the other way around, when the maximum effect increase, the controller was able to reduce the amplitudes and also minimize the tumor evolution, leading to the conclusion that drugs with more effect are better for treatment. Afterwards, it was considered the variation of the carrying capacity and it was possible to conclude that when the carrying capacity increase, the minimization of the tumor volume require more drug concentration, since the growing force of the tumor is also increased. In the Modelling Errors section, a study about the impact of parameters errors have in the controller solution was made. It was possible to conclude that, for the same solution, when the initial volume and carrying capacity increase, the tumor increase in size. When the drug maximum effect was increase, the tumor decreased in size, which lead to the conclusion that is important to invest in the drug investigation in order to create drug that has more effect on the tumor. Quantization in the control variables was then considered, and it was possible to conclude that the quantization decreases both drug dosages and time intervals. The decrease in the dosages may imply a lower drug concentration in the organism. However, the decrease in the time intervals compensated the decrease in the dosages, leading to a non decrease of the average drug concentration in the organism. This means that the impact of the quantization in the tumor volume evolution is almost none. Finally, the Gompertz model was considered as the tumor growth model. Because the tumor growth represented by the Logistic model is lower than when represented by the Gompertz model, it was possible to conclude that the amount of drug concentration necessary to minimize the tumor volume is higher using the Gompertz model than using the Logistic.

## 7.1 Future Work

In a more general view, there are some substantial changes that can be considered in this work:

- The architecture defined in figure 1.4 can be considered;

- The administration of more than one drug can be considered;
- Other PK, PD and Tumor Growth models can be considered, as well as other subsystems that influence tumor growth.

Considering the models and the architecture used in this work, there are also other tasks that can be done in future. Note that in this work, different studies, techniques and concepts were made and applied to each of the three problems. It would be interesting to study the influence of the weights of the objective functions considered in each problem. It would be also interesting to apply a synchronous Receding Horizon Control to the second problem of this work, which could result in a treatment with different time intervals. A deeper investigation about pseudo-spectral approach and different optimization algorithms and methods is also interesting.

# Bibliography

- [1] R. P. Araujo and D. L. S. McElwain. A history of the study of solid tumour growth: the contribution of mathematical modeling. *Bulletin of Mathematical Biology*, 66(5):1039–91, 2004.
- [2] G. Bastin and V. Guffens. Congestion control in compartment network systems. *Elsevier*, 55(8):689–696, Apr. 2006.
- [3] S. Benzekry, C. Lamont, A. Beheshti, A. Tracz, J. M. L. Ebos, L. Hlatky, and P. Hahnfeldt. Classical mathematica models for description and prediction of experimental tumor growth. *PLOS Computational Biology*, 10(8):e1003800, Aug. 2014.
- [4] A. Bermudez. Some applications of optimal control theory of distributed systems. *ESAIM*, 8:195–218, 2001.
- [5] W. E. Boyce and R. C. DiPrima. *Elementary Differential Equations*. Wiley, 3<sup>rd</sup> edition, 1977.
- [6] M. Braun. *Differential Equations and Their Applications*. Springer-Verlag, 2<sup>nd</sup> edition, 1941.
- [7] L. L. Brunton, J. S. Lazo, and K. L. Parker. *The Pharmacological Basis of Therapeutics*. MC Graw Hill, 11<sup>th</sup> edition, 2006.
- [8] L. F. Buchanan and F. E. Norton. Optimal control applications in economic systems. *Elsevier*, 8:141–187, 1971.
- [9] V. Chellaboina, S. P. Bhat, W. M. Haddad, and D. S. Bernstein. Modeling and analysis of mass-action kinetics. *IEEE Control Systems*, 29:60–78, Aug. 2009.
- [10] M. David G. Nathan. The cancer treatment revolution. *Transactions of the American Clinical and Climatological Association*, Vol. 118, 118:317–23, 2007.
- [11] M. C. F. Donkers, P. Tabuada, and W. P. M. H. Heemels. On the minimum attention and the anytime attention control problems for linear systems: A linear programming approach. *IEEE Conference on Decision and Control and European Control Conference*, arXiv.11082783, 2018.
- [12] H. Enderling and M. A. J. Chaplain. Mathematical modeling of tumor growth and treatment. *Current pharmaceutical design*, 20(30):4934–40, 2014.
- [13] L. Farina and S. Rinaldi. Positive linear systems - theory and applications. *Wiley, New York*, 2000.

- [14] J. C. Ferreira. *Introductions to the Theory of Distributions*. Longman, 1997.
- [15] D. E. Golan, J. Armen H. Tashjian, E. J. Armstrong, and A. W. Armstrong. *Princípios da Farmacologia*. Guanabara Koogan, 2<sup>nd</sup> edition, 2009.
- [16] F. Grognard, F. Jadot, L. Magni, G. Bastin, R. Sepulchre, and V. Wertz. Robust stabilization of a nonlinear cement mill model. *IEEE Transactions on Automatic Control* 46 (4), 46:618–623, 2001.
- [17] F. S. Hiller and G. J. Lieberman. *Introduction to Operations Research*. Mc Graw Hill, 7<sup>th</sup> edition, 2001.
- [18] L. Imsland, B. A. Foss, and G. O. Eikrem. State feedback control of class of positive systems: Application to gas-lift stabilization, 2003.
- [19] J. L. C. Jr., R. A. Clewell, P. R. Gentry, M. E. Andersen, and H. J. C. III. Physiological based pharmacokinetic/toxicokinetic modelling. *Methods in Molecular Biology*, 929:439–99, 2012.
- [20] W. G. Kelley and A. C. Peterson. *The Theory of Differential Equations*. Springer, 2<sup>nd</sup> edition, 2010.
- [21] V. Kumar, A. K. Abbas, and J. C. Aster. *Robbins Patología Básica*. Saunders, 9<sup>th</sup> edition, 2013.
- [22] D. G. Luenberger. *Introduction to Dynamic Systems*. John Wiley and Sons, 1979.
- [23] B. Meibohm and H. Derendorf. Basic concepts of pharmacokinetic/pharmacodynamic modelling. *International Journal of Clinical Pharmacology and Therapeutics*, 35(40):401–13, 1997.
- [24] E. Mosca. *Optimal, Predictive and Adaptive Control*. Prentice Hall, 1995.
- [25] OECD and P. E. O. H. Systems. State of health in the european union: Country health profile 2017 – portugal. Technical report, European Observatory on Health Systems and Policies, 2017.
- [26] A. N. Oppenheim, A. S. Willsky, and S. H. Nawab. *Signals and Systems*. Prentice Hall, 2<sup>nd</sup> edition, 1998.
- [27] L. K. Paalzow. Torsten teorell, the father of pharmacokinetics. *Upsala Journal of Medical Sciences*, 100:41–46, 1995.
- [28] E. S. M. Pacheco. *Cancer therapies based on Optimal Control methods*. Instituto Superior Técnico, 2017. Master Thesis.
- [29] H. Peng and B. Cheung. A review on pharmacokinetic modeling and the effects of environmental stressors on pharmacokinetics for operational medicine: Operational pharmacokinetics. Technical report, Defense Research and Development Canada, Sept. 2009.
- [30] J. G. Pierce and A. Schumitzky. Optimal impulsive control of compartment models - algorithm. *Journal of Optimization Theory and Applications*, 2, Apr. 1976.
- [31] J. G. Pierce and A. Schumitzky. Optimal impulsive control of compartment models - qualitative aspects. *Journal of Optimization Theory and Applications*, 1, Apr. 1976.

- [32] S. Pilari. *Novel Approaches to Mechanistic Pharmacokinetic/Pharmacodynamic Modeling*. PhD thesis, Freien Universität Berlin, 2011.
- [33] M. Rajabi and S. A. Mousa. The role of angiogenesis in cancer treatment. *Biomedicines*, 5(2):34, 2017.
- [34] M. I. Ribeiro. *Análise de Sistemas Lineares*, volume 2. IST Press, 2002.
- [35] G. S., M. M., R. F., B. X., B. L., D. M., and M. P. The hill equation: a review of its capabilities in pharmacological modelling. *Fundamental and Clinical Pharmacology*, 22(6):633–48, 2008.
- [36] C. M. Sakode and R. Pahi. Nonlinear impulsive optimal control synthesis with optimal impulse timing: A pseudo-spectral approach. *IFAC Journal of Systems and Control*, vol.3:pag.30–40, 2018.
- [37] H. Sbeity and R. Younes. Review of optimization methods for cancer chemotherapy treatment planning. *Computer Science and Systems Biology*, 8:2, 2015.
- [38] H. Schattler and U. Ledzewicz. *Optimal control for Mathematical Models of Cancer Therapies*. Springer, 2010.
- [39] L. Schwartz. *Théorie des Distributions*. Hermann, 1978.
- [40] S. P. Sethi and G. L. Thompson. *Optimal Control Theory - Applications to Management Science and Economics*. Springer, 2<sup>nd</sup> edition, 2006.
- [41] S. Siegmund, C. Nowak, and J. Diblík. A generalized picard-lindelöf theorem. *Electronic Journal of Qualitative Theory of Differential Equations*, (28):1–8, 2016.
- [42] G. W. Swan. Some strategies for harvesting a single species. *Bulleting of Mathematical Biology*, 37:659–673, 1975.
- [43] G. W. Swan. Applications of optimal control theory in biomedicine. *Dekker, New Yord*, 60(1), 1984.
- [44] G. W. Swan. Role of optimal control theory in cancer chemotherapyapplications of optimal control theory in biomedicine. *Mathematical Biosciences*, 101:237–284, 1990.
- [45] F. M. F. Teles. *Cancer Therapy Optimization based on Unsupervised Learning and Multiple Model Adaptive Control*. Instituto Superior Técnico, 2017. Master Thesis.
- [46] V. C. Wassim M. Haddad and Q. Hui. *Nonnegative and Compartmental Dynamical Systems*. Princeton, 2010.
- [47] S. Y. Yoo and S. M. Kwon. Angiogenesis and its therapeutic opportunities. *Hindawi Publishing Corporation*, 3013:127170, 2013.



## Appendix A

# Solution of the Logistic Equation

It is possible to rewrite equation the Logistic Equation (eq.(3.2)) in the form of a Riccati equation  $\frac{dy}{dx} = q_0(x) + q_1(x)y(x) + q_2(x)y^2(x)$

$$\frac{dV}{dt} = aV - \frac{a}{K}V^2, \quad (\text{A.1})$$

where  $q_1(t) = a$  and  $q_2(t) = -\frac{a}{K}$ . Because  $q_0(t) = 0$ , this is actually a Bernoulli equation. There are some different methods to solve the Bernoulli equation. For instance, it is possible to see that equation (A.1) is a separable differential equation where  $q_i(x)$ ,  $i = 0, 1, 2$  are constants. Applying the method to solve this kind of equations (see [6], page 29), yields

$$\int_{V_0}^V \frac{1}{a\sigma - \frac{a}{K}\sigma^2} d\sigma = \int_{t_0}^t 1 d\tau. \quad (\text{A.2})$$

To solve the right side of the equation, it is necessary to use the partial fractions method in order to separate the term into simpler fractions like

$$\frac{1}{aV - \frac{a}{K}V^2} = \frac{1}{aV} + \frac{1}{aK - aV}. \quad (\text{A.3})$$

So, equation (A.2) can be written as

$$\frac{1}{a} \int_{V_0}^V \frac{1}{\sigma} + \frac{1}{K - \sigma} d\sigma = t - t_0. \quad (\text{A.4})$$

Solving the integral, the following is obtained

$$\frac{1}{a} \int_{V_0}^V \frac{1}{\sigma} + \frac{1}{K - \sigma} d\sigma = \frac{1}{a} \left[ \ln \frac{V}{V_0} + \ln \left| \frac{a - \frac{a}{K}V_0}{a - \frac{a}{K}V} \right| \right] = t - t_0. \quad (\text{A.5})$$

Because  $a$  is usually bigger than  $b$ , the term  $\frac{a - \frac{a}{K}V_0}{a - \frac{a}{K}V}$  is always positive. Using this fact, taking the exponential of both sides of equation (A.4) and solving in order to  $V(t)$ , the following is obtained

$$V(t) = \frac{V_0 K}{V_0 + (K - V_0)e^{-a(t-t_0)}}, \quad (\text{A.6})$$

for  $\beta = 1$ .

It is also possible to solve the Bernoulli equation by noticing that it is a non-linear differential equation in the form  $\frac{dy}{dx} + P(x)y = y^n Q(x)$ , where  $P(t) = -a$ ,  $Q(t) = -\frac{a}{K}$  and  $n = 2$ . To solve this equation,

a change of variable is needed (see [5]). Suppose that  $M = V^{-1}$ . Dividing equation (A.1) by  $V^2$  and noticing that  $-\frac{dM}{dt} = V^{-2} \frac{dV}{dt}$ , it is possible to rewrite the Bernoulli equation as

$$\frac{dM}{dt} + Ma = \frac{a}{K}. \quad (\text{A.7})$$

Multiplying both sides by  $e^{at}$  the following is obtained

$$e^{at} \frac{dM}{dt} + ae^{at} M = \frac{a}{K} e^{at}. \quad (\text{A.8})$$

Analyzing the above equation, it is possible to see that the left side of the equation corresponds actually to the derivative of the function  $e^{at} M(t)$ . So,  $\frac{d}{dt} [e^{at} M(t)] = \frac{a}{K} e^{at}$ . Integrating both sides of the equation and using the initial condition  $M(0) = M_0 = \frac{1}{V_0}$ , the expression for  $M(t) = \frac{V_0 + (K - V_0)e^{-a(t-t_0)}}{V_0 K}$  is obtained. Remembering that  $V = M^{-1}$ ,

$$V(t) = \frac{V_0 K}{V_0 + (K - V_0)e^{-a(t-t_0)}}. \quad (\text{A.9})$$

For  $\beta \neq 1$

$$V(t) = \frac{V_0 K}{(V_0^\beta + (K^\beta - V_0^\beta)e^{-a\beta(t-t_0)})^{\frac{1}{\beta}}}. \quad (\text{A.10})$$

## **Appendix B**

### **Important remarks of chapter 5**

Table B.1: Important remarks of chapter 5.

		What varies		Convex problem		Algorithm/method used for optimization		Concepts and studies made		Objective function used		Conclusions	
Problem 1	Dirac impulse amplitudes	Results suggest convexity		Sequential Quadratic Programming (Matlab)		-Influence of parameter $\rho$ -Influence of parameter $T$ -Receding Horizon Control		$J(A_n) = \int_0^T V^2 dt + \rho \sum_{n=0}^{N-1} A_n^2, c \in \Omega_c$		If $\rho$ increase, $A_n$ decrease. If $T$ increase, $A_n$ increase. RHC introduces feedback			
Problem 2	Dirac impulse amplitudes and periodic time interval	Not convex		Use SQP with 10 different initial points and choose the one that gives the lowest objective function value		-Influence of the IS -Influence of the Angiogenesis Process		$J(A_n, T_1) = \int_0^T V^2 dt + \rho \sum_{n=0}^{N-1} A_n^2 + \omega_N e^{-T_1 + \tau}, c \in \Omega_c$		The IS helps reducing the tumor while angiogenesis helps tumor growth			
Problem 3	Dirac impulse amplitudes and time intervals	Not convex		Use SQP with 10 different initial points and choose the one that gives the lowest objective function value		-Minimum Attention Control(MAC) -Fixing N -Pseudo-Spectral Approach		For MAC: $J(A_n, T_n) = \int_0^T V^2 dt + \sum_{n=0}^{N-1} \rho_n A_n^2 + [\omega_{N-1}] [f(T_{N-1})]^T$ . Fixing N, three different obj. func. are considered (see section 5.6.2). For the Pseudo-Spectral Approach, 10 polynomials are used to approx. the states.		Using MAC techniques, it was possible to increase time intervals when tumor decrease. By fixing N, different perspectives were considered including minimizing the tumor final value and not of only the tumor temporal evolution. Using a Pseudo-Spectral approach with 10 polynomials, the objective function became convex. This could be the most important approach to investigate in the future.			